Stony Brook University

Regulatory mechanisms of the non-receptor tyrosine kinase Ack1

A Dissertation presented by

Victoria Prieto

To

The Graduate School

In Partial fulfillment of the

Requirements

For the Degree of

Doctor of Philosophy

In

Molecular and Cellular Biology

Stony Brook University

August 2010

Stony Brook University

The Graduate School

Victoria Prieto

We, the dissertation committee for the above candidate for the

Doctor of Philosophy Degree,

Hereby recommend acceptance of this dissertation.

W. Todd Miller, Ph.D., Dissertation Advisor
Professor, Department of Physiology and Biophysics

Deborah A. Brown, Ph.D., Chair of the Committee
Professor, Department of Biochemistry and Cell Biology

Wali Karzai, Ph.D.
Associate Professor, Department of Biochemistry and Cell Biology

Holly Colognato, Ph.D.
Assistant Professor, Department of Pharmacology

M. Raafat El-Maghrabi, Ph.D.
Research Associate Professor, Department of Physiology and Biophysics,
Stony Brook University

This dissertation is accepted by the graduate School

Lawrence Martin
Dean of the Graduate school

Abstract of the Dissertation

Regulatory mechanisms of the nonreceptor tyrosine kinase Ack1

By

Victoria Prieto

Doctor of Philosophy

in

Molecular and Cellular Biology

Stony Brook University

2010

Ack1 is a non-receptor tyrosine kinase that participates in tumorigenesis, cell survival and migration. Relatively little is known about mechanisms that regulate Ack1 activity. First, this dissertation will address the effect of naturally occurring somatic mutations on Ack1 function and activity and the use of these mutations to gain insight into the regulation of Ack1. Second, I will describe the study of the role of the N-terminal domain on Ack1 regulation.

As my first aim, I studied four somatic missense mutations of Ack1 that were recently identified in cancer tissue samples. The effects of these cancer-associated mutations on Ack1 activity and function have not been described. These mutations occur in the N-terminal region, the C-lobe of the kinase domain, and the SH3 domain. Here, I show that the cancer-associated mutations increase Ack1 autophosphorylation in mammalian cells without affecting localization, and increase Ack1 activity in immune complex kinase assays. The cancer-associated mutations potentiate the ability of Ack1 to promote proliferation and migration, suggesting that point

mutation is a mechanism for Ack1 deregulation. I propose that the C-terminal Mig6 homology region (MHR) (residues 802 to 990) participates in inhibitory intramolecular interactions. The isolated kinase domain of Ack1 interacts directly with the MHR, and the cancer-associated E346K mutation prevents binding. Likewise, mutation of a key hydrophobic residue in the MHR (F820) prevents the MHR-kinase interaction, activates Ack1, and increases cell migration. Thus, the cancer-associated mutation E346K appears to destabilize an autoinhibited conformation of Ack1, leading to constitutively high Ack1 activity.

The second set of experiments focused on the role of the N-terminal domain on Ack1 regulation. When overexpressed in mammalian cells, NKD (N-terminus and Kinase domain) is autophosphorylated while KD (Kinase domain alone) is not, indicating that the N-terminus is needed for Ack1 autophosphorylation. The purified kinase domain is autophosphorylated and active towards a peptide substrate *in vitro* and can be activated by increasing its local concentration, suggesting that an intermolecular interaction promotes activation. NKD localizes at the plasma membrane while KD shows a more diffuse cytosolic localization. Co-immunoprecipitation data show an interaction between NKD and full-length wild type Ack1. Taken together these studies suggest that the N-terminal domain of Ack1 is involved in a dimerization or self-association event that is required for autophosphorylation.

Table of contents

List of figures

List of tables

List of abbreviations

ATP	adenosine triphosphate
ADP	adenosine diphosphate
Cdc42	Cell division cycle 42
Cas	Crk-associated substrate
cpm	counts per minute
DACK	*Drosophila melanogaster* Ack
DMEM	Dulbecco's modified Eagle's medium
DNA	deoxyribonucleic acid
DOGS	1,2-dioleoyl-*sn*-glycero-3-succinate
E3	ubiquitin-protein isopeptide ligase
EDTA	ethylene diamine tetra acetate
EEA1	early endosome antigen 1
EGF	epidermal growth factor
EGFR	EGF receptor
EV	empty vector
FBS	fetal bovine serum
GFP	Green fluorescent protein
Grb2	Growth factor receptor-bound protein 2
GST	glutathione S-transferase
HA	Hemagglutinin
Hck	Hemopoietic cell kinase
HEPES	4-(2-hydroxyethyl)-1-piperazineethanesulfonic acid
HRP	horseradish peroxidase
IB	immunoblot
IgG	Immunoglobulin G
IP	immunoprecipitation
Kcl	Potassium chloride
MgCl2	magnesium chloride
mg	milligram
mg/ml	milligram per milliliter
MHR	Mig6 homology region
ml	milliliter
nm	nanometer
NADH	nicotineamide adenine dinucleotide hydrogenase
NaCl	Sodium chloride
NaF	sodium fluoride
Ni-NTA	nickel-nitrilotriacetic acid
NP40	nonidet P40
PBS	Phosphate-buffered saline
PC	Phosphatidylcholine
PCR	Polymerase chain reaction
PDGF	platelet derived growth factor

PMSF	phenylmethylsulfonyl fluoride
pTyr	phosphotyrosine
PVDF	Polyvinylidene fluoride
pY	phosphotyrosine
SH2	Src homology 2
SH3	Src homology 3
SNX9	sortin nexin 9
Sf9	*Spodoptera frugiperda* 9
TEL	translocation Ets leukemia
Tnk1	thirty-eight-negative kinase 1
WASP	Wiskott-Aldrich syndrome protein
WCL	whole cell lysate
WT	wild type
Yop	Yersinia outer protein
β-ME	beta-mercaptoethanol
μg	microgram
μl	microliter
μM	micromolar

Acknowledgments

I would like to thank Dr. Todd Miller for giving me the opportunity to work in his group. I appreciate his constant support and advice. He is a role model as a scientist and it was such a big privilege for me to have the chance to learn from him. I would like to be as knowledgeable and focused as he is. He is the best example of a true researcher, one that is motivated by curiosity and enjoys his work. He is always available and he always provides the right perspective to make the most of all situations. The PhD was an intellectual adventure but it was also a journey that challenged my perseverance and emotional resilience. Todd was always there to support me in every stage of the process. For his wisdom and guidance I am extremely grateful.

I want to thank the members of my committee for their encouragement and advice during our meetings. In particular, Dr. Deborah Brown was extremely generous with her time and every comment she made challenged me and made my work better. I am thankful for the support and positive feedback that I received from Dr. Holly Colognato, Dr. Wali Karzai and Dr. Richard Lin during our discussions. I want to thank Dr. Raafat El-Maghrabi for his kindness and for agreeing to review my work.

I thank Azad Gucwa for the immunofluorescence studies she did in Deborah Brown's lab. It was a pleasure to collaborate with her and she made important contributions to this work.

I thank Dr. Nicolas Carpino for giving me the Phoenix cells that I used to produce the retroviruses.

I want to thank everyone in the Miller lab for making it a very productive as well as enjoyable place to work. Barbara Craddock is such an important person in the lab. Her excellent

work is crucial to our success from making sure that we have what we need to conduct our experiments to doing research and sharing her expertise. I shared work with very inspiring and smart people and I have tried to learn from every person in the lab. I appreciated Parag's focus and meticulousness, Shalini's passion, Wanqing's strength and sharpness and Kira's wit and intelligence. Thank you guys for all the collaboration and good times. Tiffany and Saadat are recent additions and they will be assets to the group. I loved learning what it means to be a mentor with Angelina, Tori and Tiffany. I thank Tori who during her rotation helped making two of the cancer-associated mutations that I discuss in this dissertation. I want to acknowledge the work done the Dr. Noriko Yokoyama who initiated the research on Ack1 in our lab and contributed to the field with three important publications.

I want to thank everyone in the Physiology and Biophysics Department for making me feel at home. I thank Chris Gordon for letting me change the temperature of his incubator for long periods of time and for taking the pictures of my infected cells. I want to thank Marc Bowen for allowing me to use his lab to make my SUVs and especially Jim for his infinite patience to teach me. I thank Melanie Bonette, Robin Green and Charlotte Duff for their kindness and efficiency.

I would like to thank the Molecular and Cellular Biology program. I thank Dr. Rolf Sternglanz for his encouragement. I thank Carol Juliano and Beverly Piazza for taking care of the important paperwork.

In this time I also had some important lessons in life and friendship. I am grateful to my friends in Uruguay that stayed in touch, so important to keep our roots in place. I thank Juancho, Sergio and Pepen for being good friends and providing the closest thing to a home during our first month in New York City. Natalia, Alberto, Victor and Emilio were our family away from

home. I thank them for their warmth that was so important for us through the toughest moments of our first year in Stony Brook. I will always treasure Roberta's friendship and I thank her for sharing her wisdom with me. I am happy to have shared this adventure with Barbara and I thank her for her kindness and empathy. I thank Angelo for teaching by example how to enjoy life. I thank Pablo who was a friend beyond the obvious reasons of language and geographical origin.

I want to thank my parents for their love and support through everything I choose to do. Since I was very young, they always insisted in the importance of critical and independent thinking, and that shaped my curiosity and my will to learn. I love my sisters Cecilia and Elena and I thank them for staying close. I am grateful to my parents in law for their constant support and generosity. I thank Lila for supporting me since the beginning when I was doing interviews for Grad School and in the moments when we most needed it.

Finally, I want to thank my husband Jose. I am grateful for his relentless support and commitment. I am extremely proud of him and of our relationship and this is the kind of success that matters the most to me.

CHAPTER 1

Introduction

Tyrosine phosphorylation and tyrosine kinases

Tyrosine phosphorylation is a post-translational modification that was first discovered in polyomavirus infected mouse 3T6 cells (*1*). In the 30 years since the discovery of tyrosine phosphorylation, it has emerged as a mechanism widely used by cells to mediate signal transduction pathways that regulate crucial processes such as cell growth, differentiation and survival in multicellular organisms (*2, 3*). The reaction is catalyzed by protein tyrosine kinases that can be divided into two classes: receptor tyrosine kinases (RTK) and cytosolic non-receptor tyrosine kinases (NRTK). Receptor tyrosine kinases are type I transmembrane proteins with N-terminal extracellular domains that can bind to ligands such as growth factors, and C-terminal intracellular portions that contain the catalytic domains (*4*). The binding of a ligand such as a growth factor induces receptor oligomerization and autophosphorylation of tyrosine residues. Tyrosine phosphorylation activates the catalytic domain and generates binding sites for downstream signaling proteins containing phospho-tyrosine binding domains such as Src Homology-2 (SH2) domains or protein tyrosine binding (PTB) domains (*5*).

The non-receptor tyrosine kinases are classified into ten families: Src, Abl, Jak, Ack, Csk, Fak, Fes, Frk, Tec and Syk (Fig. 1-1) (*5*). They all contain a closely related catalytic domain and additional non-catalytic domains that are important in enzyme regulation and substrate recognition (*2*). Like all eukaryotic kinases, NRTK catalytic domains have an N-terminal lobe (N-lobe) that contacts ATP and a larger C- terminal lobe (C-lobe). The conformation of a flexible segment contained in the C-lobe (the activation loop) has a central role in the regulation of the enzyme activity (*6*). In addition, activation of the tyrosine kinases involves an alpha helix (αC) located in the N-lobe and oriented towards the substrate-binding pocket. In the active conformation, the αC helix tilts towards the kinase domain C-lobe and activating interactions

stabilize this orientation (*3*). The regulatory importance of the phosphorylation of the activation loop varies in the different kinases known to date. For instance, Src activation is strongly dependent on autophosphorylation (*7*), while Csk lacks the autophosphorylation site (*8*).

Regulation of non receptor tyrosine kinases

One of the NRTK families that has been most studied and the best characterized is the Src family of cytosolic tyrosine kinases (Fig. 1-2). These enzymes have a N-terminal myristoylation site followed by an SH3 domain, an SH2 domain and a kinase domain. Two tyrosine residues are important for their activity: Tyr 416 in the activation loop and Tyr 527 in the C-terminal tail. Structural studies showed the spatial arrangement of Src domains in the inactive state, in which the non-catalytic domains mediate intramolecular interactions that maintain the enzyme in a closed, inactive conformation. In this conformation, the SH3 domain is bound to a proline-rich helix located between the SH2 domain and the kinase domain, and the SH2 domain is bound to the phosphorylated Tyr 527 (*9, 10*). Activating signals provided by protein-protein interactions that destabilize these intramolecular interactions may be of three types (Fig. 1-3) (*2*): the binding of the linker proline-rich helix to an SH3-containing protein (*11*); the dephosphorylation of the Tyr527 in the C-terminal tail (*12*); and the binding of the SH2 domain to other phospho-Tyr containing proteins (*13*). These signals disrupt the intramolecular inhibition and activate the enzyme. In addition, the non-catalytic domains provide surfaces for different types of interactions that couple the activation of the catalytic domain to substrate recognition (*2, 14, 15*).

Although in all the NRTKs the noncatalytic domains are important for regulation, the specific domain arrangement or the molecular mechanisms involved vary between the different

NRTK families. For example, Abl kinases have similar domain arrangements as Src, but the regulatory mechanisms are different and this has important implications in how their activity can be pharmacologically inhibited (*3*). Similar to Src, the autoinhibition of c-Abl involves a set of intramolecular interactions between the kinase domain and the other domains of the N-terminal portion of the polypeptide: SH3, SH2 and the myristoyl group. However, the molecular details of these interactions are different for the two kinases. The interaction of the SH3 domain with a poly proline helix in the linker region between the SH2 domain and the kinase domain is common in both structures. However, the structures of c-Src and c-Abl differ in that the SH2 domain of abl interacts in a phospho-Tyr independent manner with the C-terminal lobe of the kinase domain. An additional difference is that an N-terminal cap and a myristoyl group wrap around the base of the kinase domain and stabilize the inhibited structure (*16*). Importantly, the conformation of the inhibited activation loop is unique to the c-Abl catalytic domain. The inhibitor STI-571 (Gleevec) has been particularly successful due to its ability to target specifically the active site of Abl (*16*).

As new structures of tyrosine kinases are solved, new molecular mechanisms for enzyme regulation are revealed. Moreover, it is becoming apparent that a diversity of combinations is possible, depending on the role of each particular kinase. For example in Syk kinases that include Syk and ZAP-70, phosphorylation of the activation loop does not seem to be important for activation. Syk kinases have two SH2 domains located N-terminal to the kinase domain, separated by a inter-SH2 domain linker and followed by a kinase-SH2 domain linker (*7*). In the inactive conformation, the tandem SH2 domains are maintained in an inhibited conformation by interactions between the linker regions and the kinase domain. The activation of Syk kinases involves the cooperative binding to the SH2 tandem, which allows for enzyme activation (*3*). In

addition, the phosphorylation of pairs of Tyr residues in the linker regions have been shown to be important for activation (*7*).

The Csk family of NRTKs share a high homology with Src, with the difference that Csk lacks the tyrosine at the C-terminal tail. The crystal structures of inactive Csk suggest a set of autoinhibitory interactions different from the ones present in Src kinases. The SH2 and SH3 domains bind to the N-lobe of the kinase domain and stabilize the inactive conformation (*17*). Csk may be activated by an SH2 domain binding ligand (*18*). Upon activation, the SH2 domain is rotated and makes critical interactions with the N-lobe that stabilize the active conformation (*19*).

The Fes family of tyrosine kinases has a N-terminal F-BAR domain, an SH2 domain and a kinase domain. The intramolecular interaction between the SH2 and the kinase domain of Fes kinases promotes an active conformation. The SH2 domain binds directly to the αC helix and stabilizes the active conformation. The binding of a ligand to the SH2 domain further stabilizes the activation. In addition, the F-BAR domain forms oligomeric structures and binds to phospholipids in curved regions of membrane. Thus, it appears to act in concert with the SH2 domain to simultaneously target Fes kinases to its substrates while promoting its activation (*3*).

Although the modular domain composition and the biochemical properties of the basic modules are conserved among the different families of NRTK, there is a wide diversity of molecular mechanisms acting to regulate each individual family. Tyrosine phosphorylation is essential to normal cell signaling, but it also plays a crucial role in the pathogenesis of a number of infectious and neoplasmic diseases. The understanding of the molecular mechanisms of tyrosine kinase regulation has proved to be central to the development of inhibitors that target tyrosine kinases aberrantly activated in cancer. Prominent examples are STI-571 (imatinib or

Gleevec), an inhibitor of Brc-Abl which is used for the treatment of chronic myeloid leukemia, and gefitinib and erlotinib, EGFR inhibitors which are used for the treatment of non small cell lung cancer (*4*). Despite the emergence of resistance, tyrosine kinase inhibitors are one of the most promising areas of development in cancer treatment (*20*). As will be discussed below, Ack1 has been implicated in several stages and types of cancer (*21-24*). Therefore, it is emerging as a molecule of interest and a possible target for inhibition in cancer treatment.

The domain architecture of human Ack1 is shown in Figure 1-4 (top). Ack1 is a 120 kDa protein with an N-terminal sterile alpha motif (SAM) domain (*25*), a kinase domain, an SH3 domain, and a Cdc42-binding domain (CRIB). The large C-terminal portion of Ack1 contains several proline-rich sequences as well as a clathrin-binding motif (*26*), a ubiquitin binding domain (*27*) and a region homologous to Mig6 (*28*). The domain arrangement of Ack1 is unique among NRTKs; it is the only NRTK with a CRIB domain, and the position of the SH3 domain (C-terminal to the kinase domain) differs from all other families of NRTKs. Due to its unique domain composition, Ack1 is likely to use regulatory mechanisms different from the ones known for other NRTKs. In the following sections, we review the information available on the biological roles of Ack1 in normal and cancer cells, its biochemical properties and regulatory mechanisms and describe the known substrates and ligands.

Ack family kinases

Ack1 belongs to a family of non-receptor tyrosine kinases that includes Ack1, also called Tnk 2 (Tyrosine kinase non-receptor protein 2), and homologous proteins in mouse, cow, Drosophila and *Caenorhabditis elegans* (*29, 30*). Although all the members share the overall domain architecture shown in Figure 1-4 (i.e. kinase domain, SH3 domain), there are differences

in the length of the protein and in the presence or absence of the CRIB domain (Fig. 1-4) (*30*). The proteins Tnk1 from human, DACK from Drosophila and Kos1 from mouse do not have CRIB domains (*30*).

Ack1, the first member of the Ack family, was cloned from a human hippocampal expression library by its ability to bind GTP-bound Cdc42 specifically and not Rac1 or RhoA (*31*). The gene encoding Ack1 is located on chromosome 3q29 in humans, a region that is associated with recurrence of prostate cancer and is a predictor of metastasic relapse in breast cancer (*24*).

In *Drosophila melanogaster*, there are two members of the Ack family: DACK and DPR2. The roles of DPR2 and DACK have not been dissected but they are thought to be different because DPR2 has a Cdc42-binding domain, while DACK lacks one. Cdc42 regulates the expression of DACK in Drosophila embryos (*30*). The Ack tyrosine kinase activity has been implicated downstream of Cdc42 in the pathway that leads to dorsal closure of the epidermis during embryogenesis (*30*). In *C. elegans*, ARK-1 (A Ras-regulating Kinase 1), a cytoplasmic tyrosine kinase that is related to Ack1, acts as a negative regulator of EGFR signaling. In a yeast two-hybrid analysis, ARK-1 interacts with the Grb2 homologue, Sem5 (*29*).

Tnk1 (thirty-eight-negative kinase 1) was originally cloned from hematopoietic stem/progenitor cells from umbilical cord blood in humans (*32*). Tnk1 is a member of the Ack family with a predicted size of 72 kDa and the same domain architecture as Ack (*32*). Kos1 is the murine homologue of Tnk1 (*33*). In contrast with the other members of the Ack family (namely Ack1/Tnk2, Ack2, DPR2), but similarly to DACK, Tnk1 and Kos1 lack the CRIB domain (*30, 33*). Tnk1 was found to be specifically expressed in umbilical blood and not other hematopoietic tissues and to interact with phospholipase C-γ1 through its proline-rich region (*34*). It has been

reported that during embryonic development, Tnk1 blocks NF-κB activation and thereby promotes apoptosis mediated by the TNFα signaling pathway (*35*). Kos1 is a 47 kDa protein that was cloned from differentiating murine embryonic stem cells (*33*). The *Kos1* gene is located in chromosome 11 in mice and it is thought to be a murine splice variant of the human Tnk1 (*33*). Tnk1/Kos1 have been reported the have pro-apoptotic or tumor-suppressor functions. Kos1 inhibits Ras activation and negatively regulates cell growth (*33*). Tnk1/Kos1 knockout in mice results in a increased rate of tumor development (*36*).

Ack2 was first cloned from a bovine brain expression library. Ack2 has a predicted size of 83 kDa and contains the same basic domain structure as Ack1. The differences are located at the N-terminus and C-terminus. The Ack2 N-terminal region is 56 residues shorter than the N-terminal region of Ack1 (which contains 110 residues). The Ack2 C-terminal region contains a 15-residue insert and has 344 fewer amino acids than Ack1 (*37*). Ack2 is thought to be an isoform of Ack1 that is generated by alternative splicing and is not encoded by a different gene. In humans there is no evidence for the existence of an Ack2 homologue (*24, 25*). However, a number of the reports that provide information on Ack (activation pathways, biochemical properties and biological roles) were originated by the study of Ack2 and will be discussed throughout this dissertation.

Activation pathways

Ack1 is ubiquitously expressed in mammals, with highest expression in spleen, thymus and brain (*25*). Ack1 is phosphorylated and activated in response to a number of stimuli, including EGF, PDGF (*25*), bradykinin (*37*), agonists of the M3 muscarinic receptor (*38*), and integrin-mediated cell adhesion (*39, 40*).

Upon EGF stimulation, Ack1 phosphorylates and activates the guanine exchange factor Dbl. The interactions of Ack1 with Cdc42 and the adaptor protein Grb2 are essential for this pathway (*41*). The association of Ack1 with Grb2 has been shown in several studies through different approaches. *In vitro* studies showed that Ack1 associates with several SH3 domains, including the SH3 domain from Grb2 (*42*). Ack1 association to multiple receptor tyrosine kinases is dependent on Grb2 (*43*).

Ack is involved in integrin β1-mediated signaling pathways that modulate processes such as cell migration, cell adhesion and cell spreading. Ack2 is present in a complex with integrin β1; it is activated by cell adhesion to a fibronectin-coated surface in a Cdc42-dependent manner and it activates the phosphorylation of Jnk (*40*). Cdc42 is a member of the Rho family of GTPases. These proteins regulate the cytoskeletal rearrangements that occur during cell migration and cell adhesion. In response to Cdc42 activation, Ack1 mediates the phosphorylation of p130Cas to promote cell migration (*39, 44*). Ack1 activation by Cdc42 has been documented in the regulation of melanoma cell spreading by melanoma chondroitin sulphate proteoglycan (MCSP), a proteoglycan that is expressed on the surface of melanoma cells. Clustering of MCSP recruits a signaling complex formed by Cdc42, Ack1 and p130Cas. Ack1 promotes the phosphorylation of p130Cas, which in turns activates α4β1 integrin-mediated cell spreading (*44*). In breast cancer cells, collagen induces migration in a pathway activated by integrin. Collagen stimulation induces the formation of a complex involving Cdc42, activated Ack1, Crk and p130Cas (*39*). The expression of Ack2 in HeLa cells increases cell migration in a mechanism that also involves p130Cas and CrkII (*45*).

Although the physiological functions of Ack1 are not completely understood, several studies have focused on the role of Ack1 in EGF receptor trafficking and dynamics. Ack1 is

recruited to EGFR following EGF stimulation (*27*), and overexpression of Ack1 interferes with the proper trafficking of EGFR (*46*). EGFR stability and recycling are regulated by interactions between Ack1 and multiple protein partners including ubiquitin (*27*), clathrin heavy chain (*26, 47*), and SH3PX1 (*48, 49*). In HeLa cells, knocking down or overexpressing Ack1 results in the accumulation of EGFR in membranous compartments that are possibly derived from endosomes (*46*). In breast cancer cells, the binding of Ack1 to EGFR is independent of Ack1 activity and knock down of Ack1 reduces the amount of EGFR expressed at the surface of the cell. Thus, in breast cancer cells Ack1 acts to keep EGFR expressed at the cell surface (*50*). However, it is not known whether or not the effect of Ack1 on EGFR processing is dependent on Ack1 activity. On the other hand, in Cos7 cells overexpression of Ack1 promotes EGFR degradation by binding to ubiquitinated EGFR (*27*). Increased stability of Ack1 results in defective EGFR downregulation (*51*).

Biochemical properties of Ack1

The crystal structure of the isolated kinase domain of ACK has been solved in both phosphorylated and unphosphorylated forms. In these structures, the activation loop conformations are similar and do not occlude the substrate-binding site, suggesting that the phosphorylation of the activation loop may not play a stimulatory role (*52*).

A major autophosphorylation site has been mapped to the Y284 in the activation loop (*42*). A construct containing residues 1- 476, corresponding to the N-terminus, the kinase domain, the SH3 domain and the CRIB domain (Nt-Kinase-SH3-CRIB) is the longest construct that has been purified to homogeneity (*42*). This construct is activated, although modestly (3-fold), by the phosphorylation of Y284. Proteomic approaches have identified other

phosphorylation sites in Ack1. A study that followed changes in phosphorylation patterns caused by STI-571 treatment of BCR-ABL transformed cell lines, identified sites of phosphorylation in Y826, Y856 and Y857 (*53*) (Fig. 1-5). The phosphorylation of Y826 was also identified in a study of phosphorylated proteins downstream of insulin signaling (*54*). Y857 of Ack1 was identified in a mass spectrometry study in which protein phosphorylation events downstream of the EGFR-family member HER2 were analyzed (*55*). In addition, the phosphorylation of Y518 was identified in a study of global tyrosine phosphorylation patterns in cancer cells (*56*). The biological significance of these phosphorylation sites remains to be determined. Interestingly, Y826, Y857 and Y858 are located in the Mig6-homology region (MHR) that we showed participates in inhibitory intramolecular interactions (*57*) (discussed in Chapter 3). It is possible that the MHR of Ack1 is a substrate for oncogenic BCR-ABL, or insulin and EGF receptors, resulting the disruption of autoinhibition.

Relatively little information is available about the regulatory mechanisms of Ack1 and the roles that each domain plays in Ack1 regulation. The purified Nt-Kinase-SH3-CRIB polypeptide is active *in vitro* and can be used in enzymatic assays (*42*). The peptide substrates that are the most efficiently phosphorylated by this construct are EAIYAAPFAKKKG (Abl substrate) or KVIYDFIEKKKKG (peptide derived from WASP phosphorylation site) (*58*). Ligands for the SH3 domain and the CRIB domain bind to this construct, but fail to activate it, although addition of Cdc42 *in vivo* does increase Ack1 Y284 phosphorylation (*42*). Residues important for the interaction between Ack1 and Cdc42 have been identified from the NMR structure of the complex formed by a peptide spanning the residues 548-489 of Ack1 (CRIB domain is 548- 475) and Cdc42 (*59*).

One way of studying the role of each domain in Ack1 regulation is to assess the effects of point mutations on the enzyme's phosphorylation state. The relevant residues are shown in Figure 1-5. A mutation that occurs naturally in ovarian endometroid carcinoma (E346K) has been helpful to gain insight into the role of the Mig6 homology region (MHR). We have proposed that there is an autoinhibitory interaction between the C-lobe of Ack1 kinase domain and the MHR (*57*). Mutations such as V365R (in the kinase domain) or F820A and E346K (in the MHR) destabilize this conformation and activate Ack1 (*57*). We also showed that other cancer-associated mutations located in the SAM domain (R34L and R99Q), and in the SH3 domain (M409I) activate Ack1, but the mechanism by which they do so is not as yet clear. The details of this study will be discussed in Chapter 3. Several studies have produced a constitutively active Ack1 by the point mutation of L487F in the CRIB domain (*22, 60*). The position of this mutation is thought to be analogous to L107F in Pak1, which is known to prevent an autoinhibitory interaction (*61*), but the structural basis for this activation of Ack1 is not known. A mutation designed to prevent the binding of the SH3 domain to its ligand (W426K) was reported to produce activation of Ack1. In constrast, a point mutation that disrupts Cdc42 binding (H464D) reduced Ack1 autophosphorylation (*25*). Deletion of the N-terminal SAM domain has a similar effect (*25*), and results are described in Chapter 4. These results suggest that the individual domains of Ack1 are involved in regulatory interactions that could be either inter- or intramolecular.

The role of Ack1 in cancer

Ack1 has been implicated in several stages and several types of cancer. In breast cancer, Ack1 promotes the phosphorylation and activation of Akt, an important mediator of signaling

pathways that lead to transformation (*62*). Ack1 expression is required for the survival of cells transformed by v-Ras (*23*). Also, a peptide derived from the Ack1 CRIB domain blocked the Ras-mediated transformation of NIH-3T3 cells (*63*).

In a study of ~180 advanced-stage cancers, 9% of the lung tumors and 14% of the ovary tumors, had an amplification of the *Ack1* gene on chromosome 3. In addition, 42% of the aggressive lung tumors and 77% of metastatic hormone refractory prostate tumors showed overexpression of the Ack1 mRNA. Ack1 overexpression enhanced migration of human mammary epithelial cells (HMEC) and increased metastasis in the mouse mammary 4T1 breast cancer system (*24*). Moreover, overexpression of Ack1 produced several epithelial-to-mesenchymal transition (EMT) phenotypes in the human breast cancer cell line MDA-MB-231. Thus, overexpression of Ack1 is associated with poor prognosis and metastatic phenotypes in human tumors (*24*). This suggests a role for Ack1 as a metastasis determinant, perhaps as a modifier of other pre-metastatic lesions.

The mechanistic basis of Ack1's involvement in prostate tumorigenesis has been explored in detail. In the cultured prostate cancer cell line LNCaP, the tumor suppressor Wwox is phosphorylated and marked for degradation by Ack1 (*22*). The androgen receptor (AR) is a transcriptional activator that plays important roles in the development of advanced stage (androgen-independent) prostate cancer. Activated Ack1 has been shown to phosphorylate and activate AR function and to promote the progression of prostate cancer (*64*). In addition, Ack1 Tyr 284 phosphorylation was recently found to correlate with disease progression and proposed to be prognostic of progression of prostate cancer (*65*).

In a large study of somatic mutations in cancer, four missense mutations were identified in Ack1 (*21*). Two mutations in the N-terminus (R34L and R99Q) were identified in lung

adenocarcinoma and ovarian carcinoma, respectively; a mutation in the kinase catalytic domain (E346K) was identified in ovarian endometroid carcinoma, and a mutation in the SH3 domain (M409I) was found in gastric adenocarcinoma (Figure 1-5). From this study, Ack1 emerged as a candidate whose mutations are relevant to oncogenesis (*21*). We showed that the cancer-associated mutations activate Ack1 and promote anchorage independent growth and cell migration. However, the effect of Ack1 on cell proliferation is independent of Ack1 activity (*57*). In a phosphoproteomic study of the action of the antitumor drug dasatinib in lung cancer, Ack1 emerged as a signaling node that represents a possible target in cancer treatment. This study highlighted a possible scaffolding function of Ack1 in the context of control of cell growth (*66*). Consistent with our findings on the role of Ack1 in cell growth, the level of Ack1 protein expression was shown to be important in the control of cell proliferation, whereas Ack1 kinase activity was not crucial (*66*). An additional somatic mutation found in renal cancer, S985N, located in the UBA domain of Ack1, increases Ack1 stability and enhances oncogenic signaling through EGFR (*51*).

These data suggest a role for Ack1 independent of its kinase activity in cell proliferation. On the other hand, the activation state of Ack1 appears to be important in processes that involve enhanced cell motility, which are important in the metastatic stage of cancer progression and correlate with poor prognosis.

Known ligands and substrates of Ack1

A number of SH3 containing proteins have been identified as ligands for the proline rich region of Ack1, such as Hck (*42*), Grb2 and SNX9 (*49, 67*). Recently, the E3 ubiquitin ligase was shown to bind to a PPXY motif of Ack1 and to regulate its proteolytic degradation (*68*).

Other identified substrates of Ack1 include WASP (*69*) and the sorting nexin SH3PX1 (*49*). The complete list of Ack1 substrates and interacting proteins was recently reviewed by Mahajan, K. in (*70*) (Tables 1-1 and 1-2) and it includes diverse molecules involved in signaling such as receptor tyrosine kinases (MERK, EGFR, PDGFR, AXL, ALK, LTK), membrane proteins (integrin, MCSP), adaptor molecules (Grb2, HSH2), nucleotide exchange factors (Dbl), a transcription activator (AR), a tumor suppressor (Wwox), and a proto-oncogene (Akt/PKB). Other Ack1 interactors include proteins involved with vesicle dynamics (clathrin, SNX9) and cytoskeleton remodeling (WASP).

Summary and overview of this dissertation

Non-receptor tyrosine kinases share several common features. The non-catalytic modular domain composition and the biochemical properties of the individual domains are conserved. However, the molecular bases for the regulatory mechanisms are diverse and vary between the different families of NRTKs. Since 51 out of the 90 tyrosine kinases and about half of the NRTKs are involved in cancer, they represent significant targets for the development of inhibitors (*5*) and, the diversity of regulatory mechanisms becomes an added advantage towards the development of specific inhibitory drugs.

Ack1 may be activated by gene amplification and protein overexpression, by somatic mutations, or by signaling pathways activated by RTK or other membrane proteins such as integrins. Although the role that each individual domain plays in Ack1 regulation is not completely understood, we have shown that the Mig6-homology region in the C-terminus interacts with the C-lobe of the kinase domain and stabilizes an inhibited conformation (discussed in Chapter 3). Also, the SAM domain located in the N-terminus of Ack1, appears to

promote autophosphorylation (discussed in Chapter 4). We discuss the individual interactions, and the roles they play in normal Ack1 physiology and in cancer.

Substrates	*Cellular functions*	*Regulatory role*	*Refs.*
Akt/PKB	Proto-oncogene	Phosphorylated at Y176, leading to Akt activation	(*62*)
Androgen Receptor (AR)	Steroid receptor	Phosphorylated at Y267 and Y363, leading to androgen-independent transcriptional activation	(*64, 65*)
p130Cas	Adaptor molecule	Phosphorylated at Y165, Y249, Y410, promotes cell migration Associates with Ack1 via SH3 domain	(*39*)
WASP (Wiskott-Aldrich syndrome protein)	Cdc42 effector	Phosphorylated at S242 and Y256	(*69*)
Wwox	Tumor suppressor	Phosphorylated at Y287, leading to polyubiquitination and degradation	(*22*)

Table 1-1: Substrates of Ack1.
Adapted from Mahajan, K and Mahajan, N.P. (2010). (*70*).

Interacting proteins	*Cellular functions*	*Regulatory role*	*Refs.*
Cdc42	GTPase	Direct binding with Ack1 inhibits GTPase activity	(*31*)
Clathrin Heavy Chain	Trafficking	Ack1 binds to Clathrin and regulates clathrin distribution	(*26*)
Dbl	Guanine nucleotide exchange factor	Association with Ack1 facilitates GEF activity	(*41*)
MERK, EGFR, PDGFR, Axl, Alk, Ltk	Receptor tyrosine kinases	Associate with Ack1 leads to Ack1 activation	(*22, 25, 27, 43, 50*)
Grb2	Adaptor protein	Associates with Pro-rich region of Ack1	(*25*)
Hck	Non-receptor tyrosine kinase	SH3 domain interacts with Ack1 Pro-rich region	(*71*)
HSH2	Adaptor protein	Associates with Pro-rich region of Ack1 and regulates cytoline signaling	(*72*)
Hsp90β	Chaperone	Binds to Ack1 and maintains Ack1 conformation	(*22*)
MCSP (Melanoma chondroitin sulfate proteoglycan)	Cell surface antigen	Regulates cell spreading trough Ack1 and p130Cas	(*44*)
Nck	Adaptor protein	Binds to Ack1 via Nck SH2 domain	(*25*)
Nedd4-1 and Nedd 4-2	E3-ubiquitin ligase	Ubiquitination and degradation of Ack1	(*68, 73*)
Nephrocystin	Epithelial cell organization	Partially colocalizes with Ack1 at cell to cell contacts	(*74*)
PTPN12, PTPRJ and PTPRC	Tyrosine phosphatases	Associate with Ack1	(*75*)
SNX9	Vesicle dynamics	Binds to Ack1 (residues 920-955)	(*49*)

Table 1-2: Interacting proteins of Ack1.
Adapted from Mahajan, K and Mahajan, N.P. (2010). (*70*).

Figure 1-1: Human cytoplasmic protein-tyrosine kinases.

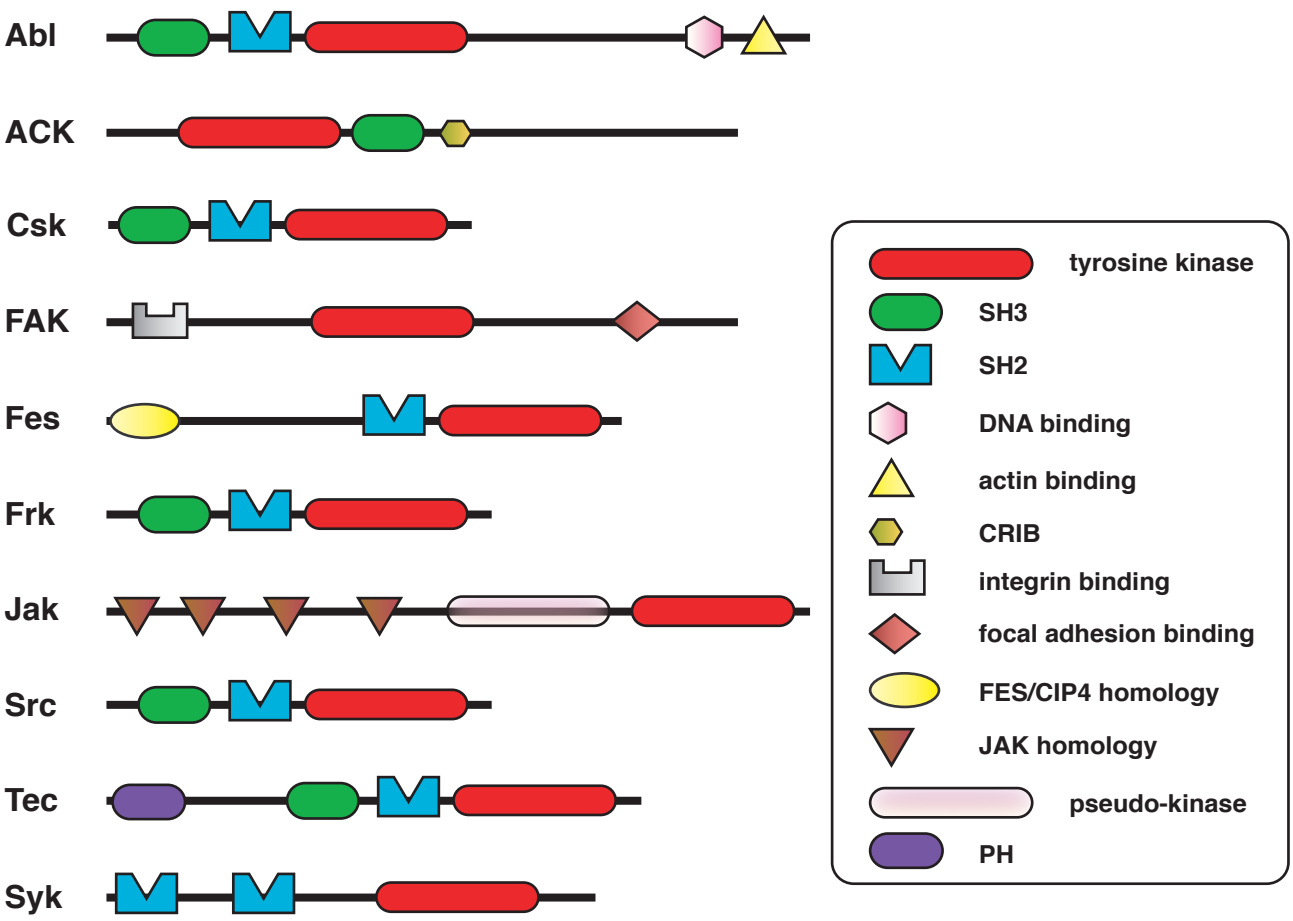
Abl
ACK
Csk
FAK
Fes
Frk
Jak
Src
Tec
Syk
tyrosine kinase
SH3
SH2
DNA binding
actin binding
CRIB
integrin binding
focal adhesion binding
FES/CIP4 homology
JAK homology
pseudo-kinase
PH

Figure 1-1

Figure 1-2: The three-dimensional structure of the Src family kinase Hck.

The SH3 domain is yellow, the SH2 domain is green, and the catalytic domain is blue. Phosphorylation sites at Tyr416 (in the activation loop) and Tyr527 (in the C-terminal tail) are indicated. Reproduced from Miller, WT. (2003) (*2*).

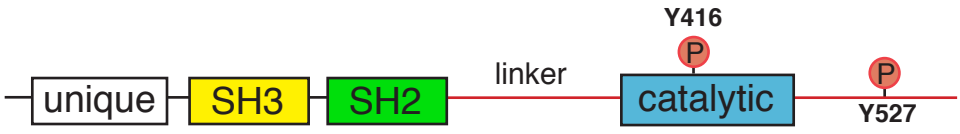
Y416
P
unique
SH3
SH2
linker
catalytic
P
Y527

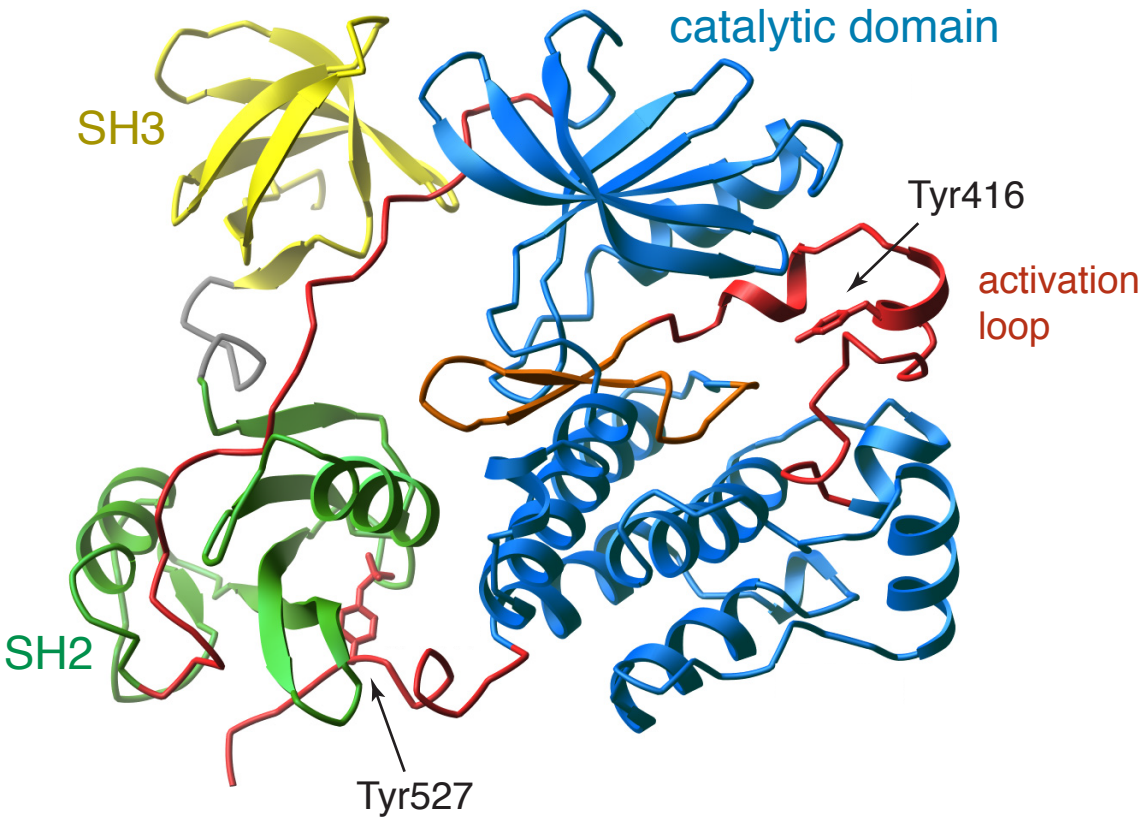
catalytic domain
SH3
Tyr416
activation
loop
SH2
Tyr527

Figure 1-2

Figure 1-3: Mechanisms for Src kinase activation.

The inactive form of the kinase is depicted at the upper left. Three processes can lead to increased autophosphorylation at Tyr416 and enhanced catalytic activity: Tyr527 dephosphorylation, SH2 ligation, or SH3 ligation. pY represents phosphorylated tyrosine. Reproduced from Miller, WT. (2003) (*2*).

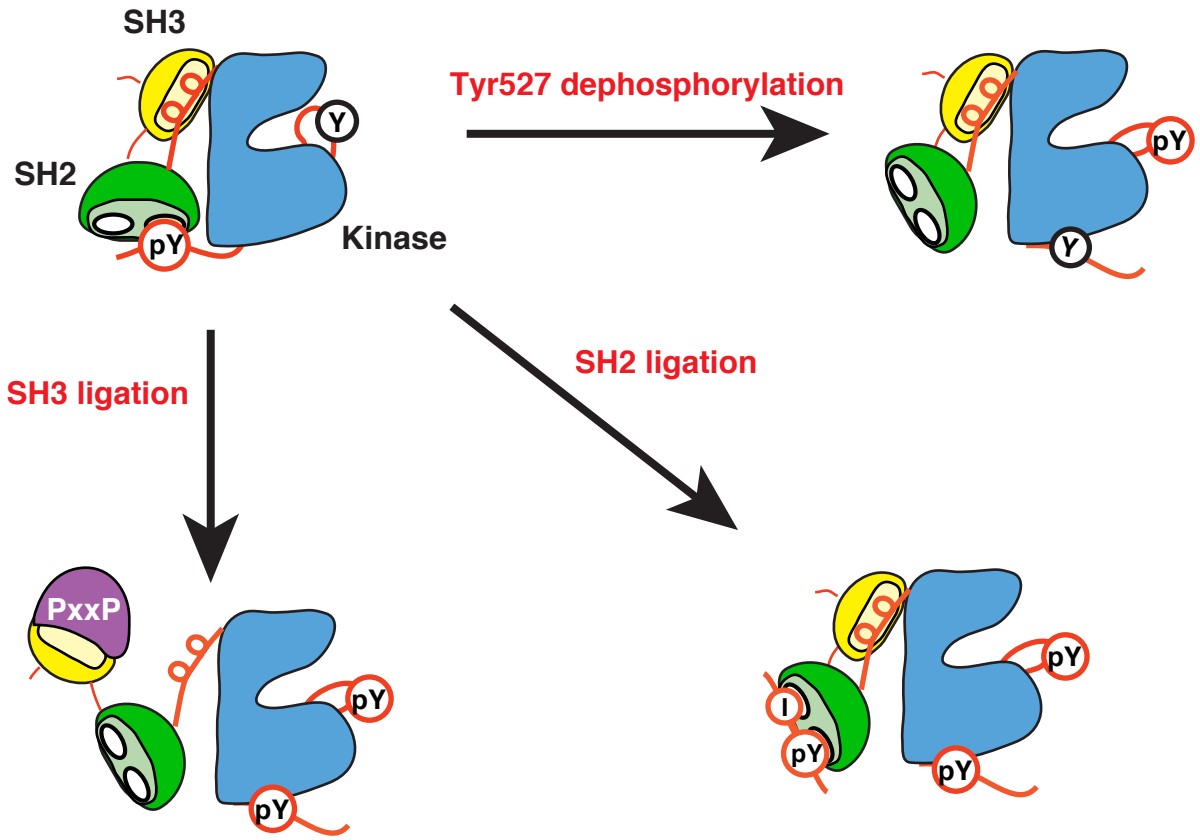
SH3
SH2
Y
pY
Kinase
Tyr527 dephosphorylation
pY
Y
SH3 ligation
SH2 ligation
PxxP
pY
pY
I
pY
pY
pY

Figure 1-3

Figure 1-4: Ack family kinases.

Domain arrangement of the members of the Ack family discussed in this dissertation.

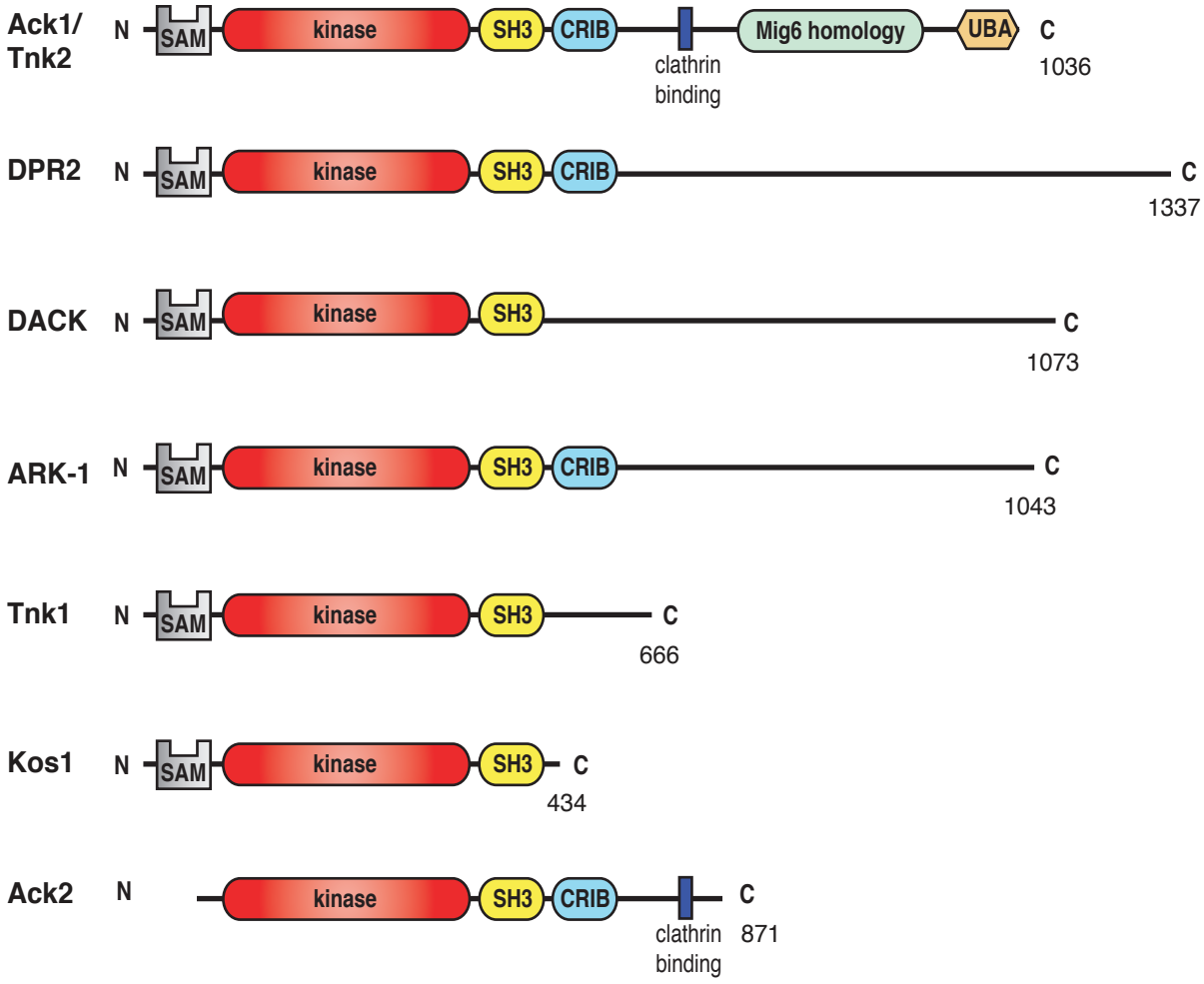
Ack1/
Tnk2
N
SAM
kinase
SH3
CRIB
clathrin
binding
Mig6 homology
UBA
C
1036
DPR2
N
SAM
kinase
SH3
CRIB
C
1337
DACK
N
SAM
kinase
SH3
C
1073
ARK-1
N
SAM
kinase
SH3
CRIB
C
1043
Tnk1
N
SAM
kinase
SH3
C
666
Kos1
N
SAM
kinase
SH3
C
434
Ack2
N
kinase
SH3
CRIB
clathrin
binding
C
871

Figure 1-4

Figure 1-5: Residues important for Ack1 function.

Phosphorylation sites are indicated in black. Tyr284 is the major site of autophosphorylation (*42*). Tyr518, Tyr826, Tyr857 and Tyr858 were identified in proteomic studies (*53-56*). Cancer-associated mutations are in blue (*21*). Point mutations reported to affect Ack1 autophosphorylation are shown in green (*22, 25, 60*). The numbering scheme used corresponds to the accession number Q07912.

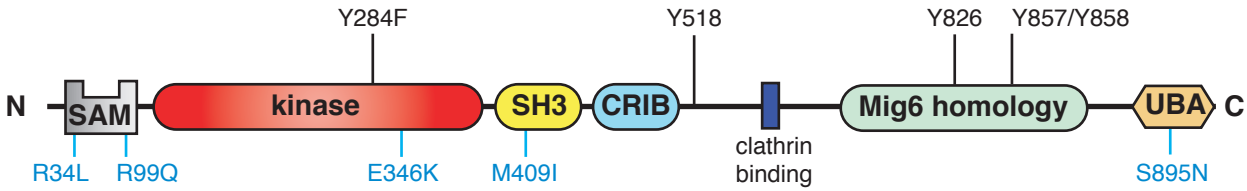
Y284F
Y518
Y826
Y857/Y858
N
SAM
kinase
SH3
CRIB
Mig6 homology
UBA
C
clathrin
binding
R34L
R99Q
E346K
M409I
S895N

Figure 1-5

CHAPTER 2

Materials and methods

Reagents and antibodies

Bovine serum albumin, leupeptin, aprotinin, PMSF, sodium vanadate, sodium fluoride, polybrene, chloroquine, pyruvate kinase/lactate dehydrogenase enzymes from rabbit muscle, and EZview red anti-FLAG M2 affinity gel were obtained from Sigma. EGF was from Sigma or Peprotech Inc. Trypsin-EDTA solution was from Mediatech Inc. Staurosporine was from Cell Signaling technology Inc. Egg PC and DOGS-NTA-Ni were from Avanti Polar lipids, Inc. Primary antibodies were obtained from the following companies: rabbit polyclonal anti-Ack1, rabbit polyclonal anti-pY284 Ack1, rabbit polyclonal anti-N-WASP, rabbit polyclonal anti-phospho-N-WASP (Tyr256), and mouse monoclonal anti-phosphotyrosine clone 4G10 were from Millipore, mouse monoclonal anti-His_6 was from Covance, mouse monoclonal anti-tubulin clone GTU-88 was from Sigma, rat monoclonal anti-HA high affinity clone 3F10 was from Roche, rabbit polyclonal anti-p130 Cas (C-20) was from Santa Cruz Biotechnology. Rabbit polyclonal antibodies anti-Erk1/2, anti-phospho-Erk1/2(Thr202/Thr204), anti PARP, anti-cleaved Caspase-3(Asp175) and anti-phospho-p130 Cas(Tyr249) were from Cell Signaling technology. The primary antibodies used for immunofluorescence were mouse monoclonal anti-HA from Applied Biological Materials, mouse anti-EEA1 from BD Biosciences and rabbit anti-HA tag from Sigma-Aldrich. Horseradish peroxidase linked secondary antibodies (donkey anti-rabbit IgG and sheep anti- mouse IgG horseradish) were from GE Healthcare. Alexa Fluor (AF)-594-transferrin and AF-488- and AF-594-goat anti-mouse and goat anti-rabbit IgG secondary antibodies were from Molecular Probes, Invitrogen.

Cell culture

Mammalian cells were maintained in DMEM (Cellgro, Mediatech, Inc) supplemented with 10% fetal bovine serum (Sigma) and 1000 IU/ml penicillin, 1000 IU/ml streptomycin, 25ng/ml amphotericin B (Cellgro, Mediatech, Inc). The Sf9 insect cells were maintained in Sf-900 medium (Gibco) supplemented with 5% fetal bovine serum and and 1000 IU/ml streptomycin, 25ng/ml amphotericin B (Cellgro, Mediatech, Inc).

Cloning and site-directed mutagenesis

Plasmid pXJ-HA-Ack1, encoding full length Ack1 was a kind gift from Dr. Edward Manser (Institute of Molecular and Cell Biology, Singapore). A plasmid encoding EGFP-clathrin light chain A in pEGFP-C3 (*76*) was the gift of Lois Greene (National Heart, Lung, and Blood Institute, National Institutes of Health, Bethesda, MD).

To produce GFP-tagged Ack1, we subcloned the Ack1 gene into pBMN-I-GFP (Addgene plasmid 1736, developed by Garry Nolan). The Mig6 homology region (Ack1 803-880) was amplified by PCR and cloned into pGEX4T-1 (GE Healthcare) using the restriction sites BamHI and NotI. For baculovirus expression of Ack1 kinase domain, a fragment encoding residues 110 to 385 was cloned into the vector pFastBac HTb (Invitrogen) using the restriction sites BamHI and NotI. Site-directed mutagenesis was performed using the Stratagene Quikchange kit, following the manufacturer's directions.

The plasmid pXJ-HA-Ack1 was modified to produce the different constructs used in this study. The ΔNt construct was generated by PCR amplification of DNA encoding residues 330-1085 using primers that contained the restriction sites BamHI and HindIII. To generate the NKD

construct, a termination signal (TGA) was inserted after codon 385 by site-directed mutagenesis. The KD construct was made by subcloning the region encoding Ack1 kinase domain (residues 110 to 385) into pXJ-HA. To produce FLAG-tagged Ack1, the coding region region for full length Ack1 was subcloned from pXJ-HA into the plasmid p(3X)FLAG CMV 7.1 (Sigma) using the restriction sites BamHI and HindIII.

Cell transfection and Western blotting

Cos7 cells ($1x10^6$ or $3 x10^6$) were plated in 10 cm or 15 cm diameter dishes, respectively. After 24 hours, the cells were transfected using 10-15 μg or 30-60 μg DNA with TransIT reagent (Mirus) at a ratio of 2 μl TransIT per μg of DNA. After 24 hours, the reagent was removed, and the cells were cultured for an additional 24 hours. The cells were harvested, washed twice in PBS, and lysed using RIPA buffer (50 mM Tris-HCl pH 7.4, 150 mM NaCl, 5 mM EDTA, 1% sodium deoxycholate, 1% Nonidet P-40) supplemented with the protease inhibitors leupeptin (10 μg/ml), aprotinin (10 μg/ml), PMSF (200 μM) and the phosphatase inhibitors Na_3VO_4 (0.2 mM) and NaF (10 mM). Lysates (30 μg) were separated by 10% SDS-PAGE, transferred to PVDF membrane, and probed with appropriate antibodies.

For immunofluorescence, the transfection was carried out as follows: Cos7 cells were maintained in Dulbecco's modified Eagle's medium with 10% iron-supplemented calf serum (JRH) and penicillin/streptomycin. Transient transfection of cells seeded on acid-washed glass coverslips was performed using fully-deacylated polyethylenimine (PEI) reagent, prepared from 200 kDa poly(2-ethyl-2-oxazoline) (Sigma-Aldrich) as described (*77*). Transfection mixtures contained 2 μg DNA and 12 μl PEI reagent per 35 mm dish. Cells were examined one day after transfection.

Fluorescence microscopy

These experiments were performed by Azad Gucwa in Deborah Brown's laboratory at the Department of Biochemistry and Cell Biology, Stony Brook University.

Cells grown on glass coverslips were fixed in phosphate-buffered saline (PBS; 150 mM NaCl, 20 mM phosphate buffer, pH 7.4) containing 3% paraformaldehyde for 30 minutes, permeabilized with PBS containing 0.5% Triton X-100 and blocked with PBS containing 3% bovine serum albumin (BSA) and 10 mM glycine for 1 hour. Cells were incubated with primary antibodies for 1 hour and secondary antibodies for 30 minutes, both in PBS with 3% BSA and 10 mM glycine. Where indicated, cells were incubated with AF-594-Tf (35 µg/ml) for 20 minutes at 37°C before fixation. For the images in Chapter 3, the cells were photographed and images were captured using a Zeiss Inverted Axiovert 200 M Microscope with a two-photon laser scanning confocal system and a 100x oil immersion objective. Images were processed with Zeiss LSM software. For the images in Chapter 4, the cells were photographed and images were captured using a Zeiss LSM 510 META NLO laser scanning confocal microscope using a 100x oil immersion objective. For quantification, a region of interest (ROI) was drawn around individual cells, and the histogram macro on the Zeiss LSM software was used to quantify the mean fluorescence intensity of each cell in both red and green channels, and the ratio of anti-pY284 to anti-HA staining in each cell was calculated. Acquisition parameters were the same for all cells, and images shown as well as those used for quantitation were not further processed. 30 cells expressing each construct were analyzed in each of three separate experiments.

IP kinase assay

Cell lysates (2 mg) were incubated overnight at 4°C with 2 µg rat high affinity anti-HA antibody (Roche) and 90 µl of protein G-Agarose beads (Roche). The immunocomplexes were washed with PBS supplemented with 1 mM Na_3VO_4. After the last wash, the beads were resuspended in 300 µl of PBS supplemented with 1 mM Na_3VO_4. Aliquots were withdrawn for gel analysis or for kinase assays, which were performed in duplicate. The kinase activity of immunoprecipitated Ack1 was determined using the phosphocellulose paper assay with a synthetic peptide substrate derived from the WASP phosphorylation site (sequence: KVIYDFIEKKKKG) (*58*). Reaction mixtures contained 20 mM Tris-HCl (pH 7.4), 10 mM $MgCl_2$, 0.4 mM ATP, 1 mM peptide, and [γ^{32}P]-ATP (30-50 cpm/pmol). After 30 min at 30 °C, the reaction was stopped by the addition of 10% TCA and the samples were spotted on p81 phosphocellulose paper. Incorporation of ^{32}P into peptide was determined by scintillation counting. For gel analysis, proteins were separated by SDS-PAGE, transferred to PVDF a membrane and immunoblotted using anti-Ack1 antibodies. The activity was normalized to the total protein immunoprecipitated.

Retrovirus production and infection

The ecotrophic virus stock was produced by transfecting subconfluent Phoenix-Eco packaging cells with Ack1 constructs cloned in pBMN-I-GFP. To transfect a 10 cm diameter plate, 10 µg of plasmid DNA was mixed with 438 µl of H2O, 62 µl 2M $CaCl_2$ and 500 µl of 2X HBS (50 mM HEPES pH 7.5, 10 mM KCl, 12 mM dextrose, 280 mM NaCl, Na_2HPO4 pH 7.05). The DNA mixture was transferred to a plate containing 4 ml of cell culture medium and 25 µM chloroquine. The plates were incubated at 32°C for 48 hours, and the supernatant containing the

retrovirus stock was collected, filtered, aliquoted and stored at -80^{o}C or used to infect cells. NIH-3T3 cells were infected by incubating confluent cells with an inoculum of virus stock in the presence of 4 μg/ml polybrene at 37^{o}C. After 48 hours, cells were visualized using a fluorescence microsocope. The GFP positive cells were selected by preparative cell sorting and the infected cells were then used in the migration, anchored growth and nonanchored growth assays.

Transwell migration assay

Migration assays were performed using 24 well plates with 8.0 μm inserts (Corning). For each cell line (WT or mutant), 200,000 cells were seeded in triplicate or quatruplicate in 200 μl of complete culture medium in the top compartment. The bottom compartment contained 500 μl of complete culture media. The cells were allowed to migrate for 6 hours at 37^{o}C. Afterwards, the inserts and media were removed, and the cells that migrated to the bottom compartment were collected in 100 μl of trypsin-EDTA solution (0.25% Trypsin and 2.21 mM EDTA in HBSS). The cell suspension was combined with 100 μl media containing 10% fetal bovine serum and the cells were counted using a hemocytometer.

Cell growth curves

For the anchored growth curves, 20,000 cells were seeded in duplicate in 12 well plates. Each day, the cell culture medium was aspirated and cells were detached with trypsin for 5-10 min. The cell suspensions were combined with complete culture medium to a final volume of 500 μl or 1 ml. The cells were counted in a hemocytometer.

For the non-anchored growth, 20,000 cells were seeded in duplicate in 24 well ultra low attachment plates (Corning). The plates were incubated at 37^{o}C for 6 days. Cells growing in solution were transferred to a fresh tube, centrifuged, treated with 150 µl of trypsin-EDTA solution for 15-30 min, and counted in a hemocytometer.

Protein expression and purification

The pFastbac HTb vector encoding the Ack1 kinase domain (wild type or E346K) was used to transfect Sf9 cells using the Bac-to-Bac system (Invitrogen). Baculovirus stocks were produced by transfecting Sf9 cells. After 2 rounds of amplification, virus titers on the order of 10^9 pfu/ml were obtained and used to infect 400 ml of Sf9 cells at $2x10^6$ cell/ml with MOI~5. After 48 hours, infected cells were collected and lysed in a French pressure cell in 20 mM Tris-HCl buffer (pH 8.0), containing 5 mM 2-mercaptoethanol, 10 µg/ml leupeptin, 10 µg/ml aprotinin, 1 mM PMSF, and 1 mM Na_3VO_4. Cell lysates were centrifuged at 40,000 g for 30 min, filtered using a 0.8 um filter, and applied to a 4 ml Ni-NTA column (Qiagen). The column was washed with 120 ml of 20 mM Tris-HCl buffer (pH 8.0) containing 2 mM imidazole, 0.5 M NaCl, 10% glycerol, 5 mM 2-mercaptoethanol, 2 mM Na_3VO_4 and further washed with 40 ml of 20 mM Tris-HCl buffer (pH 8.0) containing 1 M NaCl followed by a last wash with 40 ml of 20 mM Tris-HCl buffer (pH 8.0). The His_6-tagged proteins were eluted with 20 mM Tris-HCl buffer (pH 8.0) containing 100 mM imidazole, 5 mM 2-mercaptoethanol and 10% glycerol. The 1 ml fractions containing Ack1 kinase domain were pooled, supplemented with 20% glycerol, aliquoted and stored at -80^{o}C.

The Mig6 homology region (WT or F820A) was expressed as a GST fusion in E.coli BL21 cells. Expression was induced by adding 0.25 mM IPTG for 4 hours at 30^{o}C. The cells

were collected and lysed in a French press cell in lysis buffer containing 50 mM Hepes buffer (pH 7.4), 100 mM NaCl, 100 mM EDTA, 1% Triton X-100, 10 mM DTT, 10% glycerol, 5 μg/ml aprotinin, 5 μg/ml leupeptin, and 1 mM PMSF. The lysates were centrifuged at 11,000 g for 10 minutes and the supernatant was incubated for 2 hours at 4^{o}C with 7 ml of glutathione-agarose beads preequilibated in 50 mM Hepes buffer (pH 7.4) containing 100 mM EDTA. The beads containing the immobilized Mig6 homology region were washed once with 50 ml lysis buffer, three times with 50 ml 50 mM Hepes buffer (pH 7.4) containing 100 mM EDTA, and twice with 50 mM Tris-HCl buffer (pH 8.0).

Binding reactions

Purified WT or mutant Ack1 kinase domain (100 pmol) was incubated for 2 hours at 4^{o}C with immobilized GST-Mig6 homology region (WT or E346K, 160 ng) in a final volume of 500 μl of buffer A (50 mM Hepes pH 7.4, 0.1 M NaCl, 100 mM EDTA, 1% Triton X-100, 10 mM DTT and 10% glycerol). After binding, the beads were washed once with 1 ml of buffer A, once with 1 ml of buffer containing 50 mM Hepes pH 7.4, 1 M NaCl, 100 mM EDTA, 1% Triton X-100, 10 mM DTT and 10% glycerol, and once more with 1 ml of buffer A. Bound proteins were eluted with SDS-PAGE loading buffer and separated by 12% SDS-PAGE. The proteins were then transferred to a PVDF membrane and analyzed by Western blotting with anti-His6 antibodies.

Co-immunoprecipitation studies.

Cos 7 cells were transfected with full length FLAG-Ack1 alone or cotransfected with HA-tagged Ack1 (NKD or KD) and lysed after 48 hours using RIPA buffer, as described for the

Western blotting experiments. Cell lysates (450-750 μg) were incubated overnight at 4°C with 40 μl of FLAG M2 affinity gel. The immunocomplexes were washed 5 times with 1 ml RIPA buffer, eluted from the beads using 35 μl of 2X Laemmli buffer and separated by SDS-PAGE. The proteins were transferred to PVDF membranes and analyzed by immunoblotting using anti-HA antibody and anti-FLAG antibody.

Preparation of small unilamellar vesicles.

The lipids egg PC and DOGS-NTA-Ni were mixed in different molar ratios in glass tubes. The chloroform from 500 μl of the mixture was evaporated under an argon stream to form a thin film, and the lipids were dried under vacuum for at least one hour. The dried lipids were resuspended to create large multilamellar vesicles by the addition of 500 μl of rehydration buffer (20 mM Tris pH 7.4 and 10 mM $MgCl_2$) followed by 4 cycles of freezing, thawing and 30 seconds vigorous vortexing. Small unilamellar vesicles were produced by passing the large multilamellar vesicles through a polycarbonate filter (pore size: 100 nm) 10 times, using a mini-extruder (Avanti Polar lipids, Inc). The vesicles were used for *in vitro* assays on the same day of preparation.

Autophosphorylation in solution and with vesicles.

Purified His_6-Ack1 kinase domain was dephosphorylated by incubating 10 μg of protein with immobilized GST-tagged *Yersinia* phosphatase (Yop) for 30 minutes at room temperature. For the solution autophosphorylation reactions, dephosphorylated Ack1 kinase domain was diluted to final concentrations of 100 nM or 1 μM and incubated with kinase buffer (100 mM Tris-HCl pH 7.4, 10 mM $MgCl_2$, 25 mM vanadate, and 500 μM ATP). As a control, 1 μM Ack1

kinase domain was also incubated in the absence of ATP. The reaction proceeded for 15 minutes at room temperature and was stopped by adding Laemmli buffer and boiling for 5 minutes. Samples (100 ng per lane) were analyzed by SDS-PAGE. The proteins were transferred to PVDF membranes and analyzed by immunoblotting using anti-phosphoAck1 (Y184) and anti-His6 antibodies.

For the autophosphorylation reactions on vesicles, dephosphorylated Ack1 (500 ng) was incubated with kinase buffer in the presence of vesicles containing different mole fractions of DOGS-NTA-Ni (0%, 2% or 5%). The reactions were carried out for 15 minutes at room temperature and were analyzed as described above.

In vitro kinase assay in solution and with vesicles

The catalytic activity of the purified Ack1 kinase domain towards a peptide substrate was measured using a continuous spectrophotometric assay (*78, 79*). Reactions were performed at 30^{o}C in a final volume of 50 μl. The substrate used was a peptide containing the tyrosine phosphorylation site in the protein WASP that is phosphorylated by Ack1 (*69*). The reactions contained 100 mM Tris pH 7.4, 10 mM $MgCl_2$, 2 mM ATP, 1.5 mM phosphoenolpyruvate (PEP), 90 units/ml pyruvate kinase, 109 units/ml lactate dehydrogenase, and 1.2 mg/ml NADH. For determination of kinetic constants, the peptide substrate concentration was varied from 5 μM to 5 mM. The kinetic constants were derived from the non-linear fitting using the Michaelis-Menten equation using the program MacCurveFit. For the experiments with vesicles, the enzyme concentration was kept in the range from 250 to 500 nM and the peptide concentration was 625 μM.

CHAPTER 3

Cancer-associated mutations activate Ack1

The contents of this chapter have been published in

Journal of Biological Chemistry April 2, 2010, vol. 285, pages 10605-10615.

Abstract

Ack1 participates in tumorigenesis, cell survival and migration. Relatively little is known about mechanisms that regulate Ack1 activity. Recently, four somatic missense mutations of Ack1 were identified in cancer tissue samples, but the effects on Ack1 activity and function have not been described. These mutations occur in the N-terminal region, the C-lobe of the kinase domain, and the SH3 domain. Here, we show that the cancer-associated mutations increase Ack1 autophosphorylation in mammalian cells without affecting localization, and increase Ack1 activity in immune complex kinase assays. The cancer-associated mutations potentiate the ability of Ack1 to promote proliferation and migration, suggesting that point mutation is a mechanism for Ack1 deregulation. We propose that the C-terminal Mig6 homology region (MHR) (residues 802 to 990) participates in inhibitory intramolecular interactions. The isolated kinase domain of Ack1 interacts directly with the MHR, and the cancer-associated E346K mutation prevents binding. Likewise, mutation of a key hydrophobic residue in the MHR (F820) prevents the MHR-kinase interaction, activates Ack1, and increases cell migration. Thus, the cancer-associated mutation E346K appears to destabilize an autoinhibited conformation of Ack1, leading to constitutively high Ack1 activity.

Introduction

Recent data implicate Ack1 in different stages of cancer. Amplification of the Ack1 gene correlates with metastasis and poor prognosis in lung and prostate cancer, and overexpression increases invasiveness (*24*). In v-Ras-transformed mammalian cells, Ack1 is required for the maintenance of the transformed phenotype (*23*). Ack1 contributes to prostate tumorigenesis by phosphorylating the tumor suppressor protein Wwox, leading to its degradation (*22*), and by phosphorylating androgen receptor (*64*).

The activities of other NRTKs are controlled through intramolecular interactions, and by conformational changes in the kinase activation loops (*80*). In Src family kinases, the inactive conformation is stabilized by an interaction between the SH3 domain and a polyproline type II helix, and an interaction between the SH2 domain and the C-terminal phosphotyrosine (*9, 10*). Activating signals (such as SH3 or SH2 ligands) disrupt these interactions and promote the phosphorylation of Y416 in the activation loop of Src (*11, 81-83*). In c-Abl, the SH2 and SH3 domains also participate in autoinhibitory interactions. These interactions are stabilized by an N-terminal cap region, and by an interaction between the N-terminal myristoyl group and the base of the kinase catalytic domain (*84*). Based on the unique domain organization of Ack1, its regulatory mechanisms are likely to differ from those of Src and Abl.

Using purified Ack1, we previously showed that the major autophosphorylation site is Y284 in the activation loop (*42*). The crystal structure of the isolated kinase domain of Ack1 has been solved in both the phosphorylated (p-Y284) and unphosphorylated forms (*52*). In both of these structures, the conformation of the activation loop resembles the conformation seen in other active kinases. Phosphorylation of Y284 in Ack1 stimulates kinase activity (*42*), but not as

strongly as in Src or Abl NRTKs. Thus, the regulatory importance of Ack1 autophosphorylation appears to be intermediate between Src/Abl (strongly phosphorylation-dependent) (*52*), and kinases such as EGFR or Cdks (in which formation of the activated state is phosphorylation-independent) (*5, 6, 85*). Ligands for the SH3 or the CRIB domains of Ack1 do not activate the purified enzyme (*42*); thus, the regulatory mechanism for Ack1 is poorly understood at present.

Recently, the genes encoding 518 protein kinases were sequenced in a large collection of human cancers to identify somatic mutations (*21*). Four missense mutations were identified in Ack1: two mutations in the N-terminus (R34L and R99Q) were identified in lung adenocarcinoma and ovarian carcinoma, respectively, a mutation in the kinase catalytic domain (E346K) was identified in ovarian endometroid carcinoma, and a mutation in the SH3 domain (M409I) was found in gastric adenocarcinoma (Fig. 1-5). The probability of each mutation being a "driver" (i.e., a mutation that confers an advantage to the cancer cell, and that is therefore subject to positive selection pressure) was estimated by comparing the rate of non-synonymous and synonymous somatic mutations in each gene. The genes were ranked according to their probability of carrying at least one driver mutation, and Ack1 ranked in the top 5%. The effects of these mutations on Ack1 activity and downstream signaling are unknown.

The aims of this study were: (1) to test the effects of the cancer-associated mutations on Ack1 function and activity; and (2) to use the mutations to gain insight into the regulation of Ack1. We report that cancer-associated mutations stimulate Ack1 activity without affecting its subcellular localization, suggesting that point mutations represent a new mechanism for the oncogenic activation of Ack1. Moreover, we propose that an autoinhibitory interaction exists between the kinase domain and the C-terminal Mig6 homology region, and that mutations that disrupt this interaction (such as the cancer-associated mutation E346K) activate Ack1.

Results

Cancer–associated mutations activate Ack1

To evaluate the effect of the cancer-associated mutations on Ack1 activity in cells, we introduced the point mutations into full-length Ack1 by site-directed mutagenesis. We expressed wild-type and mutant forms of Ack1 in Cos7 cells, and analyzed their activities in whole cell lysates by probing for autophosphorylation of Y284. As a negative control, we also analyzed kinase-dead Ack1 (K158R). The level of Ack1 autophosphorylation was increased by all the cancer-associated mutations. The N-terminal mutations R34L and R99Q increased Ack1 autophosphorylation by 3- and 4-fold, respectively. The mutation in the C-lobe of the kinase domain (E346K) produced a 6-fold increase, and the mutation located in the SH3 domain (M409I) produced a 3-fold increase in the level of Ack1 autophosphorylation (Fig. 3-1B). To measure kinase activity towards an exogenous substrate, we immunoprecipitated the Ack1 proteins and incubated them with a synthetic peptide substrate in an *in vitro* assay (Fig. 3-1C). The peptide used was derived from the Ack1 phosphorylation site of WASP; this is the best *in vitro* peptide substrate reported to date (*58*). EGF treatment increased Ack1 activity towards the Tyr-containing peptide, confirming earlier observations on EGF activation of Ack1 (*25*). The activity of Ack1 was also increased by all the cancer-associated mutations. The degree of activation ranged from 4.2-fold for E346K to 9.6-fold for M409I. The kinase dead Ack1 (K158R) was not autophosphorylated in cells and was inactive in the IP-Kinase experiment, which underscores the role of autophosphorylation in Ack1 activation.

Cell localization studies

One potential explanation for the increased activity of the cancer-associated mutant forms of Ack1 would be a change in subcellular localization. To test this possibility, we examined the localization of wild type and mutant Ack1 proteins in Cos7 cells by fluorescence microscopy. These studies were performed by Azad Gucwa at Dr. Deborah Brown's laboratory. The Ack1 proteins all had similar distribution patterns: all were localized to small discrete puncta and larger amorphous perinuclear structures (Fig. 3-2). As reported earlier for wild-type HA-Ack1 (*26, 27, 46*), all the Ack1 proteins showed partial colocalization with EEA1 on early endosomes (Fig. 3-2). Also as reported earlier for the wild-type protein (ref. 24), Ack1 and all the mutants were also present on larger amorphous perinuclear structures. These did not stain for EEA1, but often appeared to surround and embed EEA1-positive endosomes (Fig. 3-2). These structures are probably the same as large reticular complexes and endosome-associated tubules seen in Ack1-overexpressing cells by electron microscopy (*46*), and may be endosome-derived tubules. Furthermore, all the Ack1 proteins caused a dramatic accumulation of clathrin (visualized using co-expressed GFP-clathrin light chain A) on the amorphous structures (Fig. 3-3) and inhibited transferrin internalization (Fig. 3-4), as reported earlier for wild type Ack1 (*26*). These results suggested that Ack1 over-expression induced the accumulation of endosome-associated tubular structures that sequestered clathrin, inhibiting transferrin internalization by reducing the amount of clathrin available for coated pit formation at the plasma membrane. All the cancer-associated mutants showed the same behavior as wild-type Ack1, suggesting that activation of the mutants did not stem from differences in cellular localization.

Effects of the cancer-associated mutations on cell growth and migration

Next, we analyzed the growth properties of NIH3T3 cells overexpressing wild type Ack1 or the cancer-associated mutants. In order to obtain homogeneous populations of Ack1-expressing cells, we generated retroviruses encoding GFP along with the various forms of Ack1. GFP fluorescence was used to monitor the infection, and GFP-positive cells were selected by preparative FACS. The adherent cells were grown on a normal cell culture surface to measure anchored growth, as well as on ultra low attachment plates to measure nonanchored growth (Fig. 3-5A). We confirmed the expression and autophosphorylation of Ack1 in these cell lines (Fig. 3-5B). As in the transiently-transfected cells, autophosphorylation of the cancer-associated mutant forms of Ack1 was higher than wild-type.

Figure 3-6A shows the anchored growth curves of the cells. Compared to cells infected with control virus (EV), cells expressing wild-type or mutant forms of Ack1 were able to grow to higher saturation densities before significant cell death was observed (~300,000 cells/well for EV compared to ~700,000 cells/well for Ack1), suggesting a partial loss of contact inhibition. Cells expressing the kinase dead version of Ack1 (K158R) exhibited similar growth properties as cells expressing WT Ack1, indicating that the effect of Ack1 on anchored cell growth is independent of kinase activity.

The ability of cells to grow in suspension is a hallmark of cell transformation. We studied the growth of the infected cells in conditions that prevent their attachment to any surface (Fig. 3-6B). The initial number of cells seeded in each well was 20,000. After 6 days in culture, the cells infected with control virus exhibited significant cell death; their number was reduced by 50%. Cells expressing wild type Ack1 survived, although without multiplying. The cells expressing the cancer-associated mutations R34L, R99Q or M409I did not differ significantly from the cells

expressing WT Ack1 (Fig 6B). However, the cells expressing E346K Ack1 were able to multiply, and the population nearly doubled in the period of time they were in culture (Fig. 3-6B). Thus, the mutation E346K increased the ability of Ack1 to override anchorage dependence.

We examined the cells for signs of apoptotic cell death at different stages of growth, corresponding to early exponential phase (2 days) and late stationary/death phase (8 days). After 2 days in culture, there was no apparent apoptosis, as judged by cleavage of caspase 3 and poly (ADP-ribose) polymerase (Fig. 3-7). On the other hand, after 8 days in culture, cells expressing vector alone showed significant apoptosis, while cells expressing Ack1 (wild-type or mutants) had reduced levels (Fig. 3-7). These results are consistent with the growth curves shown above in Fig. 3-6.

Overexpression of Ack1 in cancer cell lines increases the invasiveness of the cells *in vitro* and *in vivo* (*24*). We studied the migration properties of the Ack1-expressing cells in a transwell migration assay (Fig. 3-8). Consistent with previous findings, the expression of WT Ack1 increased cell migration as compared with the cells infected with control virus. The cancer-associated mutations produced a range of effects. R34L and M409I produced the largest increase over WT, followed by E346K. The migration of cells infected with the kinase dead Ack1 (K158R) was similar to control cells, indicating that most of the observed effect is due to the kinase activity. Thus, the dependence on kinase activity differed in the three different assays. The effect of Ack1 on anchored cell growth did not depend on kinase activity (Fig. 3-6A), and as a consequence, the cancer-associated mutants behaved similarly to WT. In the nonanchored growth experiments (Fig. 3-6B), the kinase-dead form of Ack1 promoted growth as efficiently as wild-type, but the E346K mutation gave additional stimulation. Finally, cell motility did depend on Ack1 kinase activity (Fig. 3-8), and the cancer-associated mutants with

higher *in vitro* activity also enhanced the migration rate in intact cells. These functional data on the cancer-associated mutations show that increased Ack1 kinase activity has the potential to be manifested in anchorage independence and increased motility in cancer cells.

Although relatively few downstream partners of Ack1 have been identified, we carried out experiments to identify potential alterations in signaling in cells expressing the cancer-associated mutants. Wiskott-Aldrich syndrome protein (WASP) is a Cdc42 effector that plays an important role in the formation of new actin filaments. Phosphorylation of WASP at Y256 and S242 by Ack1 stimulates actin polymerization (*69*). We examined WASP Y256 phosphorylation in NIH3T3 cells using a phosphospecific antibody (Fig. 3-9A). Phosphorylation of WASP was increased in cells expressing the R99Q, E346K, and M409I mutants relative to wild-type Ack1, consistent with the observed enhanced migration (although R34L did not show enhanced WASP phosphorylation). The Crk-associated substrate (Cas) has also been shown to be a substrate of Ack1 (*24*). In NIH3T3 cells we observed elevated Cas phosphorylation by the E346K mutant and (to a lesser extent) the M409I mutant of Ack1 (Fig. 3-9B). There was a small increase in Erk phosphorylation by several of the mutants relative to wild-type Ack1 in NIH3T3 cells (Fig. 3-10). A more detailed mechanistic understanding of the growth- and migration-promoting effects of the Ack1 mutants will be possible when additional downstream signaling pathways of Ack1 have been identified.

A mechanism for intramolecular regulation of Ack1

Next, we focused on the mechanism of Ack1 activation by the cancer-associated mutation E346K. This mutation lies in the large C-terminal lobe of the kinase catalytic domain. Sequence comparisons indicate that the kinase domain of Ack1 is very similar to the kinase

domain of the epidermal growth factor receptor (EGFR) (*86*). Activation of EGFR is achieved by formation of an asymmetric dimer in which one of the kinases acts as an activator of the other (*87*). Mig6 is a feedback inhibitor of EGFR, and the inhibition is by binding to the kinase domain of EGFR and inhibit its activity (*88*). Structural studies showed that Mig6 inhibits EGFR by blocking the formation of the activating dimer (*28*). The C-terminal region of Ack1 shows high sequence homology with Mig6 (Fig. 3-11A), and this region was found to bind to EGFR (*27*). Furthermore, the Mig6-binding region is conserved in sequence and structure in Ack1. Thus, we hypothesize that an intramolecular interaction exists in Ack1 between the kinase domain and Mig6 homology region, analogous to the Mig6/EGFR interaction. Using the structure of EGFR bound to Mig6, Zhang et. al. superimposed the solved structure of Ack1 kinase domain on the EGFR kinase domain, and created a model of the Ack1-Mig6 interaction. (Fig. 3-11B) (*28*). In the model, the side chain of E346 is oriented towards the interface with the Mig6 peptide. Thus, mutations at this position could potentially destabilize the inhibited conformation.

Mutations designed to disrupt the intramolecular interaction activate Ack1

In order to test this hypothesis, we introduced point mutations into Ack1 at positions analogous to sites that are important in the Mig6/EGFR interaction (*28*): L120 and L197 are located in the N-lobe of the Ack1 kinase domain, V365 is in the C-lobe of the kinase domain, and F820 and Y826 are located in the Mig6 homology region (Fig. 3-12A). For comparison, we included a mutation in Y284, the major autophosphorylation site. The V365R and F820A mutations produced large increases in Ack1 autophosphorylation when they were expressed in cells (Fig. 3-12B). The Y826A produced a smaller but significant increase, while the L120 and L197 mutations had no effect. When the V365R and F820A mutants were tested in a peptide

phosphorylation assay they also showed increased kinase activity (Fig. 3-12C). This activation appeared to be stronger than the activation caused by the N-terminal mutations (R34L and R99Q), as the increases for V365R and F820A surpassed the activation produced by EGF stimulation (compare Fig. 3-1C and Fig. 3-12C).

As shown above, the cancer-associated mutations potentiated the effects of Ack1 to promote migration, proliferation, and anchorage independent growth. We expected that if the Mig6 homology region-kinase domain interaction were functionally significant, then the introduction of an activating mutation should recapitulate the effects of the naturally occurring mutations. We selected F820A, because the analogous Phe makes a key contact in the Mig6-EGFR structure (*28*), and because of the strong activation of Ack1 by this mutation (Fig. 3-12). Indeed, the F820A mutation produced an increase in both cell migration (Fig. 3-13A) and non anchored growth (Fig. 3-13B) as compared with the effect caused by wild type Ack1.

Direct binding between Ack1 kinase domain and Mig6 homology region

To test for a direct interaction between the kinase domain and Mig6 homology region, we introduced the isolated Ack1 kinase domain into a recombinant baculovirus, expressed the protein in insect cells, and purified it to homogeneity. We expressed the Mig6 homology region (Ack1 residues 803-880) in bacteria as a GST fusion protein and purified it. The immobilized Mig6 homology region was able to bind to the purified kinase domain, and the introduction of the F820A mutation into the GST-Mig6 homology region prevented this binding (Fig. 3-14A). We also produced the E346K mutant form of the kinase domain in insect cells, containing the cancer-associated mutation in the C-lobe. Binding of E346K to immobilized Mig6 homology region was reduced as compared to the binding to the wild type kinase domain (Fig. 3-14B).

To test whether the E346K mutation increases the intrinsic catalytic activity of Ack1, we carried out kinetic experiments on the isolated catalytic domains, using varying concentrations of the WASP peptide substrate. The *in vitro* activity of purified E346K Ack1 kinase domain (k_{cat}/k_M~20 $min^{-1}\mu M^{-1}$) was somewhat lower than the activity measured for WT Ack1 (k_{cat}/k_M~70 $min^{-1}\mu M^{-1}$), demonstrating that the mutation itself does not increase the kinase activity. These *in vitro* data indicate that there is a direct association between the two regions of Ack1, and that mutations in the Mig6 homology region (F820A) or the kinase domain (E346K) interfere with binding. Collectively, our data suggest a model in which this interaction is autoinhibitory (Fig 3-14C); the E346K mutation would activate Ack1 by destabilizing this conformation.

Discussion

Ack1 has previously been implicated in tumorigenesis (*22, 64*), cell survival (*23*), and metastasis (*24*). The Ack1 gene is amplified and overexpressed in a number of tumors, and the copy number change correlates with later-stage, more aggressive tumors (*24*). Prior to this study, it was not clear whether mutations represent an additional mechanism for the oncogenic activation of Ack1. The four non-synonymous mutations in Ack1 studied in this paper were identified in a study in which 210 cancer tissue samples were screened for somatic mutations in protein kinase genes (*21*). Using this approach, Ack1 emerged as a likely candidate to carry driver mutations. We show here that point mutations activate Ack1, and that cells expressing the cancer-associated mutants exhibit aspects of the transformed phenotype. Mutations located in the N-terminus (R34L and R99Q), in the C-lobe of the kinase domain (E346K), and in the SH3 domain (M409I) activated Ack1 in functional and biochemical assays. Our data reinforce the previous characterization of Ack1 as an oncogene, and suggest that the somatic mutations may contribute to cancer development.

Consistent with published data (*24*), we found that the overexpression of wild type Ack1 promotes the transformed phenotype. Cells overexpressing WT Ack1 showed higher levels of migration than control cells (Fig. 3-8). The expression of WT Ack1 also caused loss of contact inhibition in cells growing attached to a surface, and allowed the cells to survive in non-anchored conditions (Figs. 3-6A,B). Our studies were carried out in NIH3T3 cells, and they are similar to results obtained in human mammary epithelial cells and in 4T1 mouse mammary tumor cells, suggesting that Ack1 promotes cell growth and migration independently of cell context.

The two cancer-associated mutations located in the N-terminus of Ack1 increased the level of Ack1 autophosphorylation in cells (Fig. 3-1B). This was due to enhanced Ack1 kinase

activity, since the mutants also phosphorylated a synthetic peptide at a higher rate (Fig. 3-1C). Neither of the N-terminal mutations displayed any significant enhancement of anchored or non-anchored growth over the level observed with WT Ack1. On the other hand, the R34L mutation did increase the effect of Ack1 on cell migration. The N-terminus of Ack1 contains a region that was identified as a SAM domain (Sterile Alpha Motif) and as a membrane localization motif (*25*). The observed activation of Ack1 by these mutations could potentially have been explained by mislocalization of Ack1 due to the disruption of the membrane localization domain. However, the intracellular localization of Ack1 was not affected by the cancer-associated mutations located in the N-terminus (Fig. 3-2). Thus, our data indicate that the R34L and R99Q mutations increase Ack1 autophosphorylation and activity. While the precise mechanism is not clear, one possibility is that the N-terminal mutations disrupt an inhibitory interaction that could either be intramolecular or intermolecular (in the latter case, involving other molecules or the formation of an Ack1 homodimer). SAM domains are characteristically rich in alpha helices and have been found in more than 1000 proteins, including the Eph family of tyrosine kinase receptors (*89, 90*), diacylglycerol kinase delta (DGKδ) (*91*) and the transcriptional repressor TEL (*92, 93*). The three-dimensional structures of several SAM domains have been solved, and they form dimeric and polymeric associations. Although the biological roles of these interactions are not yet clear for all the SAM-containing proteins, DGKδ was reported to be regulated by SAM mediated polymerization (*91*). Furthermore, the deletion of the N-terminus portion of Ack1 reduces the ability of full length Ack1 to undergo autophosphorylation (*25*). We speculate that the N-terminal SAM domain may be involved in protein-protein interactions that play a role in Ack1 regulation, and that cancer-associated mutations in this region disrupt the normal regulation

mechanism, rendering the enzyme more active. Our studies in Chapter 4 focused on the role of the N-terminal region in Ack1 regulation.

The cancer-associated mutation M409I, located in the SH3 domain of Ack1, activated cellular autophosphorylation of Ack1 and promoted increased cell migration as compared to WT Ack1. On the other hand, the effect of this mutation on cell proliferation did not significantly differ from the effect of WT Ack1. The reason for this discrepancy is not clear; however, the functional assays that we used measure different biological processes. Ack1 may activate several downstream effectors and pathways through its different domains. Therefore, it is possible that the SH3 domain is involved in the regulation of motility-related, rather than cell proliferation pathways. The methionine residue mutated in Ack1 is not conserved in other closely related SH3 domains, and it is not predicted to lie in the binding site for polyproline-containing ligands. Thus, the molecular basis for Ack1 activation by M409I remains unclear.

The cancer-associated mutation E346K is located in the C-lobe of the kinase domain. We found that the expression of E346K Ack1 potentiated the effects of the expression of WT Ack1 on migration and non-anchored growth. Thus, our functional data suggested that the C-terminal portion of Ack1 plays a role in its regulation. Next, we focused on the study of this region to gain insight into a regulatory mechanism that involves the kinase domain and the C-terminal Mig6 homology region.

Relatively little information was previously available concerning Ack1 regulation. Ack1 autophosphorylation produced modest activation in a construct containing the N-terminus, the catalytic domain, the SH3 domain and the CRIB domain of Ack1 (*42*). Also, the addition of Cdc42 (ligand for CRIB domain) or poly-proline peptides (ligands for SH3 domain) did not activate this purified construct *in vitro*. However, in cells expressing full length Ack1, the co-

expression of Cdc42 did activate Ack1 (*42*). The introduction of point mutations into the CRIB domain and SH3 domain in full length Ack1 expressed in cells also produced increased autophosphorylation, suggesting that the different domains of Ack1 participate in regulatory interactions (*25*).

The structure of the kinase domain of EGFR in a complex with the inhibitor protein Mig6 (*28*), suggested that the C-lobe of the kinase domain could be important for an intramolecular interaction with the Mig6 homology region located in the C-terminus of Ack1 (Fig. 3-11B). Based on previous studies on EGFR, we introduced point mutations designed to disrupt this putative interaction. We found that point mutations located either in the C-lobe of the kinase domain (V365R) or in the Mig6 homology region (F820A) resulted in the activation of full length Ack1 (Figs. 3-12B and 3-12C). Although the mutation F820A is not a naturally occurring mutation, it was able to recapitulate the functional effects that we observed for the cancer-associated mutations. Likewise, it produced a 50% increase in cell migration and non-anchored growth (Figs. 3-13A and 3-13B). The ability of F820A mutation to produce a large (~80-fold) increase in kinase activity suggests that previous work on Ack1, which was carried out with a construct lacking the MHR, underestimated the dynamic range of kinase activation.

In order to further test the interaction predicted by the model and suggested by the cell transfection experiments, we conducted binding experiments using purified GST-tagged Mig6 Homology region (MHR) and purified His_6-tagged Ack1 kinase domain. The purified kinase domain binds to the purified WT MHR (Figs. 3-14A, 3-14B). This interaction is prevented by the F820A mutation in the MHR (Fig. 3-14A) and by the E346K mutation in the kinase domain (Fig. 3-14B). The interaction between these two minimal segments provides additional evidence for a direct interaction between the kinase domain and the MHR in the context of full-length Ack1.

Based on the data presented in this paper, we propose a model for Ack1 regulation in which the MHR interacts with C-lobe of the kinase domain to stabilize a down-regulated structure (Fig. 3-14C). The Mig6 region might interact directly with the Ack1 active site as pictured in Fig. 3-14C, or alternatively act indirectly to position an inhibitory segment in the active site. In preliminary *in vitro* experiments, the GST-MHR did not inhibit the purified Ack1 kinase domain (V.P.E. and W.T.M., unpublished observations), suggesting that additional regions of Ack1 are needed for direct or indirect autoinhibition.

The C-terminal region of Ack1 is also involved in interactions with EGFR and other upstream and downstream signaling molecules. Thus, as observed for other NRTKs such as Src (*94*), Abl (*95*) and FAK (*96*), enzymatic activation of Ack1 can be coupled to interactions between the noncatalytic domains and allosteric regulators, effectors, and potential substrates.

Figure 3-1. Cancer-associated mutations activate Ack1 in cells and in vitro.

A, Domain architecture of Ack1. The positions of the cancer-associated mutations are indicated. **B**, Western blot analysis. Lysates from Cos 7 cells expressing wild type or mutant forms of Ack1 were probed with anti-phospho Ack1(pY284), anti-Ack1, and anti- tubulin antibodies, as indicated. Densitometry readings were used to calculate the ratios of phosphorylated to total Ack1. **C**, Immunoprecipitation-kinase assay. Cos 7 cells expressing Ack1 were stimulated with EGF (50 ng/ml for 5 minutes) or left untreated. Ack1 was immunoprecipitated from these cells, or from cells expressing Ack1 mutants, with anti-HA antibodies. The immunoprecipitated proteins were used in duplicate *in vitro* kinase reactions with ^{32}P-ATP and the WASP synthetic peptide. Activities were measured in duplicate with the phosphocellulose paper assay, and were normalized to 1.0 for WT Ack1. The error bars show standard deviations.

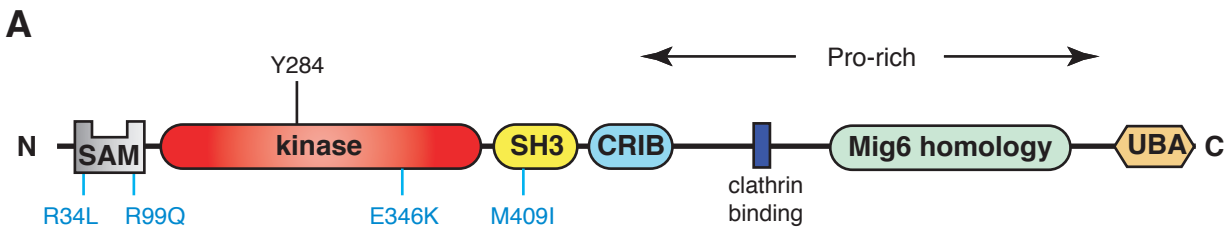
A
Y284
Pro-rich
N
SAM
kinase
SH3
CRIB
Mig6 homology
UBA
C
clathrin
binding
R34L
R99Q
E346K
M409I

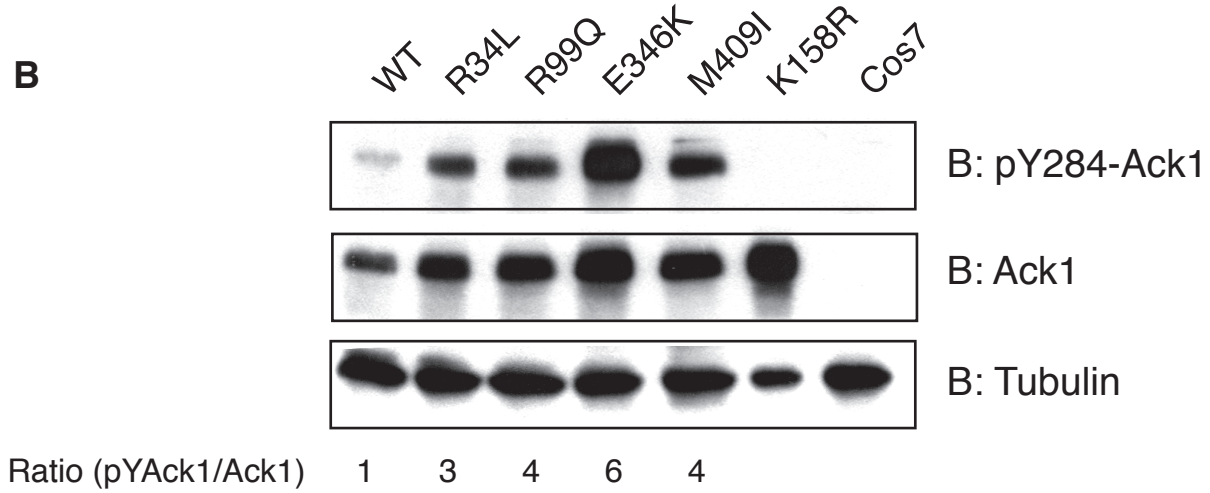
B
WT
R34L
R99Q
E346K
M409I
K158R
Cos7
B: pY284-Ack1
B: Ack1
B: Tubulin
Ratio (pYAck1/Ack1) 1 3 4 6 4

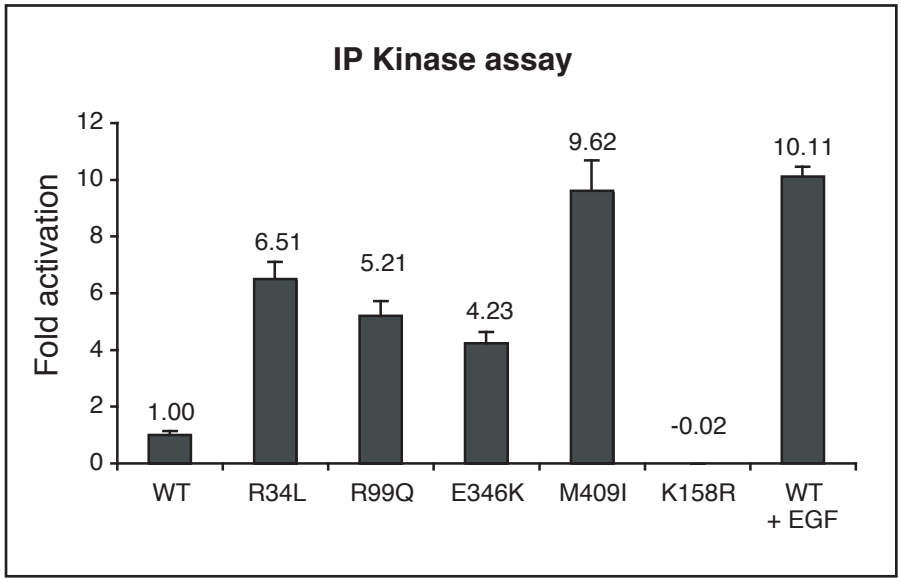
C
IP Kinase assay
Fold activation
12
10
8
6
4
2
0
1.00
6.51
5.21
4.23
9.62
-0.02
10.11
WT
R34L
R99Q
E346K
M409I
K158R
WT
+ EGF

Figure 3-1

Figure 3-2. Subcellular localization of Ack1.

Cos7 cells expressing wild-type HA-tagged Ack1 (**A**) or the indicated mutant (**B-E**) were prepared for immunostaining and confocal microscopy as described in Materials and Methods, detecting Ack1 proteins with anti-HA antibodies (left panels; green) and endogenous EEA1 (red) as indicated. Merged images are shown to the right of the EEA1 panels. Enlarged views of the boxed regions in the merged images are shown to the right of the merged images. All Ack1 proteins partially co-localized with EEA1, but were also seen in larger, amorphous structures that often surrounded punctate endosomes. Scale bar: 10 μm. Microscopy was performed by Azad Gucwa in Deborah Brown's laboratory.

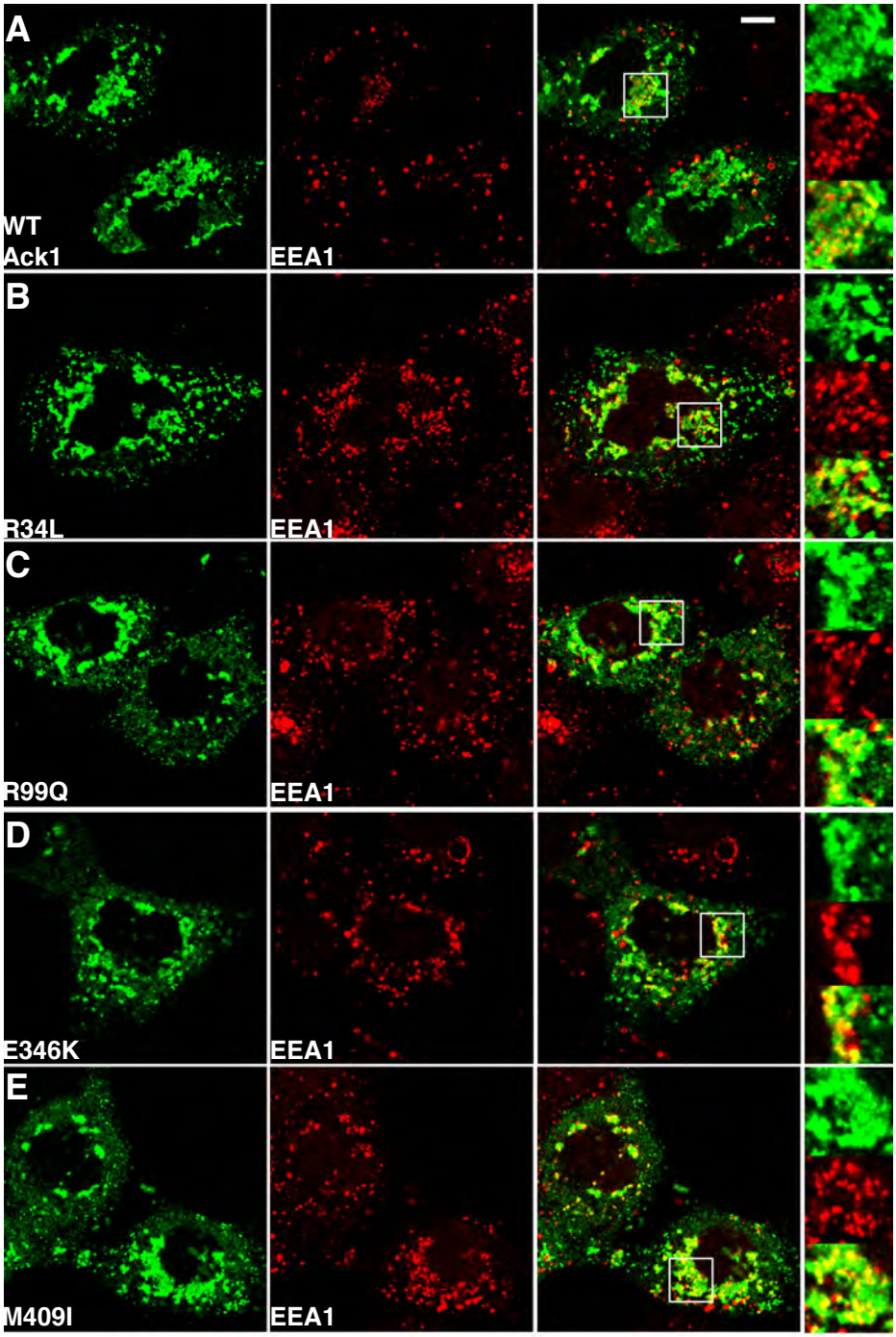

Figure 3-2

Figure 3-3. Wild-type Ack1 and cancer-associated mutants colocalize with clathrin and alter its localization.

Cos7 cells transfected with GFP-clathrin light chain A together with wild-type ACK1 (A) or the indicated Ack1 mutant (B) were prepared for immunostaining and confocal microscopy. Ack1 proteins (left-hand panels; red) were detected with anti-HA antibodies. GFP-clathrin light chain A (CLC) fluorescence is shown in green. Merged images are shown to the right of the CLC panels. Enlarged views of the boxed regions in the merged images are shown to the right of the merged images. Asterisks; cells expressing GFP-clathrin light chain A only, showing the normal clathrin localization pattern. All Ack1 constructs induced redistribution of clathrin to the amorphous structures that also contained the Ack1 proteins. Scale bar; 10 μm. Microscopy was performed by Azad Gucwa in Deborah Brown's laboratory.

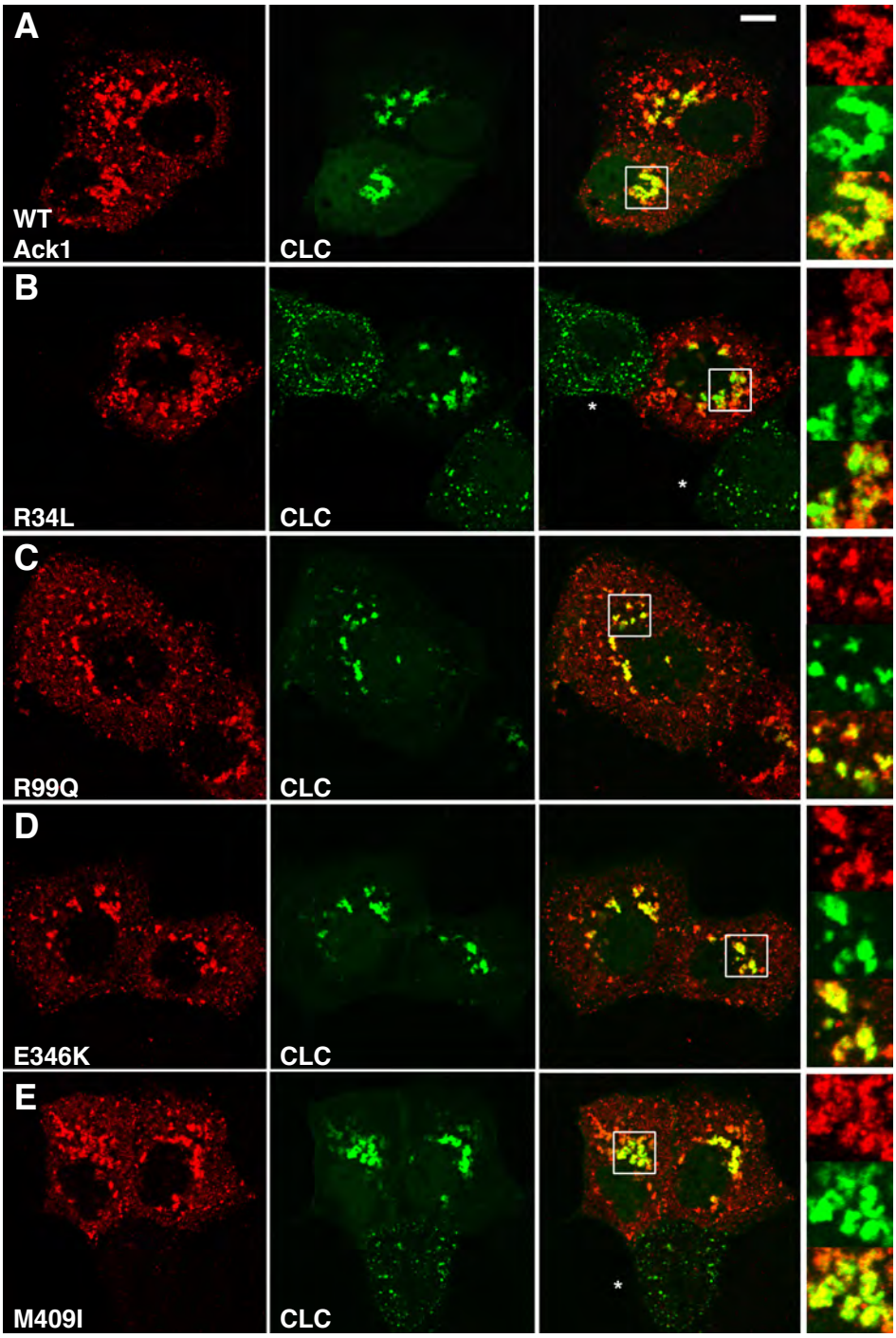

Figure 3-3

Figure 3-4. Wild-type ACK1 and cancer-associated mutants inhibit transferrin uptake.

AF-594-Transferrin (35 μg/ml) was added to Cos7 cells expressing wild-type HA-Ack1 (**A**) or the indicated Ack1 mutant (**B-E**) for 20 minutes at 37°C before fixation and processing for immunostaining and confocal microscopy. Ack1 proteins (left-hand panels; green) were detected with anti-HA antibodies. AF-594-transferrin (Tfn) fluorescence is shown in the center panels, and merged images in the right-hand panels. Transferrin internalization was blocked in cells expressing any of the Ack1 constructs, but occurred normally in neighboring untransfected cells. Scale bar; 10 μm. Microscopy was performed by Azad Gucwa in Deborah Brown's laboratory.

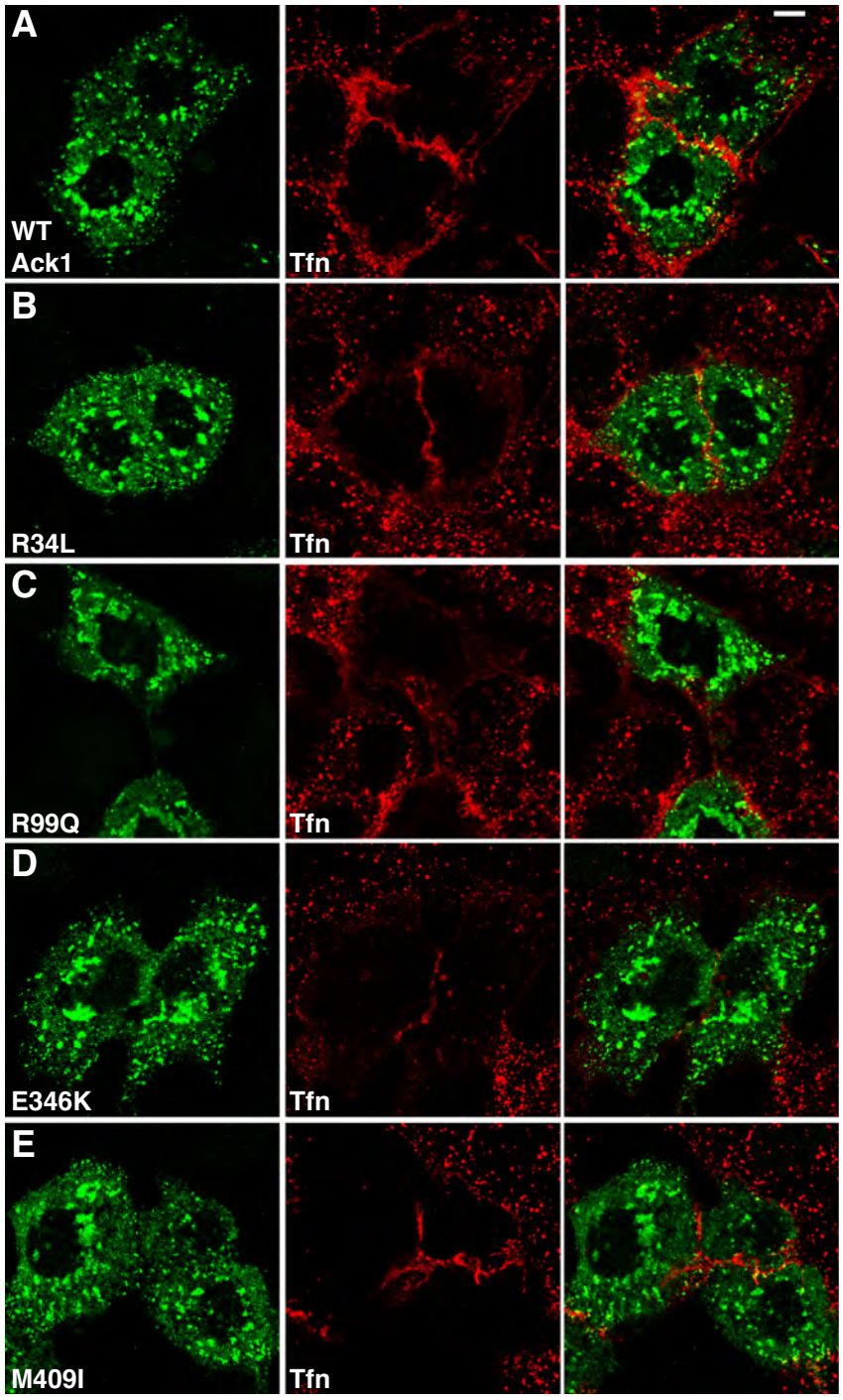

Figure 3-4

Figure 3-5. NIH3T3 cells expressing Ack1.

A, NIH 3T3 cells were infected with retroviruses encoding GFP and Ack1 (wild type or mutants) and were cultured in anchored or non anchored conditions. GFP fluorescence was used to select for infected cells by FACS. B, Lysates from NIH3T3 cells expressing wild type or mutant forms of Ack1 were probed with anti-Ack1(pY284), anti-Ack1, and anti-tubulin antibodies, as indicated. Densitometry readings were used to calculate the ratios of phosphorylated to total Ack1.

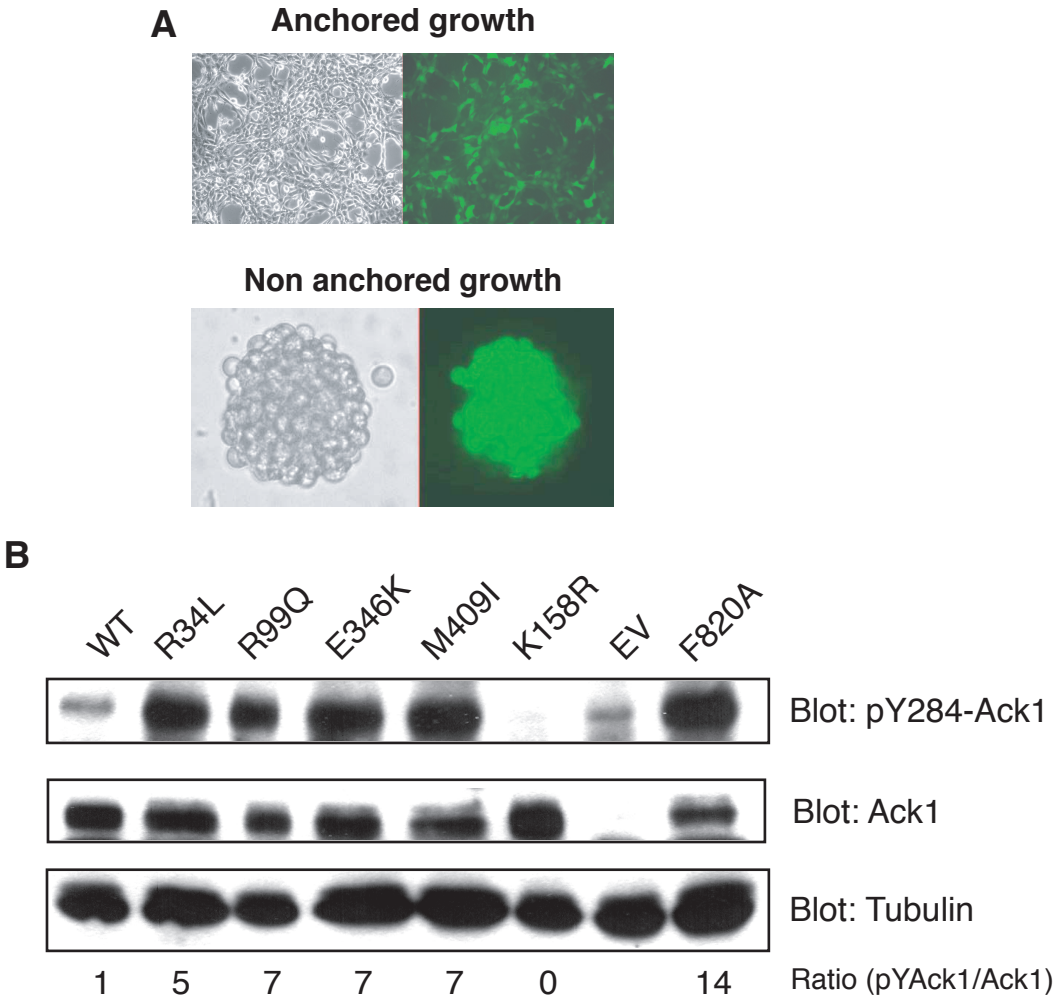
A
Anchored growth
Non anchored growth
B
WT
R34L
R99Q
E346K
M409I
K158R
EV
F820A
Blot: pY284-Ack1
Blot: Ack1
Blot: Tubulin
1
5
7
7
7
0
14
Ratio (pYAck1/Ack1)

Figure 3-5

Figure 3-6. Effects on cell growth.

A, Anchored growth: 20,000 NIH 3T3 cells infected with retroviruses carrying Ack1 (wild-type or mutant) or without Ack1 (EV) were seeded in 12-well plates and counted at the indicated times. The figure is representative of 2 experiments performed in duplicate. **B**, Non-anchored growth: 20,000 NIH 3T3 cells infected with the indicated Ack1 retrovirus or a control virus (EV) were seeded in 24-well ultra-low attachment plates and counted after 6 days. The figure is representative of 2 experiments performed in duplicate. Error bars: standard deviation.

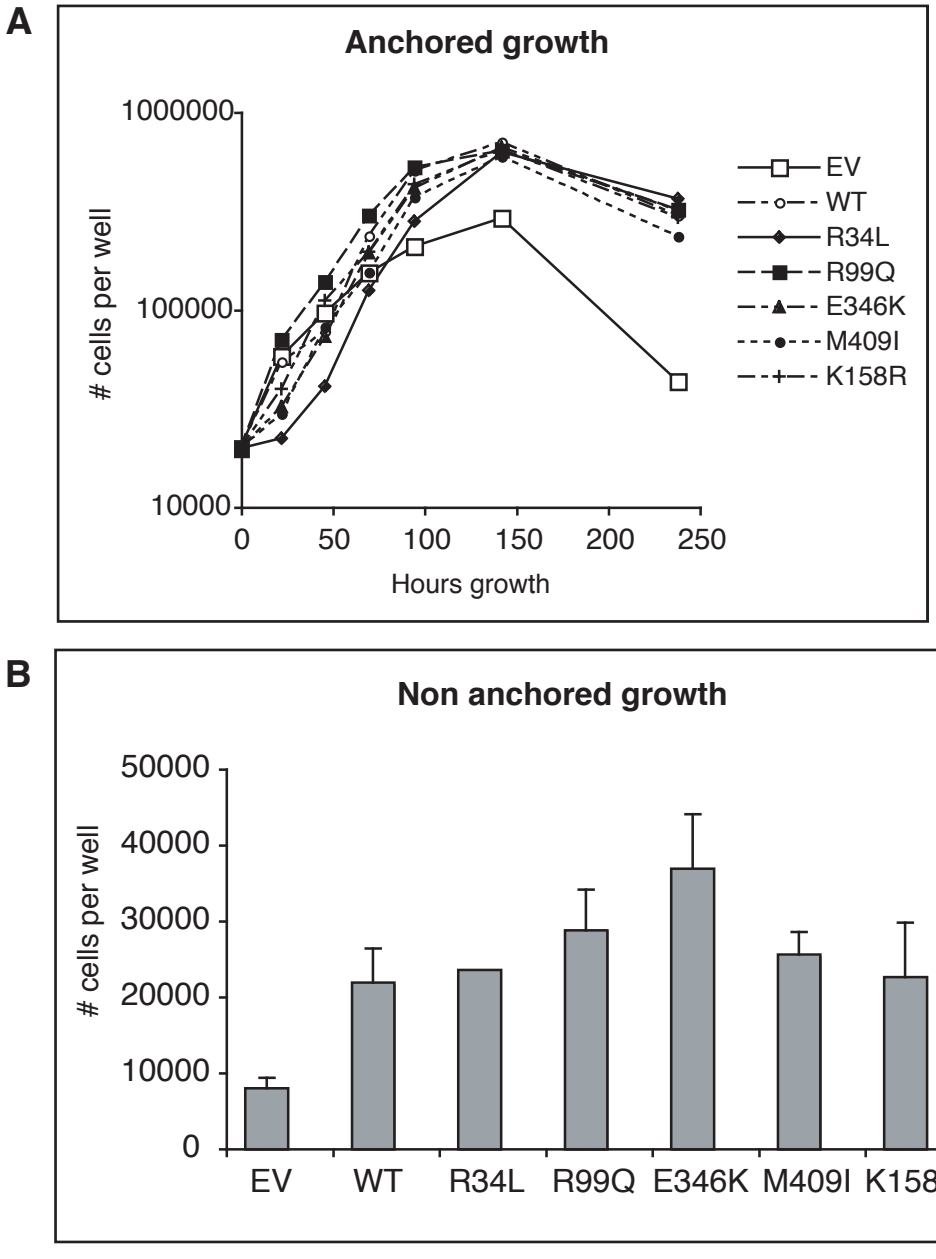
A
Anchored growth
1000000
100000
10000
cells per well
0
50
100
150
200
250
Hours growth
EV
WT
R34L
R99Q
E346K
M409I
K158R
B
Non anchored growth
50000
40000
30000
20000
10000
0
cells per well
EV
WT
R34L
R99Q
E346K
M409I
K158R

Figure 3-6

Figure 3-7. Apoptosis in Ack1-expressing cells.

NIH3T3 cells expressing wild type or mutant forms of Ack1 were harvested at different stages of growth, corresponding to early exponential phase (48hs) and late stationary/death phase (190 hs). Lysates from these cells were probed with anti-PARP and anti-cleaved caspase 3 antibodies. The detection of an 89 KDa fragment corresponding to cleaved PARP and of 19 KDa and 15 KDa fragments corresponding to cleaved caspase 3 were used as makers for apoptosis. As controls, early-phase NIH3T3 cells treated with DMSO (C) or 1 μM staurosporine for 3 hours were used as indicated.

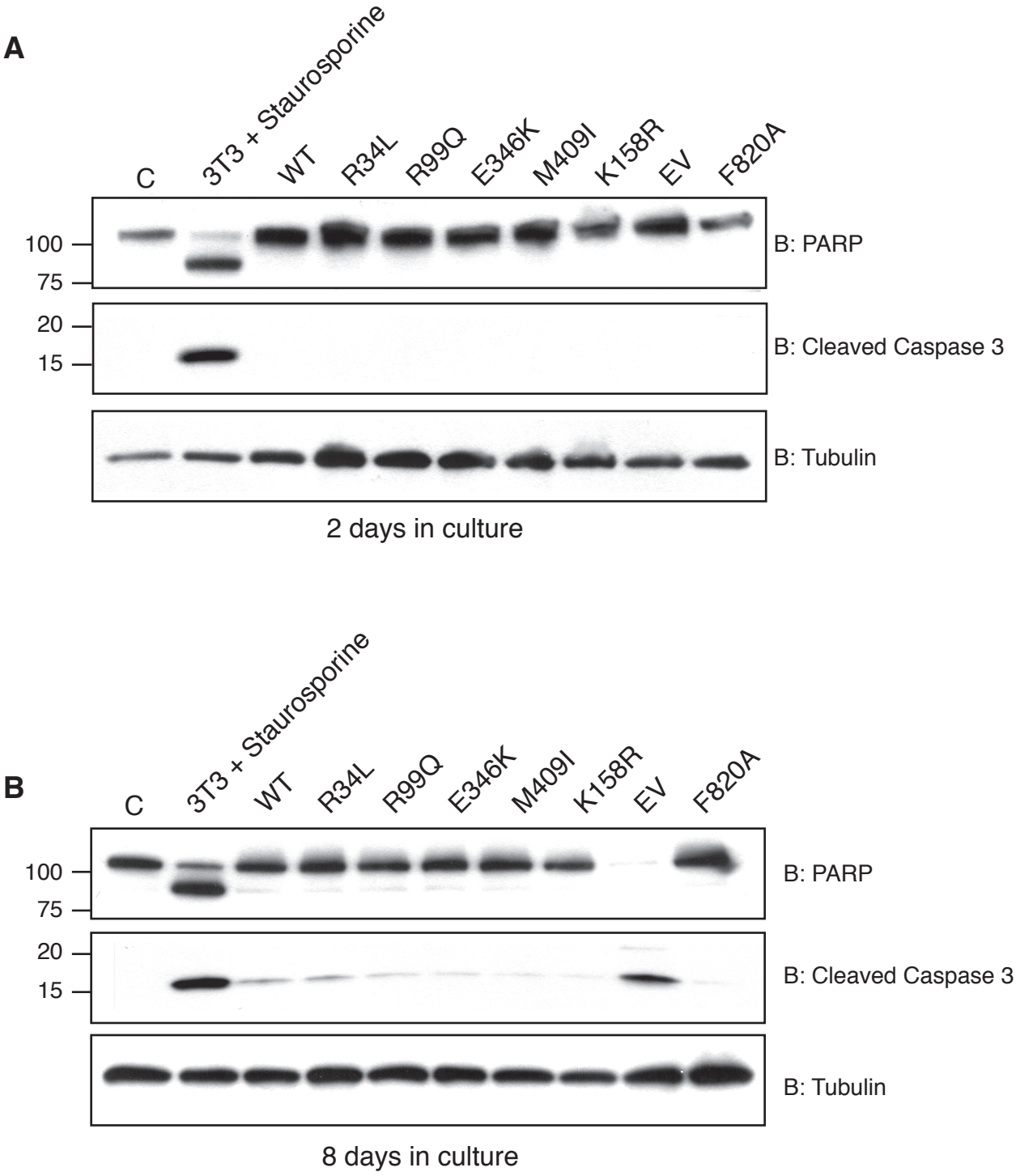
A
C
3T3 + Staurosporine
WT
R34L
R99Q
E346K
M409I
K158R
EV
F820A
100
75
20
15
B: PARP
B: Cleaved Caspase 3
B: Tubulin
2 days in culture
B
C
3T3 + Staurosporine
WT
R34L
R99Q
E346K
M409I
K158R
EV
F820A
100
75
20
15
B: PARP
B: Cleaved Caspase 3
B: Tubulin
8 days in culture

Figure 3-7

Figure 3-8. Cancer-associated mutations increase cell migration.

200,000 NIH 3T3 cells (prepared as for Figure 3-6) were seeded in the top chambers of 24-well plates that contained transwell inserts. After 6 hours, the cells that migrated through the membranes were trypsinized and counted. The percentage of cells that migrated was calculated and normalized to the percent migration of control cells (EV). The figure represents the combined results of 3 experiments performed in triplicate or quadruplicate. Error bars: SEM.

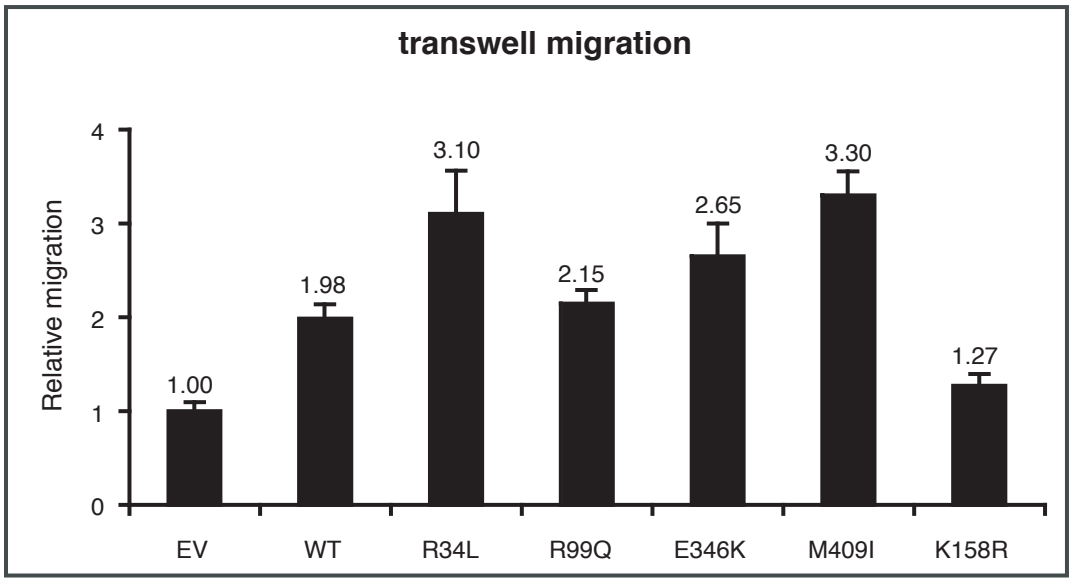
transwell migration
Relative migration
4
3
2
1
0
1.00
1.98
3.10
2.15
2.65
3.30
1.27
EV
WT
R34L
R99Q
E346K
M409I
K158R

Figure 3-8

Figure 3-9. WASP and Cas phosphorylation in Ack1-expressing cells.

A, Lysates from NIH3T3 cells expressing wild type or mutant forms of Ack1 were probed by Western blotting with anti-WASP (pY284), anti-WASP, and anti- tubulin antibodies, as indicated. Densitometry readings were used to calculate the ratios of phosphorylated to total WASP. B, Cas was isolated by immunoprecipitation from NIH3T3 cell lysates. The immunoprecipitated proteins were separated by SDS-PAGE and analyzed by Western blotting with anti-Cas and anti-pY249 Cas antibodies. Densitometry readings were used to calculate the ratios of phosphorylated to total Cas. Tubulin immunoblotting was performed on cell lysates. The figure is representative of 3 experiments.

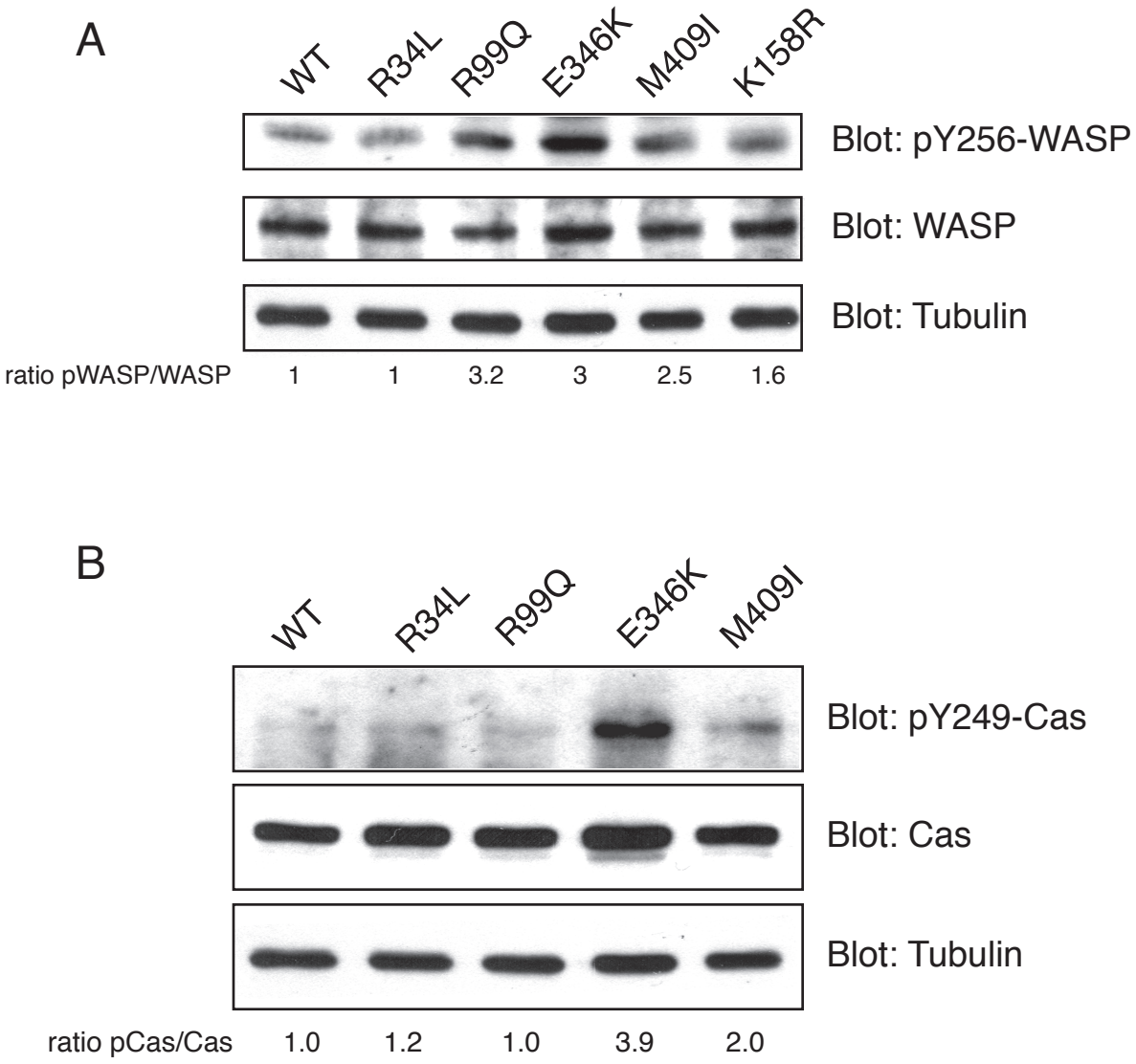
A
WT
R34L
R99Q
E346K
M409I
K158R
Blot: pY256-WASP
Blot: WASP
Blot: Tubulin
ratio pWASP/WASP
1
1
3.2
3
2.5
1.6
B
WT
R34L
R99Q
E346K
M409I
Blot: pY249-Cas
Blot: Cas
Blot: Tubulin
ratio pCas/Cas
1.0
1.2
1.0
3.9
2.0

Figure 3-9

Figure 3-10. Erk phosphorylation in Ack1-expressing cells.

Lysates from 3T3 cells expressing wild type or mutant forms of Ack1 were probed with anti-phospho-Erk, and anti-Erk antibodies, as indicated. Densitometry readings were used to calculate the ratios of phosphorylated to total Erk.

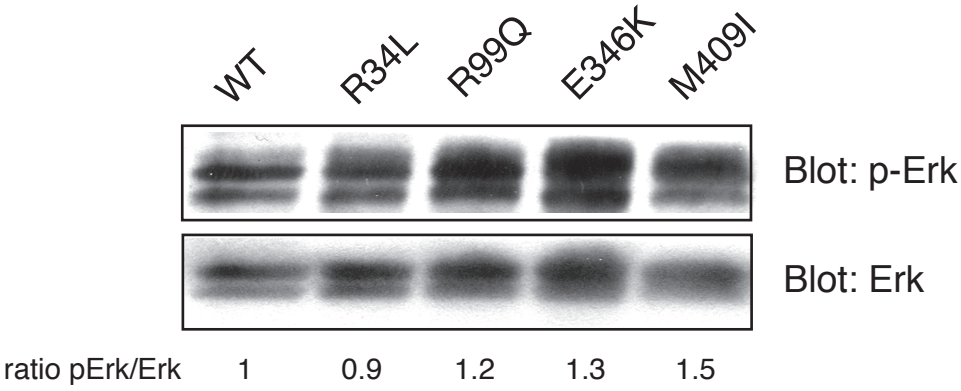
WT
R34L
R99Q
E346K
M409I
Blot: p-Erk
Blot: Erk
ratio pErk/Erk
1
0.9
1.2
1.3
1.5

Figure 3-10

Figure 3-11. A model for Ack1 intramolecular regulation.

A, Amino acid sequence conservation between residues 700 to 910 of Ack1 (accession number: Q07912) and residues 264 to 435 of Mig6 (accession number: Q9UJM3). Green shading represents identical amino acids or conservative substitutions, and the boxed region represents the fragment that was purified and used in this study. **B**, Three dimensional model of Ack1 kinase domain (blue) bound to Mig6 peptide (green) (*28*). The cancer-associated mutation E346K, and additional residues targeted for mutagenesis, are indicated.

A

B

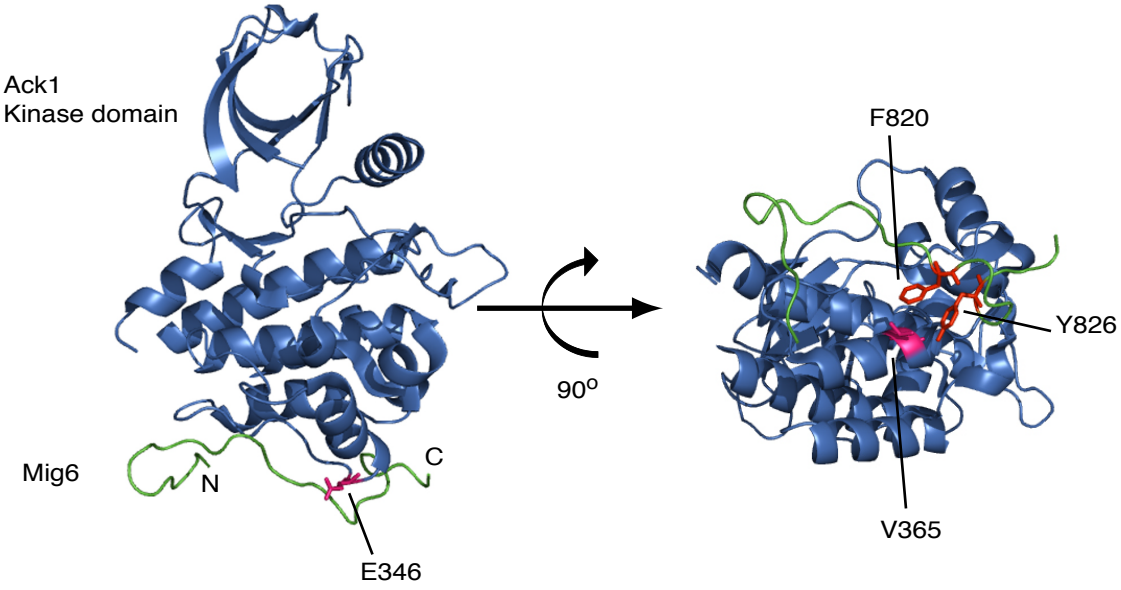

Figure 3-11

Figure 3-12. Activation of Ack1 by mutations designed to disrupt the intramolecular interaction.

A, Schematic diagram of Ack1 with sites of mutation indicated. **B**, Lysates from Cos 7 cells expressing wild type or mutant forms of Ack1 were analyzed by Western blotting with anti-Ack1 (pY284), anti-Ack1 and anti-tubulin antibodies. **C**, Immunoprecipitation-kinase assay: The following forms of Ack1 were immunoprecipitated from Cos 7 cells: WT (unstimulated or EGF-stimulated), V365R, F820A. Immunoprecipitated proteins were analyzed *in vitro* as described in the legend to Figure 3-1.

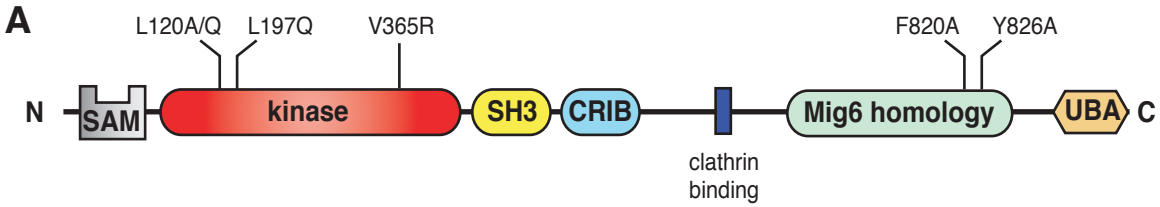
A
L120A/Q
L197Q
V365R
F820A
Y826A
N
SAM
kinase
SH3
CRIB
clathrin
binding
Mig6 homology
UBA
C

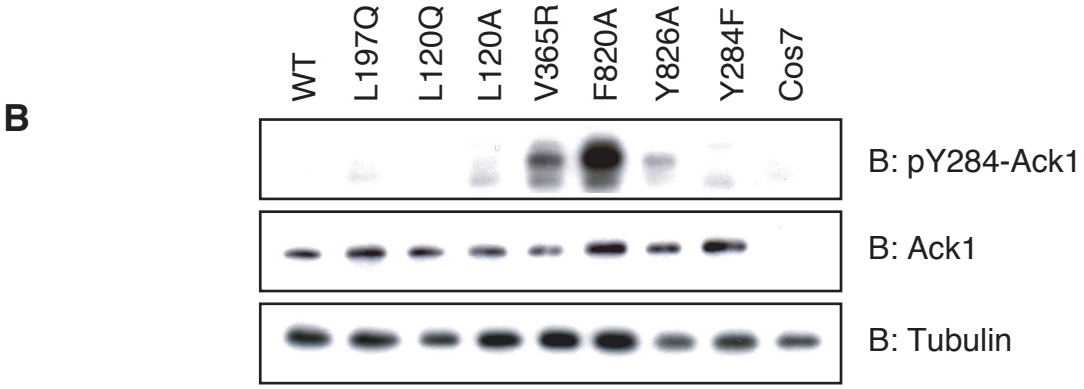
B
WT
L197Q
L120Q
L120A
V365R
F820A
Y826A
Y284F
Cos7
B: pY284-Ack1
B: Ack1
B: Tubulin

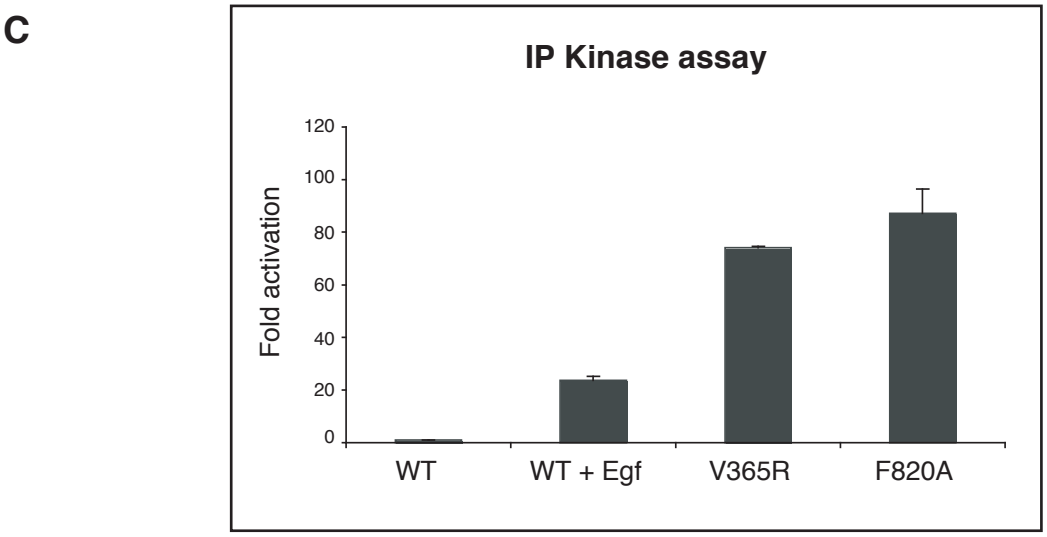
C
IP Kinase assay
Fold activation
120
100
80
60
40
20
0
WT
WT + Egf
V365R
F820A

Figure 3-12

Figure 3-13. A mutation in the Mig6-homology region recapitulates effects of cancer-associated mutations.

A, NIH 3T3 cells infected with retrovirus carrying F820A Ack1 were analyzed in a cell migration assay, as described in the legend to Figure 3-8. **B**, Non anchored growth: the same cells were grown in ultra low attachment plates and counted after 6 days, as described in the legend to figure 3-6B.

A

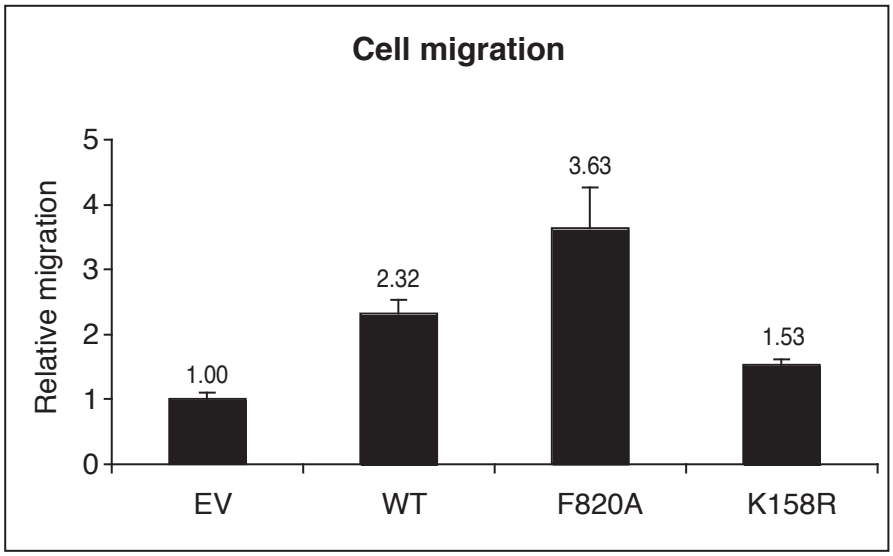

B

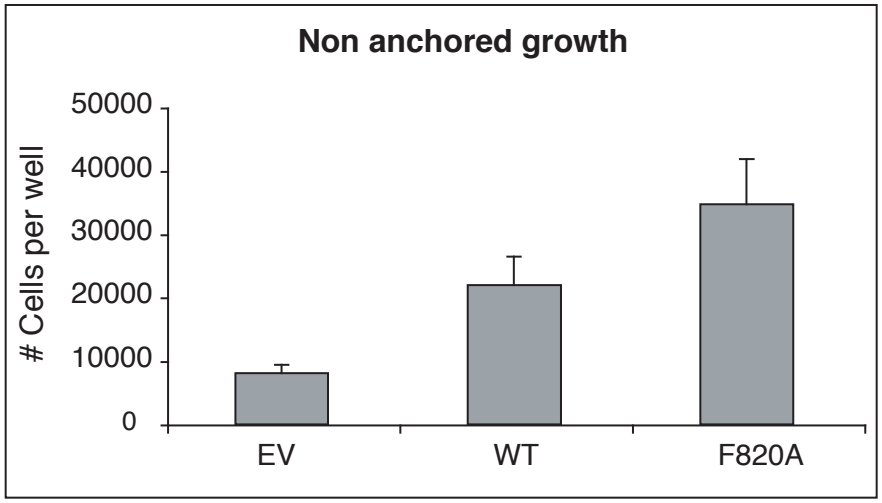

Figure 3-13

Figure 3-14. Direct binding of Mig6-homology region to the Ack1 kinase domain.

A, GST fusion proteins containing the Ack1 Mig6-homology region (MHR) (wild type or F820A) were immobilized on glutathione-agarose beads and incubated with purified His_6-tagged Ack1 kinase domain. The bound proteins were eluted from the beads with Laemmli buffer, separated by SDS-PAGE, transferred to a PVDF membrane, and analyzed by Western blotting using anti-His_6 antibodies. The PVDF membrane was stained with Ponceau S to show the GST proteins. Immobilized GST was used as a control. **B**, GST-MHR was incubated with the His_6-tagged kinase domain (WT or E346K). Bound proteins were eluted with Laemmli buffer, separated by SDS-PAGE, transferred to a PVDF membrane, and analyzed by Western blotting using anti-His_6 antibodies. The PVDF membrane was stained with Ponceau S to show GST proteins. Input proteins were detected by anti-His_6 Western blotting. **C**, Cartoon depicting the proposed interaction between MHR and kinase domain.

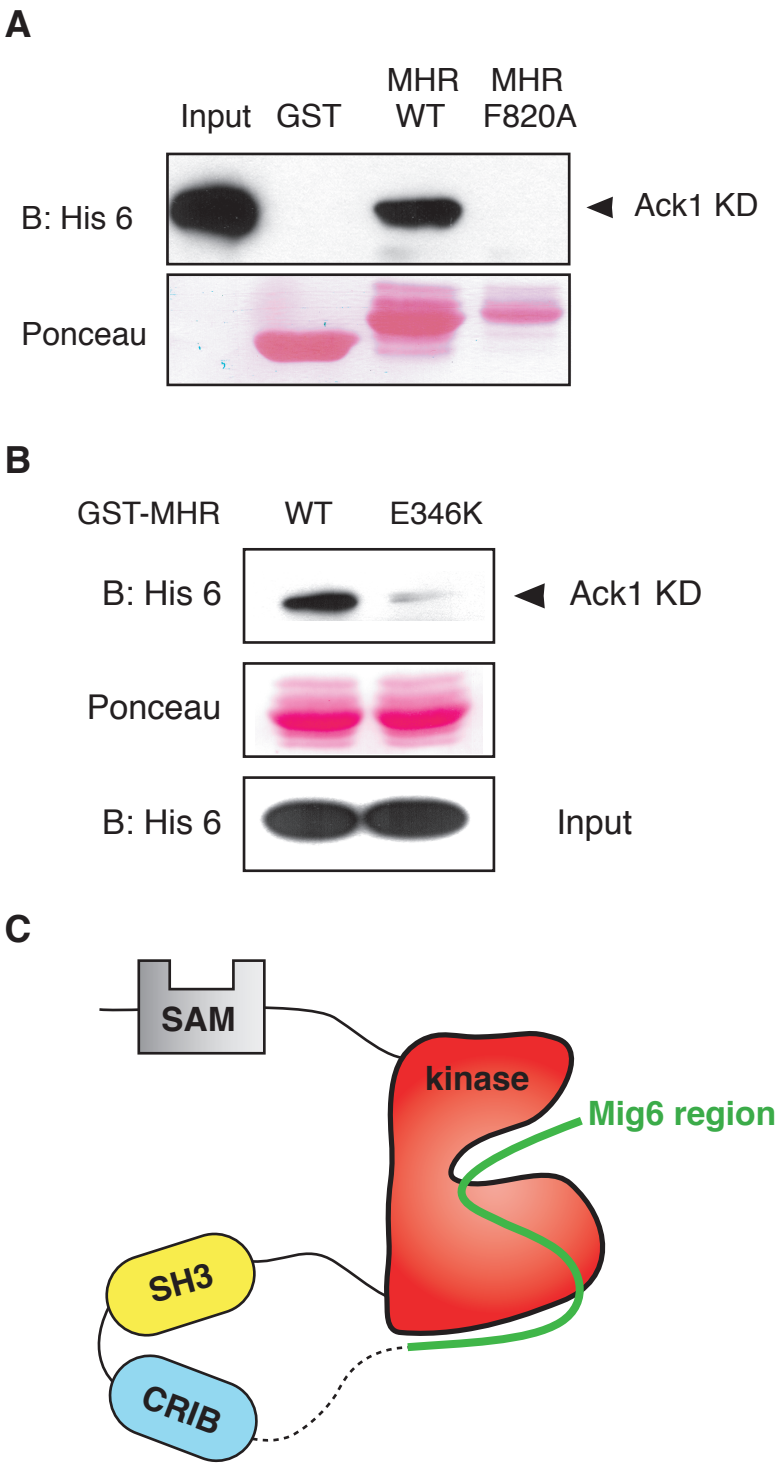
A
Input
GST
MHR WT
MHR F820A
B: His 6
Ack1 KD
Ponceau
B
GST-MHR
WT
E346K
B: His 6
Ack1 KD
Ponceau
B: His 6
Input
C
SAM
kinase
Mig6 region
SH3
CRIB

Figure 3-14

CHAPTER 4

Regulation of Ack1 localization and activity by the amino-terminal SAM domain

The contents of this chapter have been submitted for publication.

Abstract

Sterile alpha motif (SAM) domains share a common fold and mediate protein-protein interactions in a wide variety of proteins. The amino-terminal region of the nonreceptor tyrosine kinase Ack1 (activated Cdc42-associated kinase) is predicted to contain a SAM domain. Here, we used immunofluorescence and Western blotting to show that Ack1 deletion mutants lacking the N-terminus displayed significantly reduced autophosphorylation in cells. A minimal construct comprising the N-terminus and kinase domain (NKD) was autophosphorylated, while the kinase domain alone (KD) was not. When expressed in mammalian cells, NKD localized to the plasma membrane, while KD showed a more diffuse cytosolic localization. Co-immunoprecipitation experiments showed a much stronger interaction between full length Ack1 and NKD than between full length Ack1 and KD, indicating that the N-terminus was important for Ack1 dimerization. Increasing the local concentration of purified Ack1 kinase domain at the surface of lipid vesicles stimulated autophosphorylation and catalytic activity, consistent with a requirement for dimerization and trans-phosphorylation for activity. Collectively, the data suggest that the N-terminus of Ack1 promotes dimerization or multimerization at the plasma membrane to allow for autophosphorylation.

Introduction

Ack1 is a 120 kDa non-receptor tyrosine kinase (NRTK) with the domain arrangement shown in Figure 4-1A. From N- to C-terminus, Ack1 contains a sterile alpha motif (SAM) domain (*25*), a kinase domain, an SH3 domain, a Cdc42-binding domain (CRIB), a clathrin-binding motif (*26*), a region homologous to Mig6 (*28*), and a ubiquitin binding domain (*27*). The C-terminal portion of Ack1 also contains several proline-rich sequences that serve as protein-protein interaction motifs (*42, 49, 67, 68*). Members of the Ack family including Ack1 or Tnk2 in human (*31*), Tnk1/Kos1 in human and mouse (*32, 36*), bovine Ack2 (*37*), DACK and DPR2 in *Drosophila melanogaster* (*30*) and Ark-1 in *Caenorhabditis elegans* (*29*) have been identified in several organisms. The isoforms share the overall domain arrangement of Ack1 (i.e. a kinase domain followed by an SH3 domain and Pro-rich sequences), but differ in some details. For instance, Ack2 has a shorter N-terminal region and a shorter C-terminal portion (*37*). The isoforms Tnk1, Kos1 and DACK do not have a CRIB domain and are shorter than Ack1 (*30, 32, 33*).

Several proteins have been shown to interact with Ack1. GTP-bound Cdc42 binds to the CRIB domain and activates Ack1 (*31*). Ligands for the proline-rich region of Ack1 include the SH3 domains of Hck (*42*), Grb2 (*67*), SNX9 (*49, 67*), and the WW domain of the E3 ubiquitin ligase Nedd4-2 (*68*). Upon activation by Cdc42, Ack1 phosphorylates the guanine exchange factor Dbl (*41, 60*) and the adapter protein p130Cas (*39*). Although the physiological roles of Ack1 are still unclear, it has been implicated in several signaling pathways. Ack1 is phosphorylated and activated in response to multiple growth factors (*25, 67*) and integrin-mediated signals (*39, 44*). Ack1 participates in a signaling complex with EGFR (*27*). In addition, due to its interaction with proteins such as ubiquitin (*27*), clathrin heavy chain (*26, 47*) and the

sorting nexin SH3PX1 (*97*), Ack1 is thought to play a role in the regulation of EGFR stability and vesicle dynamics.

SAM (sterile-alpha motif) domains are modular domains of ~ 70 amino acids that were originally identified and named due to their essential role in sexual differentiation in yeasts. In spite of their common five-helical structure, SAM domains do not exhibit significant sequence homology (*98*). This sequence diversity reflects a large diversity of function. SAM domains have been found in nearly 1000 proteins that include a diverse array of signaling molecules such as the transcriptional repressors TEL (*92*) and Polycomb (*93*), diacyglycerol kinase δ1 (DGKδ1) (*91*), and Eph receptor tyrosine kinases (*89, 90*).

Structural studies of the SAM domains from the EphA4 receptor (*89*) and EphB2 receptor (*90*) showed that the helical arrangement creates two interfaces, suggesting a mechanism for SAM domain dimerization. These interfaces are composed of two complementary surfaces that associate mainly by hydrophobic interactions. Similar interfaces have been identified in TEL, Polycomb and DGKδ1, and these SAM domains form extended polymers that have important regulatory roles. In the lipid kinase DGKδ1, SAM domain-mediated polymerization keeps the enzyme in an inactive form and localized to cytoplasmic vesicles. Upon EGF stimulation, DGKδ1 is recruited to the plasma membrane, where its substrate is located (*91*). The SAM domain of the transcriptional repressors Polyhomeotic (*93*) and TEL (*92*) form helical polymeric filaments, suggesting a mechanism by which transcriptional repressor complexes might spread along the chromosome.

The amino-terminal 85 residues of Ack1 contain SAM domain-like sequences that are conserved across species (*25*). Fusion of the Ack1 SAM domain sequence to GFP resulted in its translocation to the plasma membrane (*25*). Deletion of the SAM domain from full-length Ack1

reduced the level of autophosphorylation in HeLa cells, suggesting the involvement of the N-terminus in enzyme regulation (*25*). Here, we explore the role of the N-terminal domain in Ack1 localization and regulation. Our data suggest that the SAM domain promotes Ack1 dimerization at the plasma membrane to allow intermolecular autophosphorylation, analogous to the role of the transmembrane domains of receptor tyrosine kinases.

Results

Analysis of Ack1 autophosphorylation by Western blotting.

To test for the importance of the amino-terminal SAM domain in Ack1 regulation, we created the deletion and truncation constructs that are shown in Figure 4-1A. In the construct ΔNt, the first 110 amino acid residues comprising the SAM domain were deleted. NKD corresponds to the first 381 residues of Ack1 including the SAM domain and the kinase domain, and KD is the kinase domain alone.

We expressed these constructs in Cos7 cells and analyzed their activities in whole cell lysates by probing for phosphorylation of Y284, the major autophosphorylation site in the activation loop of Ack1 (*42*). Phosphorylated Ack1 was detected in the lanes corresponding to NKD and WT and the lanes corresponding to KD and ΔNt did not show any detectable signal for pY284-Ack1 (Fig.4-1B, top panel). Thus, the level of Ack1 autophosphorylation was drastically reduced by the deletion of the SAM domain both in the context of the full-length protein (i.e., WT vs. ΔNt) and of the shorter constructs (NKD vs. KD). The membrane was reprobed with anti-HA antibody to determine total levels of the proteins in the blot (Fig. 4-1B, middle panel). The ratio of pY284-Ack1 signal to total Ack1 signal is quantified in Figure 1C. These results suggest that the SAM domain plays an important role in the regulation of Ack1 by promoting its autophosphorylation.

We also analyzed the overall phosphotyrosine content of cells expressing the different Ack1 constructs (Fig. 4-1B, bottom panel). Expression of full-length Ack1 resulted in the tyrosine phosphorylation of numerous cellular proteins, while fewer proteins were phosphorylated in DNt-expressing cells. For both full-length Ack1 and ΔNt, a band was present that co-migrated with the phosphorylated Ack1 protein, although the band was weaker for ΔNt.

No signal was observed for ΔNt in the pY284 blot, but this construct contains other previously identified phosphorylation sites (Y826, Y857) that may account for the signal in the pTyr blot (*53, 55*). Expression of the construct NKD did not produce any drastic change in the pattern of phosphotyrosine-containing proteins as compared to untransfected Cos7 cells, but a tyrosine phosphorylated band migrating at the position of NKD was detected. In contrast, expression of the isolated kinase domain (KD) did not stimulate phosphorylation of cellular proteins compared to untransfected control cells, and evidence for autophosphorylation was detected. This is consistent with the data in the pY284 blot, since this residue is probably the only one available for phosphorylation in KD and NKD. These data suggest that Ack1 N-terminus is important for its activation.

The deletion of Ack1 N-terminus affects subcellular localization.

As reported earlier (*46, 57*), WT Ack1 showed some colocalization with the early endosomal marker EEA1, but was also present in amorphous intracellular structures that were often closely associated with early endosomes (Fig. 4-2). ΔNT was also present in large intracellular structures (Fig. 4-2). These were not associated with early endosomes, and had a smoother-surfaced appearance than the structures containing WT Ack1. By contrast, NKD was mostly localized to the plasma membrane, while the isolated kinase domain (KD) showed a diffuse cytosolic localization. The difference between NKD and KD localization patterns was consistent with the reported ability of the SAM domain to direct Ack1 to the plasma membrane (*25*). The intracellular localization of WT Ack1 and ΔNT suggested that other regions of the protein might also contain targeting information, consistent with the fact that downstream Ack1 domains bind to a number of proteins.

Analysis of Ack1 autophosphorylation by quantitative immunofluorescence.

Next, we tested whether the various forms of Ack1 were active in all cellular sites. We studied the subcellular localization of the autophosphorylated, activated forms of Ack1 and the mutants by immunofluorescence analysis using anti-pY284 Ack1 antibody. In the cases where it was detected, the signal for pY284 Ack1 colocalized exactly with the distribution of total Ack1 (Figure 4-3).

To determine the relative activities of the constructs, we quantitated anti-pY284 staining (for autophosphorylated Ack1) and anti-HA staining (for total Ack1) (Figs. 4-3B and 4-3C). The ratios of fluorescence intensities (pY284/HA) were normalized to the value corresponding to wild type (WT=100). Figure 4-3B shows results from a representative experiment, while Figure 4-3C shows the merged data from three experiments. Consistent with the Western blotting results, the level of autophosphorylation was significantly decreased by the deletion of the N-terminus, both in the context of the full length and the minimal construct. The construct ΔNt showed a ~2-fold decrease in autophosphorylation compared to wild type, while the isolated kinase domain (KD) had a ~9-fold decrease in autophosphorylation compared to NKD.

Concentration-dependent activity of the purified Ack1 kinase domain.

A possible explanation for the negligible autophosphorylation of the KD construct (Figs. 4-1, 4-3) is that the isolated kinase domain might be inactive. Several tyrosine kinase catalytic domains (e.g., Csk, Fes) require the presence of accessory domains for activity (*8, 99*). To test this possibility, we introduced the Ack1 kinase domain into a recombinant baculovirus, expressed the protein in insect cells, and purified it to homogeneity. We tested the catalytic

activity of Ack1 kinase domain by carrying out kinetic experiments using varying concentrations of a peptide substrate derived from the Tyr256 sequence of WASP (KVIYDFEKKKG). As shown in Figure 4-4A, the purified kinase domain was active towards the peptide. Experiments with varying ATP concentrations yielded a K_M(ATP) value of 107 μM (data not shown), a typical value for NRTKs. Thus, although the kinase domain expressed in cells is inactive, the isolated kinase domain has intrinsic tyrosine kinase activity. We hypothesized that the observed activity *in vitro* may be a function of the increased protein concentration under these conditions. The SAM domains in other proteins mediate polymerization processes that regulate activity (*98*), and the SAM domain of Ack1 acts as a membrane-targeting signal (Fig. 4-2 and ref. 1). In full-length Ack1, the SAM domain may increase the local concentration by causing dimerization or multimerization at the sites where it is recruited.

Kinases that dimerize and transphosphorylate show concentration-dependent activity. In order to test the effect of Ack1 concentration on autophosphorylation, we first dephosphorylated the His_6-tagged enzyme purified from Sf9 cells using the *Yersinia* phosphatase (Yop) then incubated the Ack1 kinase domain with ATP at two different enzyme concentrations and analyzed the level of Y284 phosphorylation. After stopping the reaction, similar amounts of total protein were analyzed by Western blotting using anti-pY284 Ack1 and anti-His6 antibodies. A ten-fold increase in Ack1 kinase domain concentration in the reaction resulted in a similar increase in the relative phosphorylation level, as shown in Figure 4-4B and 4-4C. This result supported the hypothesis that increasing local concentration may be a mechanism for Ack1 activation.

To confirm these findings, we performed a similar experiment using lipid vesicles to control the local concentration of Ack1 kinase domain. Dephosphorylated Ack1 was incubated

with ATP in the presence of small unilamellar vesicles containing different mole fractions of a lipid with a Ni-NTA head group (DOGS-NTA-Ni). This method was used to demonstrate the activation of EGFR by formation of an asymmetric dimer (*87*). Thus, in these experiments, we mimicked the dimerization function of the SAM domain by using the hexahistidine tag to control the local concentrations of the isolated kinase domain. The concentration of enzyme was kept constant, and the concentration of Ni-NTA was kept constant (by varying the total vesicle concentration) to ensure that any observed effects would be due to changes in effective local concentration. The total lipid concentration was 3.3 mM for vesicles containing 0% and 2% DOGS- NTA-Ni and 1.32 mM for vesicles containing 5% DOGS-NTA-Ni. Attachment of the purified kinase domain to vesicles caused a significant increase in autophosphorylation (Fig. 4-5). The stimulation of autophosphorylation by DOGS-NTA-Ni was dose-dependent, as vesicles with 5 mole % DOGS-NTA-Ni produced a further increase over vesicles with 2 mole % DOGS-NTA-Ni. Vesicles that contained no Ni-NTA did not produce any increase in autophosphorylation compared to the activity in the absence of vesicles, indicating that that the observed effect was not due to any unspecific interaction between lipids and proteins (Fig. 4-5).

The vesicles were also used to analyze the catalytic activity of purified Ack1 kinase domain towards a peptide substrate in a continuous spectrophotometric assay (Fig. 4-6). The catalytic activity of the enzyme in the presence of vesicles containing 5 mole % DOGS-NTA-Ni was 2-fold higher than with vesicles containing no Ni-NTA, or than solution reactions (i.e., in the absence of vesicles). We confirmed that the effect was due to binding between the His_6-Ack1 kinase domain and DOGS-NTA-Ni by performing the assay in the presence of 500 mM imidazole; under these conditions the Ack1 activity was comparable to the activity observed in the absence of vesicles or in solution. Taken together, the data show that artificially increasing

the local concentration of the isolated kinase domain increases autophosphorylation and catalytic activity. The data are consistent with the proposed role of SAM domain polymerization in Ack1 regulation.

Ack1 self associates in cells.

We investigated the capacity of Ack1 constructs to self-associate in cells. Cos 7 were transfected with Flag-tagged full length Ack1 alone or together with HA-tagged NKD or KD. Flag-Ack1 was immunoprecipitated from the cell lysates using anti-Flag antibody, processed for SDS-PAGE and transferred to PVDF membranes. Blots were probed for the presence of co-immunoprecipitated HA-tagged proteins. The densitometry readings corresponding to Flag-tagged Ack1 and to HA-tagged Ack1 in the immunocomplexes were used to calculate the ratio HA-Ack1/Flag-Ack1. The HA:Flag ratio for KD was arbitrarily set to 1. We found that HA-NKD coimmunoprecipitated with Flag Ack1 3-fold more strongly than HA-KD (Fig. 4-7). These data provide evidence that self-association of Ack1 can be mediated by the N-terminal region.

Discussion

SAM domains are a diverse group of protein-protein interaction motifs that frequently mediate homo- or hetero- dimerization and oligomerization. In several enzymes, SAM domains regulate activity by localized polymerization at the membrane or in the nucleus. In this work, we show that the SAM domain of Ack1 is required for autophosphorylation. Our data suggest that the N-terminus of Ack1, containing the SAM domain mediates dimerization, and that the increased local concentrations result in increased autophosphorylation and kinase activity.

To study the role of the Ack1 N-terminus in autophosphorylation, we deleted the first 110 amino acids of the polypeptide (ΔNt) and we compared it to the full-length protein (WT). In addition, we created a minimal construct that contains only the N-terminus and the kinase domain (NKD) and we compared it to the isolated kinase domain (KD). Since Ack1 is a large protein that contains several different regions, some of whose roles are not completely understood, this simplified system proved to be useful to dissect the role of the N-terminus in Ack1 activation and intracellular localization.

The deletion of the Ack1 N-terminus produced a significant decrease in Ack1 autophosphorylation in cells. Similar trends were observed by two different methods, although the Western blot quantitation method appears to have a broader dynamic range than the quantitative immunofluorescence. Autophosphorylation of ΔNt was 15-fold lower than WT Ack1 by Western blotting (Fig. 4-1) and 2-fold lower by immunofluorescence (Fig. 4-3). The effect on the minimal NKD construct was more pronounced: autophosphorylation of KD was 27-fold lower than NKD by Western blotting and 9-fold lower by immunofluorescence. In the immunofluorescence assays (Fig. 4-3), autophosphorylation of KD was significantly lower than ΔNt. A possible explanation for this difference is that other regions of Ack1, in addition to the N-

terminus, may mediate interactions or provide inputs that result in increased autophosphorylation.

Consistent with published data (*25*), we observed that Ack1 N-terminus is a membrane-targeting domain (Figs. 4-2 and 4-3). The minimal constructs NKD and KD show very distinct intracellular localizations: NKD is clearly localized at the plasma membrane and phosphorylated, while KD is diffuse and cytosolic, and unphosphorylated at Y284 (Figs. 4-2 and 4-3). The situation is more complex in the cases of WT and ΔNt. They both show a punctate distribution that is not identical to either NKD or KD. This suggests that the localization of full-length Ack1 results from the cumulative effect of interactions mediated by the SAM domain and other regions of the protein. The cellular distribution of WT Ack1 is in structures that partially colocalize with the early endosome marker EEA1 (Fig. 4-2). It is likely that interactions between full-length Ack1 and other proteins including clathrin (*26*), sorting nexin 9 (*49*), and ubiquinated EGFR (*27*) play a determining role in subcellular localization.

In the context of full-length Ack1, the primary function of the SAM domain may be to promote enzyme activation. We used an *in vitro* system to explicitly test the hypothesis that self-association is an activation mechanism for Ack1. We found that increasing solution concentrations of Ack1 resulted in increased autophosphorylation (Fig. 4-5). Furthermore, Ack1 kinase domain attached to vesicles showed a concentration-dependent increase in autophosphorylation and in phosphorylation of an exogenous substrate (Figs. 4-5 and 4-6). We found evidence for N-terminal dependent Ack1 self-association in cells by co-immunoprecipitation experiments. FLAG-Ack1 co-immunoprecipitated more weakly with HA-KD than with HA-NKD, suggesting that the N-terminus promotes Ack1 self-association. These

results suggest that increasing the local concentration of Ack1 catalytic domain by SAM domain-mediated self-association is potentially a mechanism for enzyme activation.

Counterbalancing mechanisms presumably exist to reverse the SAM domain-mediated activation of Ack1. Although these mechanisms are undefined at present, the domain arrangement of Ack1 is complex, and it is likely that other regions of the polypeptide are involved in Ack1 downregulation. We have shown that the Mig6-homology region (MHR) located at the C-terminus of Ack1 is involved in an intramolecular autoinhibitory interaction (*57*). The MHR is also capable of binding to EGFR kinase domain *in vitro* (V.P.E., W.T.M.; unpublished observations) and in cell lysates (*27*). This Ack1-EGFR interaction could potentially be involved in the dynamic regulation of Ack1 activity. The immunofluorescence data presented here (Fig. 4-2) and elsewhere (*25*) suggest that the overall intracellular distribution of Ack1 is determined by interactions with multiple regions of the protein. Growth factor treatment of cells promotes phosphorylation of the Ack1 C-terminus [29,30], which could potentially destabilize autoinhibitory interactions and unmask the SAM domain for membrane recruitment and Ack1 activation.

Figure 4-1: The N-terminus of Ack1 is required for autophosphorylation in cells.

A, constructs used in this study: WT, full length Ack1 (accession # Q07912); ΔNt, deletion of the N-terminal 110 amino acids; NKD, amino terminus plus kinase domain (residues 1-381); KD, kinase domain alone (residues 111-381). B, Western blot analysis. Lysates from Cos7 cells expressing wild type or truncated forms of Ack1 were probed with anti- phospho Ack1 (pY284), anti-HA, and anti-phosphotyrosine antibodies as indicated. The figure is representative of five experiments. C, densitometry readings were taken from all five experiments and the average was plotted in a bar graph. Error bars indicate standard error.

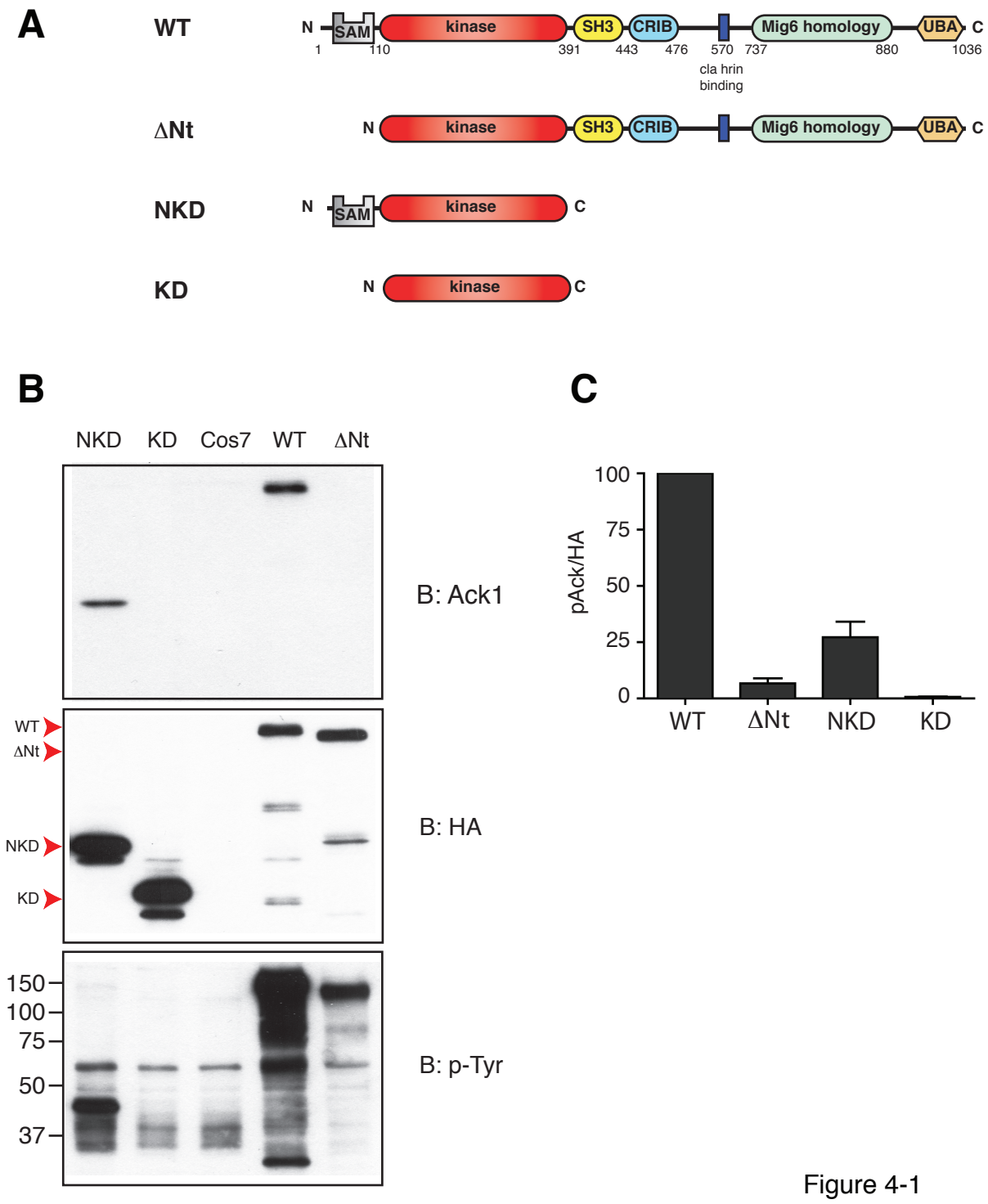
A
WT
N
SAM
kinase
SH3
CRIB
Mig6 homology
UBA
C
1
110
391
443
476
570
737
880
1036
cla hrin
binding
ΔNt
NKD
KD
B
NKD
KD
Cos7
WT
ΔNt
B: Ack1
WT
ΔNt
NKD
KD
B: HA
150
100
75
50
37
B: p-Tyr
C
pAck/HA
100
75
50
25
0
WT
ΔNt
NKD
KD

Figure 4-1

Figure 4-2: Localization of Ack1 proteins.

Cos7 cells expressing wild-type HA-tagged Ack1 (top row) or the indicated mutant (Rows 2-4) were prepared for immunostaining and confocal microscopy as described in Materials and Methods, detecting Ack1 proteins with anti-HA antibodies and early endosomes with anti-EEA1 antibodies. Anti-HA; left panels; anti-EEA1, middle panels; merged images, right panels. Microscopy was performed by Azad Gucwa in Deborah Brown's laboratory.

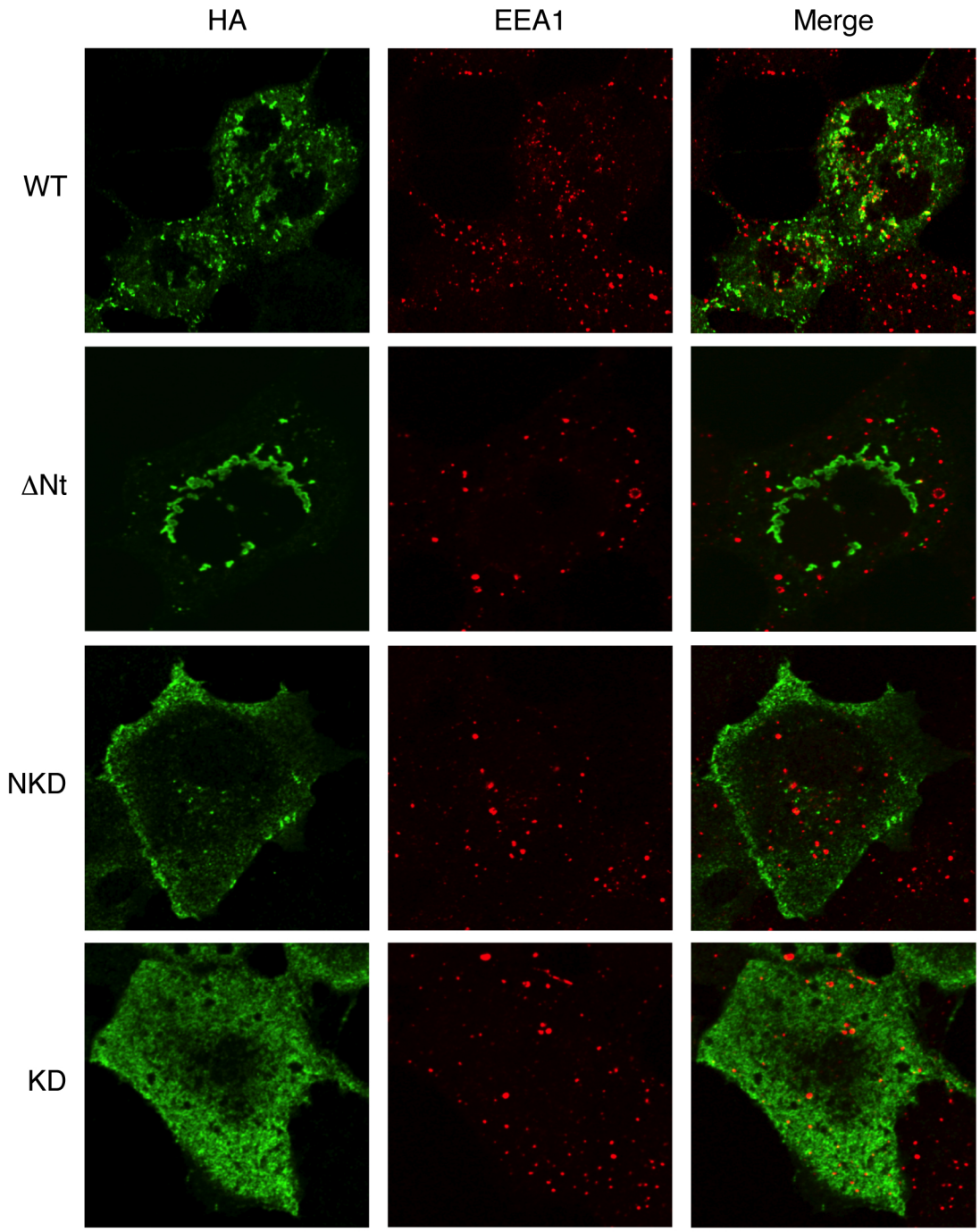

Figure 4-2

Figure 4-3: Quantitative immunofluorescence analysis.

A, Cos7 cells expressing wild type or truncated forms of Ack1 were prepared for immunofluorescence using anti- phospho-Ack1 (pY284) and anti-HA antibodies. Top row: HA staining; middle row: pY284 staining; bottom row: merged images. Microscopy was performed by Azad Gucwa in Deborah Brown's laboratory. B, the experiment shown in panel A was performed three times, measuring pY284 fluorescence and HA fluorescence in 30 cells each time. The ratio of pY284Ack1/HA in each cell was calculated and normalized with respect to WT Ack1. A scatter plot for one representative experiment, with a line at the mean is shown. C, Bar graph showing the combined data of the three experiments. The data was compared using a one-way ANOVA test followed by a Tukey's test of honest significant differences. All groups were significantly different from each other; $P < 0.001$ for all pairings, with the exception of KD vs. K158R ($P < 0.01$). Errors bars indicate standard error.

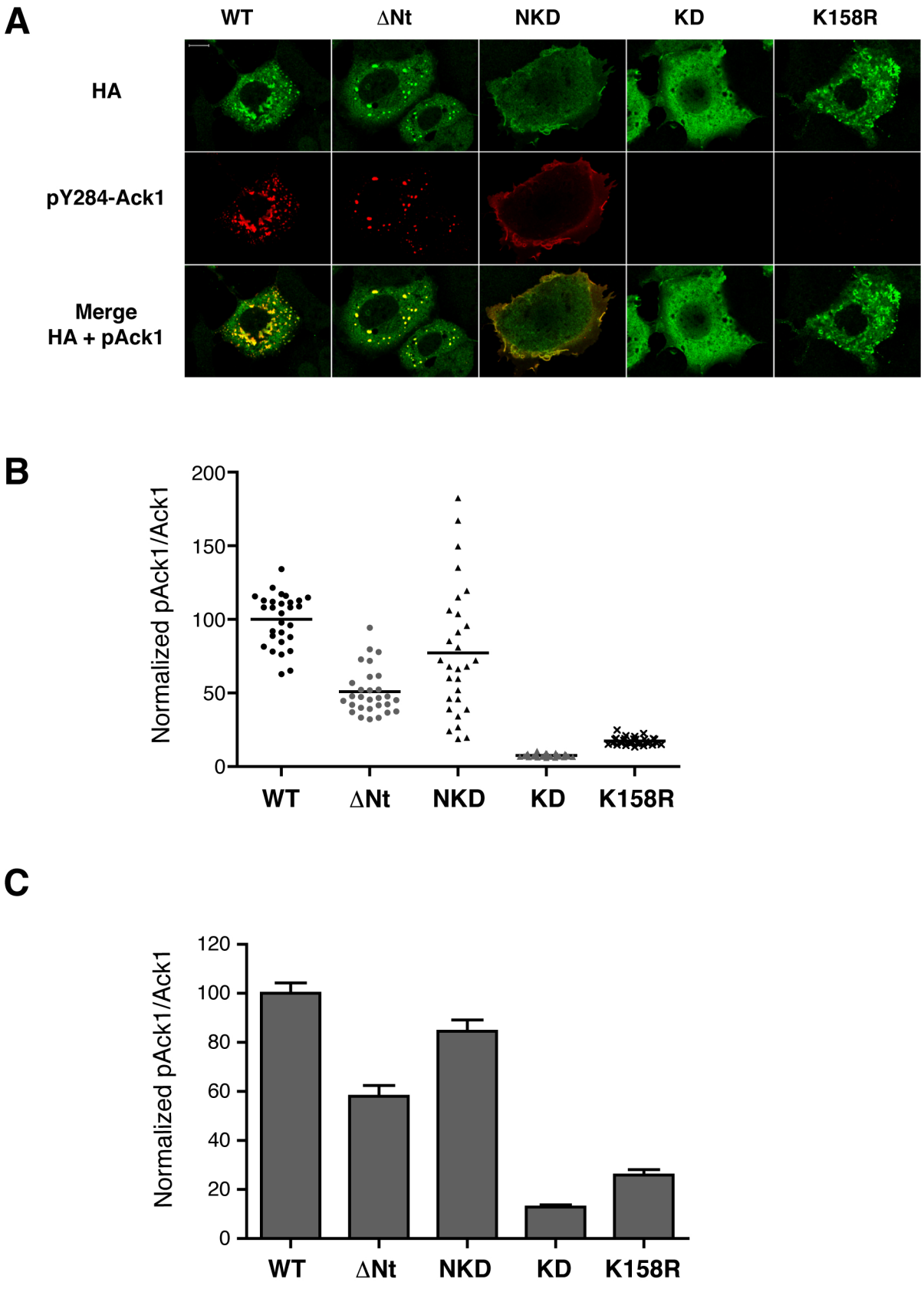
A
WT
ΔNt
NKD
KD
K158R
HA
pY284-Ack1
Merge
HA + pAck1
B
Normalized pAck1/Ack1
200
150
100
50
0
WT
ΔNt
NKD
KD
K158R
C
Normalized pAck1/Ack1
120
100
80
60
40
20
0
WT
ΔNt
NKD
KD
K158R

Figure 4-3

Figure 4-4: Autophosphorylation of purified Ack1 kinase domain in solution.

A, purified Ack1 kinase domain is active *in vitro*. The catalytic activity of varying concentrations of Ack1 kinase domain was measured towards a WASP-derived peptide was measured in a continuous activity assay with varying substrate concentrations. The figure is representative of three experiments. B, the purified Ack1 kinase domain was dephosphorylated using *Yersinia* phosphatase Yop and incubated at different concentrations in the presence of ATP. As a control, a mock reaction was carried out in the absence of ATP. Lane 1: Ack1 before dephosphorylation with Yop. Lane 2: mock reaction with 1 μM Ack1 in the absence of ATP. Lane 3: reaction with 0.1 μM Ack1. Lane 4: reaction with 1 μM Ack1. Equal amounts of protein (100 ng) were analyzed by Western blotting using anti-phospho Ack1 (pY284) and anti-His_6 antibodies. The figure is representative of three experiments. C, Densitometry readings were used to calculate the ratios of phosphorylated Ack1 (pY284 blot) to Ack1 (His_6 blot).

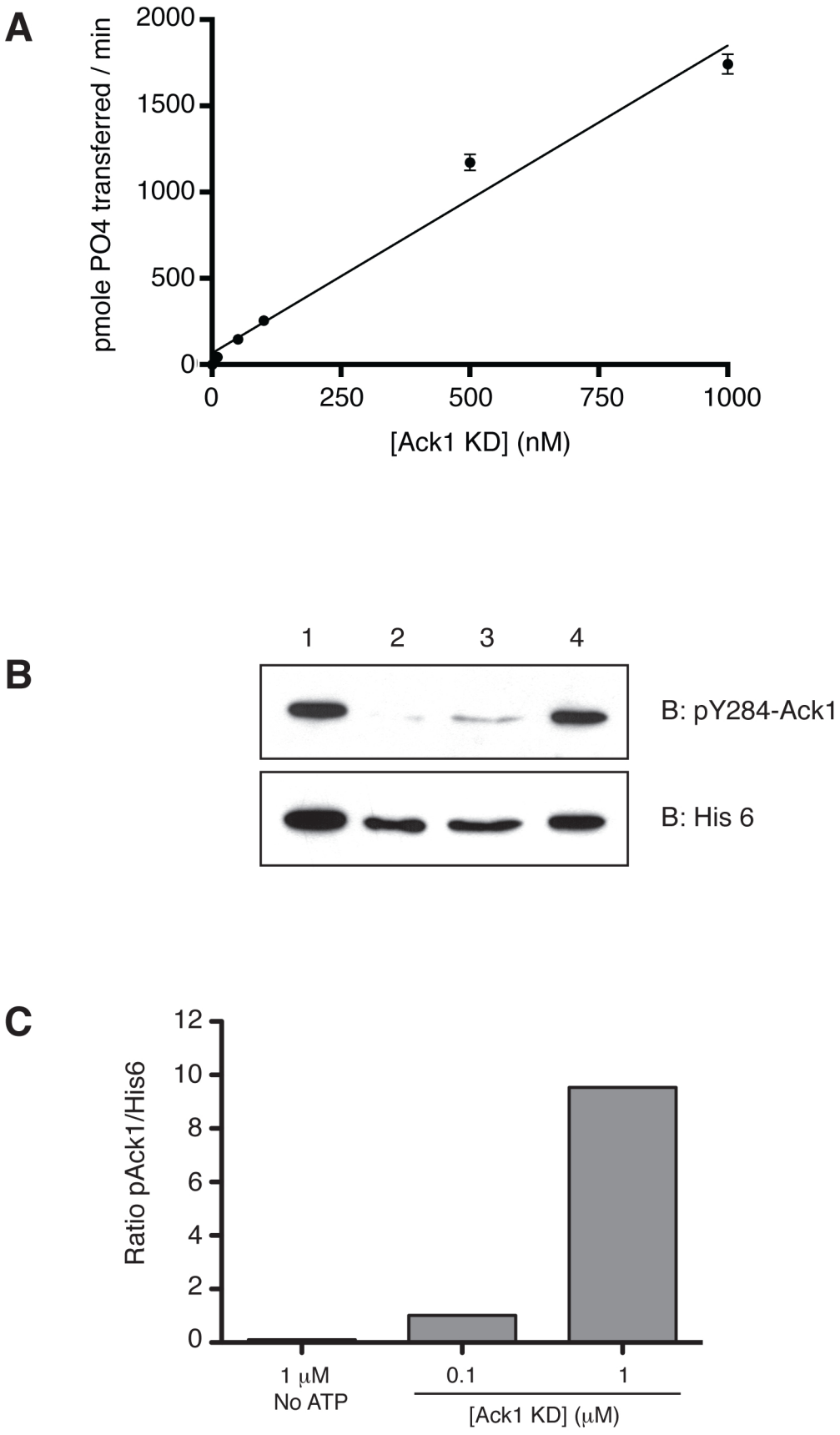
A
2000
1500
1000
500
0
pmole PO4 transferred / min
0
250
500
750
1000
[Ack1 KD] (nM)
B
1
2
3
4
B: pY284-Ack1
B: His 6
C
12
10
8
6
4
2
0
Ratio pAck1/His6
1 μM
No ATP
0.1
1
[Ack1 KD] (μM)

Figure 4-4

Figure 4-5: Increasing local concentrations of purified Ack1 kinase domain at the surface of lipid vesicles activates autophosphorylation.

A, the purified dephosphorylated Ack1 kinase domain was incubated in the presence or absence of ATP and in the presence of lipid vesicles containing different mole ratios of DOGS NTA-Ni. After the reaction, equal amounts of Ack1 kinase domain were separated by SDS-PAGE and analyzed by Western blotting using anti- phospho-Ack1 (pY284) and anti His_6 antibodies. In these experiments, the enzyme concentration was 142 μM and the Ni-NTA was kept constant at 58.5 μM. In order to keep the Ni-NTA concentration constant, the amount of total lipids was varied inversely proportionally with the mole % of Ni-NTA in the vesicles. For 0% and 2% Ni-NTA, the total lipid concentration was 3.3 mM and for 5 % Ni-NTA the lipid concentration was 1.32 mM. No ATP, reaction in the absence of vesicles and ATP. NO Ves., reaction in the absence of vesicles. The figure is representative of three experiments. B, quantitation of the western blots described in A. Densitometry readings were used to calculate the ratios of phosphorylated Ack1 (pY284 blot) to Ack1 (His_6 blot). Error bars indicate standard error.

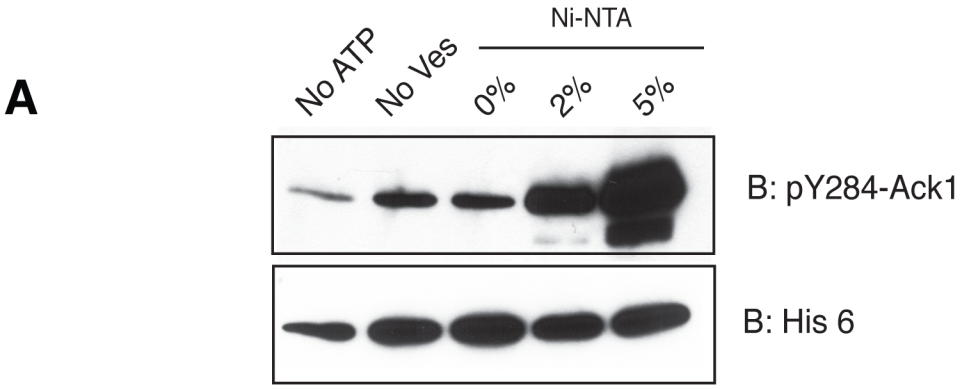
A
Ni-NTA
No ATP
No Ves
0%
2%
5%
B: pY284-Ack1
B: His 6

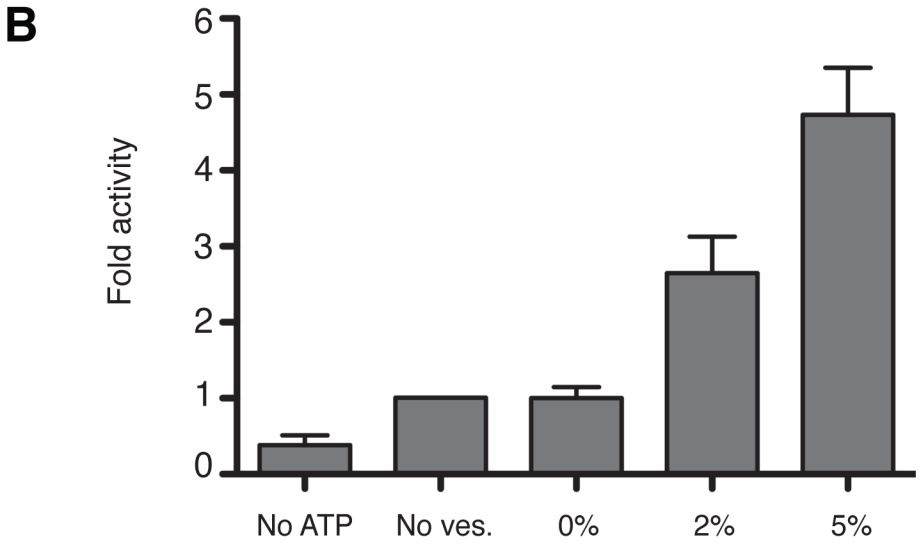
B
Fold activity
6
5
4
3
2
1
0
No ATP
No ves.
0%
2%
5%

Figure 4-5

Figure 4-6: Increasing local concentrations of purified Ack1 kinase domain at the surface of lipid vesicles increases catalytic activity.

The catalytic activity of Ack1 kinase domain towards a peptide was measured as in Figure 4-4. The activities of purified Ack1 kinase domain were measured in solution (no Ves) or with vesicles containing 0 or 5 mole % of DOGS-NTA-Ni. In one experiment (5% + Im), the reaction was carried out in the presence of 500 mM imidazole. The enzyme concentration was 250-500 nM, peptide substrate was used at 1 mM, and the Ni-NTA concentration was kept constant at 30 μM. The figure shows the combined results of nine experiments performed in triplicate. Errors bars indicate Standard error.

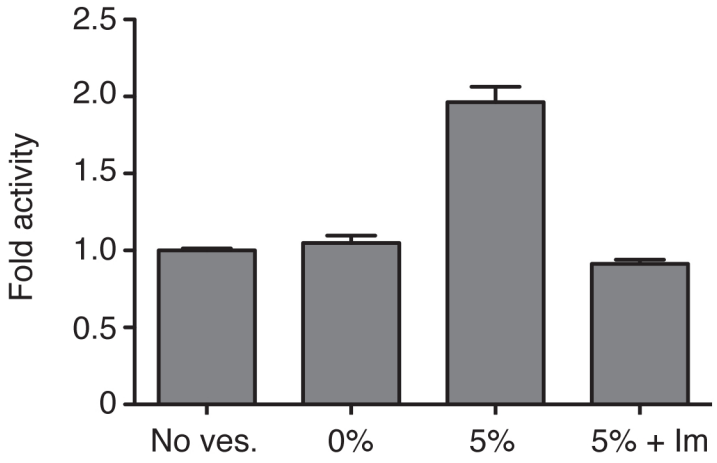

Figure 4-6

Figure 4-7: Ack1 self-associates in cells.

Cos7 cells were transfected with Flag-tagged wild type Ack1 alone or together with HA-tagged Ack1 NKD or KD. Ack1 was immunoprecipitated from cell lysates with anti-Flag antibodies, and the immunocomplexes were analyzed by Western blotting with anti-Flag and anti-HA antibodies. Densitometry readings of the immunoprecipitated proteins (top panels) were used to calculate the ratios of immunoprecipitated HA-Ack1 to immunoprecipitated Flag-Ack1 (HA/Flag). The figure is representative of three experiments.

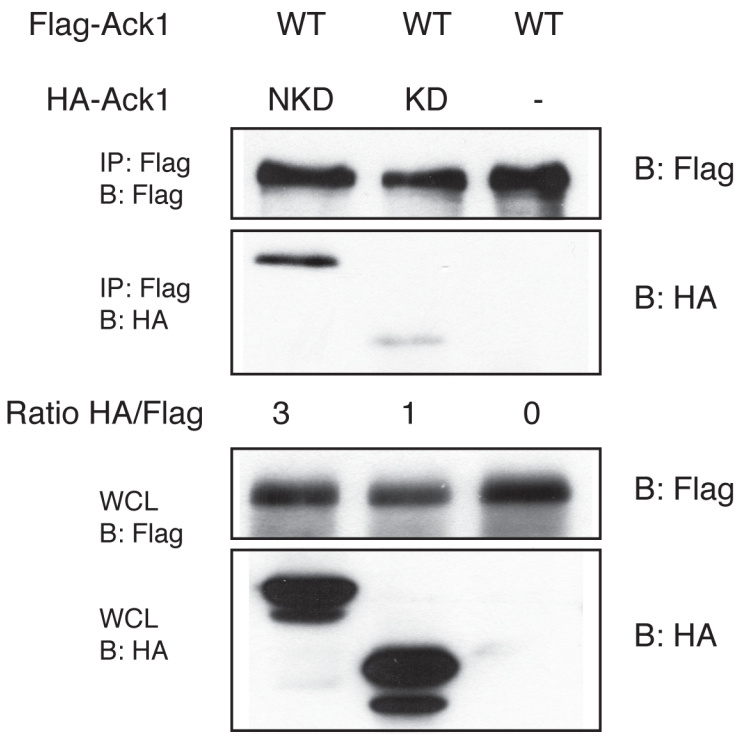
Flag-Ack1
WT
WT
WT
HA-Ack1
NKD
KD
-
IP: Flag
B: Flag
B: Flag
IP: Flag
B: HA
B: HA
Ratio HA/Flag
3
1
0
WCL
B: Flag
B: Flag
WCL
B: HA
B: HA

Figure 4-7

CHAPTER 5

Concluding discussion and future directions

The aim of this work was to understand the molecular mechanisms that regulate the activity of the non-receptor tyrosine kinase Ack1. In particular, we studied the role of the C-terminal Mig6-homology region and the N-terminal SAM domain in Ack1 regulation.

In Chapter 3, we studied the effect of cancer-associated mutations on Ack1 activity. In addition, we used one of the mutations (E346K, located in the C-lobe of the kinase domain) to identify a regulatory mechanism of Ack1. We proposed that the C-terminal region of Ack1 participates in an intramolecular inhibitory interaction, and that destabilizing that conformation potentially activates Ack1. Also, we showed that somatic point mutations located in the Ack1 N-terminal region (R34L and R99Q) have a stimulatory effect on Ack1 activity. Although the molecular mechanism for this activation is currently unclear, this result suggests that the Ack1 N-terminus participates in an additional set of interactions that downregulate the enzyme. These interactions could be either intramolecular, analogous to the ones proposed for the C-terminal MHR, or they could involve one or more binding partner. In either case, the cancer-associated point mutations would destabilize the inhibited conformation and produce an active enzyme.

In Chapter 4, we studied the role of Ack1 N-terminal SAM domain on Ack1 localization and regulation. Our data confirmed that the SAM domain has the potential to localize Ack1 to the plasma membrane, and suggested that a SAM-mediated interaction stimulates Ack1 activation. The activation of Ack1 is also achieved by increasing the local concentration of the purified kianse domain. Therefore, it is possible that the activation by Ack1 SAM domain is due to the formation of SAM-mediated Ack1 oligomers that increase local concentrations of enzyme at determined recruitment sites.

The structure and biophysical properties of the Ack1 SAM domain will be an important topic for future studies. A first step would be to produce the isolated Ack1 SAM domain and

determine its aggregation state in solution. Detailed structural information is available for other SAM domains that oligomerize. TEL-SAM (*92*), Ph-SAM (*93*) and DGKδ-SAM (*91*) have two binding surfaces (end helix, EH and middle loop, ML) that form an interface stabilized by hydrophobic patches surrounded by salt bridges (*91*). These domains form insoluble oligomers when they are expressed in *Escherichia coli*. Ph-SAM and DGKδ-SAM form insoluble filaments (*91, 93*) and TEL-SAM is found in inclusion bodies (*92*). A soluble variant of TEL–SAM was obtained by a point mutation (V80E) that is located at the polymerization interface (*92*). Rationally designed mutations based on the structure of TEL-SAM were introduced in the putative interfaces of Ph-SAM to obtain its crystal structure (*93*). A random mutational screen of DGKδ-SAM was used to select for soluble mutants and to identify residues located at the interface between monomers (*91*). Based on these findings, the Ack1-SAM domain might be predicted to be insoluble. If that is the case, a mutagenesis strategy (rational or random) could be used to increase solubility of Ack1-SAM and to provide information on which residues are important for self-association.

The availability of purified Ack1-SAM would facilitate studies on the effect of the cancer-associated mutations on Ack1-SAM solubility. The self-association of purified Ack1-SAM could be quantified by measuring affinity constants by isothermal titration calorimetry or by surface plasmon resonance. Both N-terminal cancer-associated mutations (R34L and R99Q) exchange a polar residue (arginine) for an uncharged residue. R34 is located at a position that aligns with the EH interface of the other known SAM domains and is surrounded by several hydrophobic residues (Fig.5-1). It is possible that Ack1-SAM domains form oligomers similar to the ones described for TEL, Ph or DGKδ. The presence of the charged residue would modulate the affinity of the interaction and a mutation such as R34L would increase the hydrophobicity of

the region and potentially increase the affinity. Although the secondary structure of R99 is not included in the secondary structure prediction, the substitution of the arginine for a glutamine could potentially neutralize electrostatic repulsions and increase affinity.

Thus, the role of the N-terminal SAM domain of Ack1 might be dual. On the one hand, the N-terminus could stabilize a downregulated conformation of Ack1. On the other hand, upon stimulation of Ack1 by signals such as binding of Cdc42, the SAM domain would be released and made available to self-associate bringing the active molecules to the site of recruitment and favoring trans-phosphorylation. However, we cannot rule out the possibility that the SAM domain is only required for activation by self-association. In that case, stimulatory signals would simply unmask the N-terminus and the activation observed by the cancer-associated mutations, would be the result of increasing SAM binding affinity between monomeric Ack1 molecules.

In the past, our laboratory devoted efforts to the purification of full length Ack1 from Sf9 cells, but activity was lost after the first round of chromatography (*42*). It is possible that some SAM-mediated aggregation interfered with the yield of Ack1. Thus, the deletion of the SAM domain (i.e. ΔNt) could increase Ack1 solubility and allow for purification to homogeneity. The availability of such a construct would be useful to understand more about the relationships between the domains of Ack1.

Due to its role in cancer, Ack1 is emerging as a candidate target for drug development to be used in combined therapies (*66*). We found that cancer-associated mutations that activate Ack1, also promote anchorage independent growth and cell migration. This suggests that cells transformed by the same or a different oncogenic event, and carrying a mutation on Ack1 will have increased metastatic ability. Our studies provide support for Ack1 as a possible target of drug therapies that would be effective in controlling cell motility and cancer spreading. A more

complete understanding of Ack1 physiological roles and regulation mechanism will be helpful to the rational design of drugs targeting Ack1.

The physiological role of Ack1 is unclear, although most data suggest that it plays a role in receptor endocytosis. However, this is a topic still under investigation, because the exact role of Ack1 in this process is not understood. EGFR belongs to the Erb family of receptor tyrosine kinases and is a key target for inhibition in cancer therapy (*100*). The regulation of EGFR stability is a mechanism that modulates the temporal extension of the signal by growth factors (*101*). Ack1 is activated by EGFR (*25*), and in turn it promotes EGFR degradation (*27*). EGF treatment promotes Ack1 degradation (*68*). Paradoxically we (*57*) and others (*24*) have shown that amplified and activated Ack1 has an oncogenic effect. In addition, stimulation of EGFR or HER2 leads to phosphorylation of Ack1. The role of the phosphorylation sites described in proteomic studies (Y518, Y827, Y857, Y958) (*53-55*), the stoichiometry of phosphorylation and the nature of the kinase(s) involved are unknown. Thus,the relationship between Ack1and EGFR appears to be complex and to involve mutual effects that are not understood. The elucidation of these mechanisms will be an important area of research in the future due to the central role of EGFR in tumorigenesis. In addition, a better understanding of the role of Ack1 in EGFR signaling will potentially provide a specific target for rational drug design to be used in combined cancer therapy.

The domain composition of Ack1 is complex and it is likely that in the future, additional interactions (both intra-and intermolecular) will be described that will explain in more detail the molecular mechanisms of Ack1 regulation and signaling. In the introductory chapter, we highlighted the diversity of regulatory mechanisms among the different NRTKs. The results discussed in this dissertation suggest that Ack1 is regulated by a novel mechanism that shares

basic principles with other NRTKs but also has unique features. The unique regulatory mechanism of Ack1 could potentially be exploited to generate specific inhibitors. For instance, imatinib inhibits Abl (but not Src) because it binds to a specific conformation of Abl that Src is not capable of achieving (*95*). Moreover, the inhibited conformation of Abl appears to be the result of the interplay of the non-catalytic domains (*95*). The understanding of the regulatory mechanisms that govern Ack1 activity will be crucial for the development of specific Ack1 inhibitors that could potentially be used in cancer treatment.

Figure 5-1: Sequence and structural alignment of SAM domains.

Top: Predicted secondary structure Ak1 residues 1-110. The server JPred3 at http://www.compbio.dundee.ac.uk/www-jpred was used. Yellow rectangles represent the predicted alpha helices. Bottom: alignment of diverse SAM domains that oligomerize or dimerize. Red: Residues located at the EH Surface. Cyan: Residues located at the ML surface. Magenta: cancer-associated mutations in Ack1. Green: residues at the dimer interface in EphB2 receptor

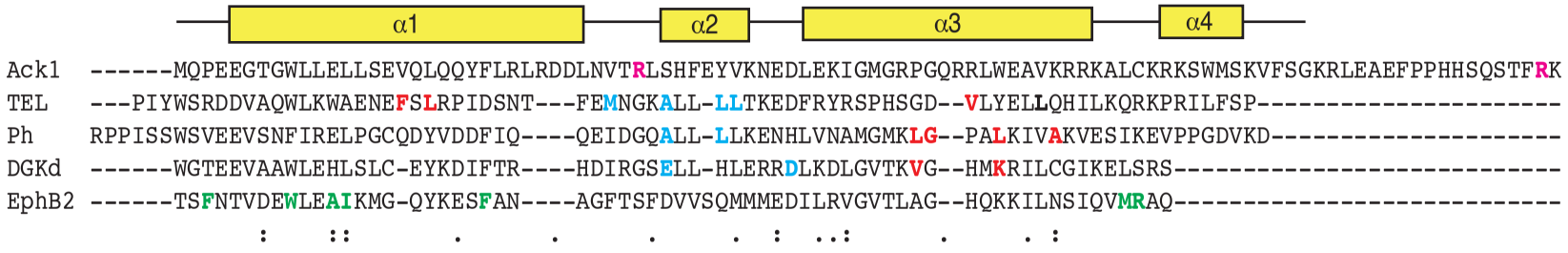
α1
α2
α3
α4
Ack1 ------MQPEEGTGWLLELLSEVQLQQYFLRLRDDLNVTRLSHFEYVKNEDLEKIGMGRPGQRRLWEAVKRRKALCKRKSWMSKVFSGKRLEAEFPPHHSQSTFRK
TEL ---PIYWSRDDVAQWLKWAENEFSLRPIDSNT---FEMNGKALL-LLTKEDFRYRSPHSGD--VLYELLQHILKQRKPRILFSP----------
Ph RPPISSWSVEEVSNFIRELPGCQDYVDDFIQ----QEIDGQALL-LLKENHLVNAMGMKLG--PALKIVAKVESIKEVPPGDVKD----------
DGKd ------WGTEEVAAWLEHLSLC-EYKDIFTR----HDIRGSELL-HLERRDLKDLGVTKVG--HMKRILCGIKELSRS----------
EphB2 ------TSFNTVDEWLEAIKMG-QYKESFAN----AGFTSFDVVSQMMMEDILRVGVTLAG--HQKKILNSIQVMRAQ----------

Figure 5-1

References

1. Eckhart, W., Hutchinson, M. A., and Hunter, T. (1979) An activity phosphorylating tyrosine in polyoma T antigen immunoprecipitates, *Cell 18*, 925-933.

2. Miller, W. T. (2003) Determinants of substrate recognition in nonreceptor tyrosine kinases, *Acc Chem Res 36*, 393-400.

3. Pawson, T., and Kofler, M. (2009) Kinome signaling through regulated protein-protein interactions in normal and cancer cells, *Curr Opin Cell Biol 21*, 147-153.

4. Hunter, T. (2009) Tyrosine phosphorylation: thirty years and counting, *Curr Opin Cell Biol 21*, 140-146.

5. Blume-Jensen, P., and Hunter, T. (2001) Oncogenic kinase signalling, *Nature 411*, 355-365.

6. Hubbard, S. R., and Till, J. H. (2000) Protein tyrosine kinase structure and function, *Annual review of biochemistry 69*, 373-398.

7. Bradshaw, J. M. (2010) The Src, Syk, and Tec family kinases: distinct types of molecular switches, *Cell Signal 22*, 1175-1184.

8. Mikkola, E. T., and Gahmberg, C. G. (2010) Hydrophobic Interaction between the SH2 Domain and the Kinase Domain Is Required for the Activation of Csk, *J Mol Biol*.

9. Sicheri, F., Moarefi, I., and Kuriyan, J. (1997) Crystal structure of the Src family tyrosine kinase Hck, *Nature 385*, 602-609.

10. Xu, W., Harrison, S. C., and Eck, M. J. (1997) Three-dimensional structure of the tyrosine kinase c-Src, *Nature 385*, 595-602.

11. Moarefi, I., LaFevre-Bernt, M., Sicheri, F., Huse, M., Lee, C. H., Kuriyan, J., and Miller, W. T. (1997) Activation of the Src-family tyrosine kinase Hck by SH3 domain displacement, *Nature 385*, 650-653.

12. Cooper, J. A., and King, C. S. (1986) Dephosphorylation or antibody binding to the carboxy terminus stimulates pp60c-src, *Mol Cell Biol 6*, 4467-4477.

13. Porter, M., Schindler, T., Kuriyan, J., and Miller, W. T. (2000) Reciprocal regulation of Hck activity by phosphorylation of Tyr(527) and Tyr(416). Effect of introducing a high affinity intramolecular SH2 ligand, *The Journal of biological chemistry 275*, 2721-2726.

14. Pellicena, P., and Miller, W. T. (2002) Coupling kinase activation to substrate recognition in SRC-family tyrosine kinases, *Front Biosci 7*, d256-267.

15. Qiu, H., and Miller, W. T. (2004) Role of the Brk SH3 domain in substrate recognition, *Oncogene 23*, 2216-2223.

16. Hantschel, O., and Superti-Furga, G. (2004) Regulation of the c-Abl and Bcr-Abl tyrosine kinases, *Nat Rev Mol Cell Biol 5*, 33-44.

17. Ogawa, A., Takayama, Y., Sakai, H., Chong, K. T., Takeuchi, S., Nakagawa, A., Nada, S., Okada, M., and Tsukihara, T. (2002) Structure of the carboxyl-terminal Src kinase, Csk, *The Journal of biological chemistry 277*, 14351-14354.

18. Takeuchi, S., Takayama, Y., Ogawa, A., Tamura, K., and Okada, M. (2000) Transmembrane phosphoprotein Cbp positively regulates the activity of the carboxyl-terminal Src kinase, Csk, *The Journal of biological chemistry 275*, 29183-29186.

19. Mikkola, E. T., and Bergman, M. (2003) Conserved hydrophobicity in the SH2-kinase linker is required for catalytic activity of Csk and CHK, *FEBS Lett 544*, 11-14.

20. Hemmings, B. A., Restuccia, D., and Tonks, N. (2009) Targeting the Kinome II, *Curr Opin Cell Biol 21*, 135-139.

21. Greenman, C., Stephens, P., Smith, R., Dalgliesh, G. L., Hunter, C., Bignell, G., Davies, H., Teague, J., Butler, A., Stevens, C., Edkins, S., O'Meara, S., Vastrik, I., Schmidt, E. E., Avis, T., Barthorpe, S., Bhamra, G., Buck, G., Choudhury, B., Clements, J., Cole, J., Dicks, E., Forbes, S., Gray, K., Halliday, K., Harrison, R., Hills, K., Hinton, J., Jenkinson, A., Jones, D., Menzies, A., Mironenko, T., Perry, J., Raine, K., Richardson, D., Shepherd, R., Small, A., Tofts, C., Varian, J., Webb, T., West, S., Widaa, S., Yates, A., Cahill, D. P., Louis, D. N., Goldstraw, P., Nicholson, A. G., Brasseur, F., Looijenga, L., Weber, B. L., Chiew, Y. E., DeFazio, A., Greaves, M. F., Green, A. R., Campbell, P., Birney, E., Easton, D. F., Chenevix-Trench, G., Tan, M. H., Khoo, S. K., Teh, B. T., Yuen, S. T., Leung, S. Y., Wooster, R., Futreal, P. A., and Stratton, M. R. (2007) Patterns of somatic mutation in human cancer genomes, *Nature 446*, 153-158.

22. Mahajan, N. P., Whang, Y. E., Mohler, J. L., and Earp, H. S. (2005) Activated tyrosine kinase Ack1 promotes prostate tumorigenesis: role of Ack1 in polyubiquitination of tumor suppressor Wwox, *Cancer Res 65*, 10514-10523.

23. Nur, E. K. A., Zhang, A., Keenan, S. M., Wang, X. I., Seraj, J., Satoh, T., Meiners, S., and Welsh, W. J. (2005) Requirement of activated Cdc42-associated kinase for survival of v-Ras-transformed mammalian cells, *Mol Cancer Res 3*, 297-305.

24. van der Horst, E. H., Degenhardt, Y. Y., Strelow, A., Slavin, A., Chinn, L., Orf, J., Rong, M., Li, S., See, L. H., Nguyen, K. Q., Hoey, T., Wesche, H., and Powers, S. (2005) Metastatic properties and genomic amplification of the tyrosine kinase gene ACK1, *Proc Natl Acad Sci U S A 102*, 15901-15906.

25. Galisteo, M. L., Yang, Y., Urena, J., and Schlessinger, J. (2006) Activation of the nonreceptor protein tyrosine kinase Ack by multiple extracellular stimuli, *Proceedings of the National Academy of Sciences of the United States of America 103*, 9796-9801.

26. Teo, M., Tan, L., Lim, L., and Manser, E. (2001) The tyrosine kinase ACK1 associates with clathrin-coated vesicles through a binding motif shared by arrestin and other adaptors, *The Journal of biological chemistry 276*, 18392-18398.

27. Shen, F., Lin, Q., Gu, Y., Childress, C., and Yang, W. (2007) Activated Cdc42-associated kinase 1 is a component of EGF receptor signaling complex and regulates EGF receptor degradation, *Mol Biol Cell 18*, 732-742.

28. Zhang, X., Pickin, K. A., Bose, R., Jura, N., Cole, P. A., and Kuriyan, J. (2007) Inhibition of the EGF receptor by binding of MIG6 to an activating kinase domain interface, *Nature 450*, 741-744.

29. Hopper, N. A., Lee, J., and Sternberg, P. W. (2000) ARK-1 inhibits EGFR signaling in C. elegans, *Molecular cell 6*, 65-75.

30. Sem, K. P., Zahedi, B., Tan, I., Deak, M., Lim, L., and Harden, N. (2002) ACK family tyrosine kinase activity is a component of Dcdc42 signaling during dorsal closure in Drosophila melanogaster, *Mol Cell Biol 22*, 3685-3697.

31. Manser, E., Leung, T., Salihuddin, H., Tan, L., and Lim, L. (1993) A non-receptor tyrosine kinase that inhibits the GTPase activity of p21cdc42, *Nature 363*, 364-367.

32. Hoehn, G. T., Stokland, T., Amin, S., Ramirez, M., Hawkins, A. L., Griffin, C. A., Small, D., and Civin, C. I. (1996) Tnk1: a novel intracellular tyrosine kinase gene isolated from human umbilical cord blood CD34+/Lin-/CD38- stem/progenitor cells, *Oncogene 12*, 903-913.

33. Hoare, K., Hoare, S., Smith, O. M., Kalmaz, G., Small, D., and Stratford May, W. (2003) Kos1, a nonreceptor tyrosine kinase that suppresses Ras signaling, *Oncogene 22*, 3562-3577.

34. Felschow, D. M., Civin, C. I., and Hoehn, G. T. (2000) Characterization of the tyrosine kinase Tnk1 and its binding with phospholipase C-gamma1, *Biochemical and biophysical research communications 273*, 294-301.

35. Azoitei, N., Brey, A., Busch, T., Fulda, S., Adler, G., and Seufferlein, T. (2007) Thirty-eight-negative kinase 1 (TNK1) facilitates TNFalpha-induced apoptosis by blocking NF-kappaB activation, *Oncogene 26*, 6536-6545.

36. Hoare, S., Hoare, K., Reinhard, M. K., Lee, Y. J., Oh, S. P., and May, W. S., Jr. (2008) Tnk1/Kos1 knockout mice develop spontaneous tumors, *Cancer Res 68*, 8723-8732.

37. Yang, W., and Cerione, R. A. (1997) Cloning and characterization of a novel Cdc42-associated tyrosine kinase, ACK-2, from bovine brain, *The Journal of biological chemistry 272*, 24819-24824.

38. Linseman, D. A., Heidenreich, K. A., and Fisher, S. K. (2001) Stimulation of M3 muscarinic receptors induces phosphorylation of the Cdc42 effector activated Cdc42Hs-associated kinase-1 via a Fyn tyrosine kinase signaling pathway, *The Journal of biological chemistry 276*, 5622-5628.

39. Modzelewska, K., Newman, L. P., Desai, R., and Keely, P. J. (2006) ACK1 mediates CDC42-dependent cell migration and signaling to p130cas, *The Journal of biological chemistry 281*, 37527-37535.

40. Yang, W., Lin, Q., Guan, J. L., and Cerione, R. A. (1999) Activation of the Cdc42-associated tyrosine kinase-2 (ACK-2) by cell adhesion via integrin beta1, *The Journal of biological chemistry 274*, 8524-8530.

41. Kato-Stankiewicz, J., Ueda, S., Kataoka, T., Kaziro, Y., and Satoh, T. (2001) Epidermal growth factor stimulation of the ACK1/Dbl pathway in a Cdc42 and Grb2-dependent manner, *Biochemical and biophysical research communications 284*, 470-477.

42. Yokoyama, N., and Miller, W. T. (2003) Biochemical properties of the Cdc42-associated tyrosine kinase ACK1. Substrate specificity, authphosphorylation, and interaction with Hck, *The Journal of biological chemistry 278*, 47713-47723.

43. Pao-Chun, L., Chan, P. M., Chan, W., and Manser, E. (2009) Cytoplasmic ACK1 interaction with multiple receptor tyrosine kinases is mediated by Grb2: an analysis of ACK1 effects on Axl signaling, *The Journal of biological chemistry 284*, 34954-34963.

44. Eisenmann, K. M., McCarthy, J. B., Simpson, M. A., Keely, P. J., Guan, J. L., Tachibana, K., Lim, L., Manser, E., Furcht, L. T., and Iida, J. (1999) Melanoma chondroitin sulphate proteoglycan regulates cell spreading through Cdc42, Ack-1 and p130cas, *Nat Cell Biol 1*, 507-513.

45. Coon, M., and Herrera, R. (2002) Modulation of HeLa cells spreading by the non-receptor tyrosine kinase ACK-2, *J Cell Biochem 84*, 655-665.

46. Grovdal, L. M., Johannessen, L. E., Rodland, M. S., Madshus, I. H., and Stang, E. (2008) Dysregulation of Ack1 inhibits down-regulation of the EGF receptor, *Exp Cell Res 314*, 1292-1300.

47. Yang, W., Lo, C. G., Dispenza, T., and Cerione, R. A. (2001) The Cdc42 target ACK2 directly interacts with clathrin and influences clathrin assembly, *The Journal of biological chemistry 276*, 17468-17473.

48. Childress, C., Lin, Q., and Yang, W. (2006) Dimerization is required for SH3PX1 tyrosine phosphorylation in response to epidermal growth factor signalling and interaction with ACK2, *Biochem J 394*, 693-698.

49. Yeow-Fong, L., Lim, L., and Manser, E. (2005) SNX9 as an adaptor for linking synaptojanin-1 to the Cdc42 effector ACK1, *FEBS Lett 579*, 5040-5048.

50. Howlin, J., Rosenkvist, J., and Andersson, T. (2008) TNK2 preserves epidermal growth factor receptor expression on the cell surface and enhances migration and invasion of human breast cancer cells, *Breast Cancer Res 10*, R36.

51. Chua, B. T., Lim, S. J., Tham, S. C., Poh, W. J., and Ullrich, A. (2010) Somatic mutation in the ACK1 ubiquitin association domain enhances oncogenic signaling through EGFR regulation in renal cancer derived cells, *Mol Oncol*.

52. Lougheed, J. C., Chen, R. H., Mak, P., and Stout, T. J. (2004) Crystal structures of the phosphorylated and unphosphorylated kinase domains of the Cdc42-associated tyrosine kinase ACK1, *The Journal of biological chemistry 279*, 44039-44045.

53. Salomon, A. R., Ficarro, S. B., Brill, L. M., Brinker, A., Phung, Q. T., Ericson, C., Sauer, K., Brock, A., Horn, D. M., Schultz, P. G., and Peters, E. C. (2003) Profiling of tyrosine phosphorylation pathways in human cells using mass spectrometry, *Proceedings of the National Academy of Sciences of the United States of America 100*, 443-448.

54. Ibarrola, N., Molina, H., Iwahori, A., and Pandey, A. (2004) A novel proteomic approach for specific identification of tyrosine kinase substrates using [13C]tyrosine, *The Journal of biological chemistry 279*, 15805-15813.

55. Wolf-Yadlin, A., Kumar, N., Zhang, Y., Hautaniemi, S., Zaman, M., Kim, H. D., Grantcharova, V., Lauffenburger, D. A., and White, F. M. (2006) Effects of HER2 overexpression on cell signaling networks governing proliferation and migration, *Mol Syst Biol 2*, 54.

56. Rush, J., Moritz, A., Lee, K. A., Guo, A., Goss, V. L., Spek, E. J., Zhang, H., Zha, X. M., Polakiewicz, R. D., and Comb, M. J. (2005) Immunoaffinity profiling of tyrosine phosphorylation in cancer cells, *Nat Biotechnol 23*, 94-101.

57. Prieto-Echague, V., Gucwa, A., Craddock, B. P., Brown, D. A., and Miller, W. T. (2010) Cancer-associated mutations activate the nonreceptor tyrosine kinase Ack1, *The Journal of biological chemistry 285*, 10605-10615.

58. Yokoyama, N., and Miller, W. T. (2006) Purification and enzyme activity of ACK1, *Methods Enzymol 406*, 250-260.

59. Mott, H. R., Owen, D., Nietlispach, D., Lowe, P. N., Manser, E., Lim, L., and Laue, E. D. (1999) Structure of the small G protein Cdc42 bound to the GTPase-binding domain of ACK, *Nature 399*, 384-388.

60. Kato, J., Kaziro, Y., and Satoh, T. (2000) Activation of the guanine nucleotide exchange factor Dbl following ACK1-dependent tyrosine phosphorylation, *Biochemical and biophysical research communications 268*, 141-147.

61. Parrini, M. C., Lei, M., Harrison, S. C., and Mayer, B. J. (2002) Pak1 kinase homodimers are autoinhibited in trans and dissociated upon activation by Cdc42 and Rac1, *Molecular cell 9*, 73-83.

62. Mahajan, K., Coppola, D., Challa, S., Fang, B., Chen, Y. A., Zhu, W., Lopez, A. S., Koomen, J., Engelman, R. W., Rivera, C., Muraoka-Cook, R. S., Cheng, J. Q., Schonbrunn, E., Sebti, S. M., Earp, H. S., and Mahajan, N. P. (2010) Ack1 mediated AKT/PKB tyrosine 176 phosphorylation regulates its activation, *PLoS One 5*, e9646.

63. Nur, E. K. M. S., Kamal, J. M., Qureshi, M. M., and Maruta, H. (1999) The CDC42-specific inhibitor derived from ACK-1 blocks v-Ha-Ras-induced transformation, *Oncogene 18*, 7787-7793.

64. Mahajan, N. P., Liu, Y., Majumder, S., Warren, M. R., Parker, C. E., Mohler, J. L., Earp, H. S., and Whang, Y. E. (2007) Activated Cdc42-associated kinase Ack1 promotes prostate cancer progression via androgen receptor tyrosine phosphorylation, *Proceedings of the National Academy of Sciences of the United States of America 104*, 8438-8443.

65. Mahajan, K., Challa, S., Coppola, D., Lawrence, H., Luo, Y., Gevariya, H., Zhu, W., Chen, Y. A., Lawrence, N. J., and Mahajan, N. P. (2010) Effect of Ack1 tyrosine kinase inhibitor on ligand-independent androgen receptor activity, *The Prostate 70*, 1274-1285.

66. Li, J., Rix, U., Fang, B., Bai, Y., Edwards, A., Colinge, J., Bennett, K. L., Gao, J., Song, L., Eschrich, S., Superti-Furga, G., Koomen, J., and Haura, E. B. (2010) A chemical and phosphoproteomic characterization of dasatinib action in lung cancer, *Nat Chem Biol 6*, 291-299.

67. Satoh, T., Kato, J., Nishida, K., and Kaziro, Y. (1996) Tyrosine phosphorylation of ACK in response to temperature shift-down, hyperosmotic shock, and epidermal growth factor stimulation, *FEBS Lett 386*, 230-234.

68. Chan, W., Tian, R., Lee, Y. F., Sit, S. T., Lim, L., and Manser, E. (2009) Down-regulation of active ACK1 is mediated by association with the E3 ubiquitin ligase Nedd4-2, *The Journal of biological chemistry 284*, 8185-8194.

69. Yokoyama, N., Lougheed, J., and Miller, W. T. (2005) Phosphorylation of WASP by the Cdc42-associated kinase ACK1: dual hydroxyamino acid specificity in a tyrosine kinase, *The Journal of biological chemistry 280*, 42219-42226.

70. Mahajan, K., and Mahajan, N. P. (2010) Shepherding AKT and androgen receptor by Ack1 tyrosine kinase, *J Cell Physiol 224*, 327-333.

71. Yokoyama, N., Reich, N. C., and Miller, W. T. (2003) Determinants for the interaction between Janus kinase 2 and protein phosphatase 2A, *Arch Biochem Biophys 417*, 87-95.

72. Oda, T., Muramatsu, M. A., Isogai, T., Masuho, Y., Asano, S., and Yamashita, T. (2001) HSH2: a novel SH2 domain-containing adapter protein involved in tyrosine kinase signaling in hematopoietic cells, *Biochemical and biophysical research communications 288*, 1078-1086.

73. Lin, Q., Wang, J., Childress, C., Sudol, M., Carey, D. J., and Yang, W. (2010) HECT E3 ubiquitin ligase Nedd4-1 ubiquitinates ACK and regulates epidermal growth factor (EGF)-induced degradation of EGF receptor and ACK, *Mol Cell Biol 30*, 1541-1554.

74. Eley, L., Moochhala, S. H., Simms, R., Hildebrandt, F., and Sayer, J. A. (2008) Nephrocystin-1 interacts directly with Ack1 and is expressed in human collecting duct, *Biochemical and biophysical research communications 371*, 877-882.

75. Barr, A. J., Ugochukwu, E., Lee, W. H., King, O. N., Filippakopoulos, P., Alfano, I., Savitsky, P., Burgess-Brown, N. A., Muller, S., and Knapp, S. (2009) Large-scale structural analysis of the classical human protein tyrosine phosphatome, *Cell 136*, 352-363.

76. Wu, X., Zhao, X., Baylor, L., Kaushal, S., Eisenberg, E., and Greene, L. E. (2001) Clathrin exchange during clathrin-mediated endocytosis, *The Journal of cell biology 155*, 291-300.

77. Thomas, M., Lu, J. J., Ge, Q., Zhang, C., Chen, J., and Klibanov, A. M. (2005) Full deacylation of polyethylenimine dramatically boosts its gene delivery efficiency and specificity to mouse lung, *Proceedings of the National Academy of Sciences of the United States of America 102*, 5679-5684.

78. LaFevre-Bernt, M., Sicheri, F., Pico, A., Porter, M., Kuriyan, J., and Miller, W. T. (1998) Intramolecular regulatory interactions in the Src family kinase Hck probed by mutagenesis of a conserved tryptophan residue, *The Journal of biological chemistry 273*, 32129-32134.

79. Barker, S. C., Kassel, D. B., Weigl, D., Huang, X., Luther, M. A., and Knight, W. B. (1995) Characterization of pp60c-src tyrosine kinase activities using a continuous assay: autoactivation of the enzyme is an intermolecular autophosphorylation process, *Biochemistry 34*, 14843-14851.

80. Huse, M., and Kuriyan, J. (2002) The conformational plasticity of protein kinases, *Cell 109*, 275-282.

81. Liu, X., Brodeur, S. R., Gish, G., Songyang, Z., Cantley, L. C., Laudano, A. P., and Pawson, T. (1993) Regulation of c-Src tyrosine kinase activity by the Src SH2 domain, *Oncogene 8*, 1119-1126.

82. Alexandropoulos, K., and Baltimore, D. (1996) Coordinate activation of c-Src by SH3- and SH2-binding sites on a novel p130Cas-related protein, Sin, *Genes & development 10*, 1341-1355.

83. Briggs, S. D., Sharkey, M., Stevenson, M., and Smithgall, T. E. (1997) SH3-mediated Hck tyrosine kinase activation and fibroblast transformation by the Nef protein of HIV-1, *The Journal of biological chemistry 272*, 17899-17902.

84. Pluk, H., Dorey, K., and Superti-Furga, G. (2002) Autoinhibition of c-Abl, *Cell 108*, 247-259.

85. Nolen, B., Taylor, S., and Ghosh, G. (2004) Regulation of protein kinases; controlling activity through activation segment conformation, *Molecular cell 15*, 661-675.

86. Manning, G., Whyte, D. B., Martinez, R., Hunter, T., and Sudarsanam, S. (2002) The protein kinase complement of the human genome, *Science (New York, N.Y 298*, 1912-1934.

87. Zhang, X., Gureasko, J., Shen, K., Cole, P. A., and Kuriyan, J. (2006) An allosteric mechanism for activation of the kinase domain of epidermal growth factor receptor, *Cell 125*, 1137-1149.

88. Anastasi, S., Baietti, M. F., Frosi, Y., Alema, S., and Segatto, O. (2007) The evolutionarily conserved EBR module of RALT/MIG6 mediates suppression of the EGFR catalytic activity, *Oncogene 26*, 7833-7846.

89. Stapleton, D., Balan, I., Pawson, T., and Sicheri, F. (1999) The crystal structure of an Eph receptor SAM domain reveals a mechanism for modular dimerization, *Nature structural biology 6*, 44-49.

90. Thanos, C. D., Goodwill, K. E., and Bowie, J. U. (1999) Oligomeric structure of the human EphB2 receptor SAM domain, *Science (New York, N.Y 283*, 833-836.

91. Harada, B. T., Knight, M. J., Imai, S., Qiao, F., Ramachander, R., Sawaya, M. R., Gingery, M., Sakane, F., and Bowie, J. U. (2008) Regulation of enzyme localization by polymerization: polymer formation by the SAM domain of diacylglycerol kinase delta1, *Structure 16*, 380-387.

92. Kim, C. A., Phillips, M. L., Kim, W., Gingery, M., Tran, H. H., Robinson, M. A., Faham, S., and Bowie, J. U. (2001) Polymerization of the SAM domain of TEL in leukemogenesis and transcriptional repression, *The EMBO journal 20*, 4173-4182.

93. Kim, C. A., Gingery, M., Pilpa, R. M., and Bowie, J. U. (2002) The SAM domain of polyhomeotic forms a helical polymer, *Nature structural biology 9*, 453-457.

94. Xu, W., Doshi, A., Lei, M., Eck, M. J., and Harrison, S. C. (1999) Crystal structures of c-Src reveal features of its autoinhibitory mechanism, *Molecular cell 3*, 629-638.

95. Nagar, B., Hantschel, O., Young, M. A., Scheffzek, K., Veach, D., Bornmann, W., Clarkson, B., Superti-Furga, G., and Kuriyan, J. (2003) Structural basis for the autoinhibition of c-Abl tyrosine kinase, *Cell 112*, 859-871.

96. Lietha, D., Cai, X., Ceccarelli, D. F., Li, Y., Schaller, M. D., and Eck, M. J. (2007) Structural basis for the autoinhibition of focal adhesion kinase, *Cell 129*, 1177-1187.

97. Lin, Q., Lo, C. G., Cerione, R. A., and Yang, W. (2002) The Cdc42 target ACK2 interacts with sorting nexin 9 (SH3PX1) to regulate epidermal growth factor receptor degradation, *The Journal of biological chemistry 277*, 10134-10138.

98. Kim, C. A., and Bowie, J. U. (2003) SAM domains: uniform structure, diversity of function, *Trends in biochemical sciences 28*, 625-628.

99. Filippakopoulos, P., Kofler, M., Hantschel, O., Gish, G. D., Grebien, F., Salah, E., Neudecker, P., Kay, L. E., Turk, B. E., Superti-Furga, G., Pawson, T., and Knapp, S. (2008) Structural coupling of SH2-kinase domains links Fes and Abl substrate recognition and kinase activation, *Cell 134*, 793-803.

100. Yoshida, T., Zhang, G., and Haura, E. B. (2010) Targeting epidermal growth factor receptor: Central signaling kinase in lung cancer, *Biochem Pharmacol*.

101. Haglund, K., Sigismund, S., Polo, S., Szymkiewicz, I., Di Fiore, P. P., and Dikic, I. (2003) Multiple monoubiquitination of RTKs is sufficient for their endocytosis and degradation, *Nat Cell Biol 5*, 461-466.

Appendix

Supplemental figures

Figure S1. Receptor and cytoplasmic tyrosine kinases.

The red Box highlights Ack family of cytoplasmic tyrosine kinases. One of the families with closest homology to Ack is the Epidermal growth factor receptor family. Reproduced from the website Cell Signaling Inc.

http://www.cellsignal.com/reference/pathway/pdfs/Tyrosine_Kinases.pdf

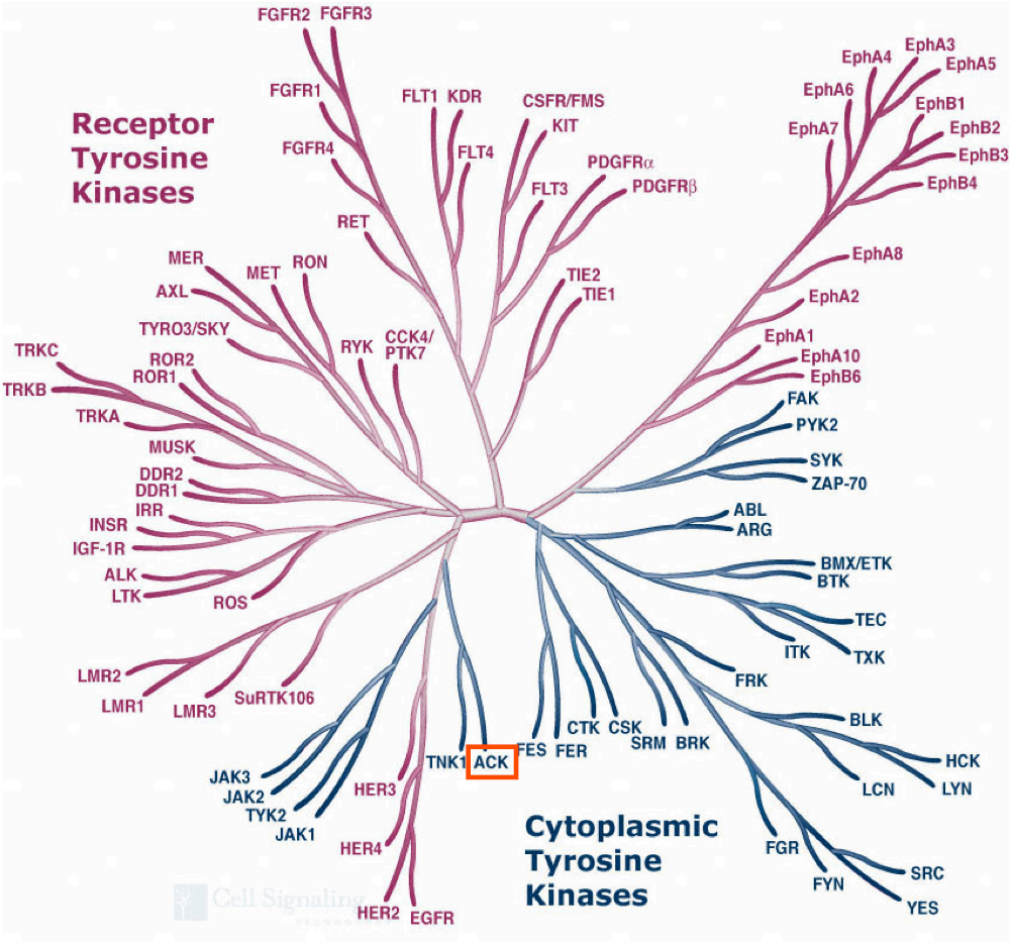

Figure S2. Controlling local concentrations of purified Ack1 at the surface of lipid vesicles.

The His_6-tagged purified Ack1 kinase domain was incubated with lipid vesicles containing 0, 2 or 5 mole% of a modified lipid that contained NTA-Ni as a head group (DGS-NTA-Ni). Increasing mole% of NTA-Ni resulted in increasing the local concentration of Ack1 kinase domain at the surface of the lipid vesicles. Similar systems were used in autophosphorylation assays and phosphorylation of a peptide.

Grey circles represent small unilamellar vesicles, light blue dots represent NTA-Ni groups and dark blue dots indicate His_6-tagged purified Ack1 kinase domain.